PREDICTION OF HEXAGONAL LATTICE PARAMETERS OF STOICHIOMETRIC AND NON-STOICHIOMETRIC APATITES BY ARTIFICIAL NEURAL NETWORKS

A THESIS SUBMITTED TO
THE GRADUATE SCHOOL OF NATURAL AND APPLIED SCIENCES
OF
MIDDLE EAST TECHNICAL UNIVERSITY

BY

ÜMİT KOÇKAN

IN PARTIAL FULLFILLMENT OF THE REQUIREMENTS
FOR
THE DEGREE OF MASTER OF SCIENCE
IN
MICRO AND NANOTECHNOLOGY

JANUARY 2009

Approval of the thesis:

PREDICTION OF HEXAGONAL LATTICE PARAMETERS OF STOICHIOMETRIC AND NON-STOICHIOMETRIC APATITES BY ARTIFICIAL NEURAL NETWORKS

submitted by **ÜMİT KOÇKAN** in partial fullfillment of the requirements for the degree of **Master of Science in Micro and Nanotechnology, Middle East Technical University** by,

Prof. Dr. Canan Özgen _____
Dean, Graduate School of **Natural and Applied Sciences**

Prof. Dr. Raşit Turan _____
Head of Department, **Micro and Nanotechnology**

Assist. Prof. Dr. Zafer Evis _____
Supervisor, **Engineering Sciences Department, METU**

Prof. Dr. Kadri Aydınol _____
Co-Supervisor, **Metallurgical and Materials Engineering Dept., METU**

Examining Committee Members:

Prof. Dr. M. Polat Saka _____
Engineering Sciences Department, METU

Assist. Prof. Dr. Zafer Evis _____
Engineering Sciences Department, METU

Prof. Dr. Kadri Aydınol _____
Metallurgical and Materials Engineering Dept., METU

Assist. Prof. Dr. Caner Durucan _____
Metallurgical and Materials Engineering Dept., METU

Assist. Prof. Dr. Hande Toffoli _____
Physics Department, METU

Date: 20.01.2009

I hereby declare that all information in this document has been obtained and presented accordance with the academic rules and ethical conduct. I also declare that, as required by these rules and conduct, I have fully cited and referenced all material and results that are not original to this work.

Name, Last Name: Ümit Koçkan

Signature:

ABSTRACT

PREDICTION OF HEXAGONAL LATTICE PARAMETERS OF STOICHIOMETRIC AND NON-STOICHIOMETRIC APATITES BY ARTIFICIAL NEURAL NETWORKS

Koçkan, Ümit

M.Sc., Micro and Nanotechnology

Supervisor: Assist. Prof. Dr. Zafer Evis

Co-supervisor: Prof. Dr. Kadri Aydınol

January 2009, 119 pages

Apatite group of minerals have been widely used in applications like detoxification of wastes, disposal of nuclear wastes and energy applications in addition to biomedical applications like bone repair, substitution, and coatings for metal implants due to its resemblance to the mineral part of the bone and teeth. X-ray diffraction patterns of bone are similar to mineral apatites such as hydroxyapatite and fluorapatite.

Formation and physicochemical properties of apatites can be understood better by computer modeling. For this reason, lattice parameters of possible apatite compounds ($A_{10}(BO_4)_6C_2$), constituted by A: Na^{+}, Ca^{2+}, Ba^{2+}, Cd^{2+}, Pb^{2+}, Sr^{2+}, Mn^{2+}, Zn^{2+}, Eu^{2+}, Nd^{3+}, La^{3+}, Y^{3+}; B: As^{+5}, Cr^{+5}, P^{5+}, V^{5+}, Si^{+4}; and C: F^{-}, Cl^{-}, OH^{-}, Br^{-1} were predicted from their elemental ionic radii by artificial neural networks techniques. Using artificial neural network techniques, prediction models of lattice parameters a, c and hexagonal lattice volumes were developed.

Various learning methods, neuron numbers and activation functions were used to predict lattice parameters of apatites. Best results were obtained with Bayesian regularization method with four neurons in the hidden layer with ‘tansig’ activation function and one neuron in the output layer with ‘purelin’ function. Accuracy of prediction was higher than 98% for the training dataset and average errors for outputs were less than 1% for dataset with multiple substitutions and different ionic charges at each site. Non-stoichiometric apatites were predicted with decreased accuracy. Formulas were derived by using ionic radii of apatites for lattice parameters a and c.

Keywords: Apatite, hydroxyapatite, artificial neural networks, lattice parameter

ÖZ

YAPAY ZEKA AĞI KULLANILARAK STOKİYOMETRİK VE STOKİYOMETRİK OLMAYAN APATİTLERİN ALTIGENEL KAFES PARAMETRELERİNİN TAHMİN EDİLMESİ

Koçkan, Ümit

Yüksek Lisans, Mikro and Nanoteknoloji

Tez Yöneticisi: Yard. Doç. Zafer Evis

Ortak Tez Yöneticisi: Prof. Dr. Kadri Aydınol

Ocak 2009, 119 sayfa

Apatit mineral grubu biyolojik uygulamalara ek olarak atıkların zehirlerinden arındırılması, nükleer atıkların elden çıkarılması ve enerji uygulamalarında da kullanılmaktadır. Kemik ve dişin mineral yapısına benzerliğinden dolayı kemik onarımı, değiştirilmesi ve metal implantların kaplanmasında yaygın olarak kullanılmaktadır. Kemiğin x-ışını difraksiyonu modelleri, mineral apatitlerinkine, örneğin hidroksiapatit ve florapatit, benzerlik göstermektedir. Bu apatitlerin oluşumu ve fizyokimyasal özelliklerinin daha iyi anlaşılabilmesi bilgisayar modellemesi ile sağlanabilir.

Bu yüzden ($A_{10}(BO_4)_6C_2$) genel formüllü muhtemel apatitlerin A: Na^{+}, Ca^{2+}, Ba^{2+}, Cd^{2+}, Pb^{2+}, Sr^{2+}, Mn^{2+}, Zn^{2+}, Eu^{2+}, Nd^{3+}, La^{3+}, Y^{3+}; B: As^{+5}, Cr^{+5}, P^{+5}, V^{+5}, Si^{+4}; ve C: F^{-}, Cl^{-}, OH^{-}, Br^{-} iyonlarının atom yarıçapları kullanılarak a ve c kafes parametrelerini tahmin eden bir yapay sinir ağları programı geliştirilmiştir ve hegzagonal kafes hacimleri hesaplanmıştır.

Apatitlerin kafes parametrelerinin tahmin edilebilmesi için çeşitli öğrenme yöntemleri, nöron sayıları ve aktivasyon fonksiyonları kullanılmıştır. En iyi sonuçlar Bayesian düzenlileştirme yöntemiyle, ara katmanda dört nöron ve 'tansig' fonksiyonu kullanılarak ve çıkış katmanında tek nöron ve 'purelin' fonksiyonu kullanılarak elde edilmiştir. Tahmin doğruluğu, eğitim veri seti için yüzde 98'in üzerinde ve çoklu yer değiştirme ve her bölgede değişik iyonik yüklerle yapılan test veri setinde hata yüzde 1'in altındadır. Stokiyometrik olmayan apatitlerin tahmin sonuçları ise daha düşük doğruluktadır. Kafes parametreleri a ve c, apatitlerin iyon yarıçapları kullanılarak formül haline getirilmiştir.

Anahtar Sözcükler: Apatit, hidroksiapatit, yapay sinir ağları, kafes parametreleri

To my family

ACKNOWLEDGEMENTS

I would like to express my deepest gratitude to my supervisor Assist. Prof. Dr. Zafer Evis and co-supervisor Prof. Dr. Kadri Aydınol for their guidance, advice, criticism, encouragements and insight throughout the research.

I would also like to thank all my friends in the Metallurgical and Materials Engineering Department for their help and friendship. Special thanks go to Taylan Örs for being a supportive friend with a great sense of humor.

Finally, I would like to thank to my family for their continuous support and encouragements during this study.

TABLE OF CONTENTS

LIST OF TABLES

TABLES

LIST OF FIGURES

FIGURES

CHAPTER 1

INTRODUCTION

Apatite is the name of a group of minerals with the chemical formula $A_{10}(BO_4)_6C_2$ where A is a divalent cation, $(BO_4)^{3-}$ is a trivalent anion and C^- is a monovalent anion [1]. Atomic structures of apatites can be substituted by large amounts of different elements, but even small substitutions may have a pronounced effect on mechanical, thermal and optical properties [2]. This material group has been getting increasingly important in the fields of biomaterials, sensors, detoxification of wastes and water and for the immobilization of radioactive wastes [2-4].

Bone is a composite material of 69-80 wt% inorganic phase (carbonated hydroxyapatite), 17-20 wt% collagen and small amounts of water and proteins [5]. Synthetic hydroxyapatite with a chemical formula of $Ca_{10}(PO_4)_6(OH)_2$ is used as a bone and dental implant and as coatings on implants, because of its chemical and crystallographic similarity to the inorganic part of the bone [6]. Residual stresses affect both bulk and interfacial properties in biological apatites and one of the main reasons for these stresses is structural mismatch induced stress including lattice distortion [7]. An effective way to reduce these structural problems is to select the right compositions with appropriate lattice parameters.

Crystal structure of apatites is shown as $P6_3/m$ which corresponds to its space group [1]. The $P6_3/m$ space group has three kinds of vertical symmetry which are a combination of screw axes, rotation axes and mirror planes that form a complex crystal structure [8].

Geological environment provides a wide range of elements for apatites and at high temperatures, almost complete range of substitution exists between end-members of chlorapatite, fluorapatite, and hydroxyapatite. However, ionic substitutions possible in biological apatite is limited to the available elements in the body such as F^-, Cl^-,Na^+, K^+, Fe^{2+}, Zn^{2+}, Sr^{2+}, Mg^{2+}, citrate and carbonate [2].

Formation and physicochemical properties of apatites were investigated experimentally but the crystal structure of apatite is too complex to determine all of their properties by only using experimental techniques [9]. There are numerous computer modelling methods available to gain a deeper knowledge about the structure of these materials and these modelling methods can be classified as "physical modelling methods" and "statistical modelling methods" [10].

Physical modelling methods, used for atomic and crystal structure calculations, are mainly first principles methods [11, 12, 13], molecular dynamics simulations [3,14] and finite element analysis [15]. However, studies like first principles methods are computationally too complex to be used by many researchers. One of the most powerful statistical modelling methods for engineering practices is artificial neural networks (ANN) and it has a wide range of applications where there is large amount of data available but no reliable physical models is present [10].

Neural networks have been used in a wide range of engineering disciplines like chemical, electronics, civil, mechanical, and computer engineering for a long time. All of these disciplines require neural networks mainly for prediction, classification, clustering and forecasting [16]. However, neural networks are relatively new for materials science, but it is being increasingly used [17].

Neural networks analysis has been a highly efficient method for materials science by giving accurate results for a wide range of phenomena which cannot be studied by physical modelling. There are numerous works of neural networks on the subjects of powder metallurgy [18], alloy design [19], ceramics [20], mechanical properties of materials [21-23], composite materials [24-28], surface properties [29,30], and biomaterials [9]. Among these subjects, biomaterials is a promising field for using artifical neural networks, because crystallographic information, mechanical and physicochemical properties databases of biomaterials are reliable enough for modelling their complex behaviour.

It is difficult to prepare single crystals of many apatites with desired properties and compositions for x-ray diffraction applications and lattice parameter determination by other diffraction techniques such as electron and neutron diffraction are not practical. Hence, it is very important to develop a computer model for the prediction of lattice parameters of apatites [9].

In this study, research was focused on predicting the lattice parameters of apatites from ionic radii values by using artificial neural networks. First, several datasets were prepared for proper training of the network. After that, several learning methods, neuron numbers, activation functions were used to achieve the highest training accuracy and test datasets with multiple substitutions and different ionic charges at each site were prepared to check the success of the network with new inputs. Finally, datasets consisting of apatites with unknown lattice parameters were prepared and their hexagonal lattice parameters were predicted.

CHAPTER 2

LITERATURE SURVEY

2.1 Apatites

Apatite is the name of a large mineral group which is found naturally in earth's crust. The name of the mineral comes from a greek word which means 'to deceive' because of its similarity to other valuable minerals such as olivine and peridot [31].

The most important property of these minerals is their versatile ionic substitution capabilities which makes them ideal candidates for a wide range of applications [2].

There are various types of apatites for different applications. For example, HPO_4^{2-} or CO_3^{2-} substituted apatites as well as Ca^{2+} and OH^- deficient apatites are typical biological apatites [32] whereas, arsenate and phosphate type apatites which include calcium and lead are used for environmental purposes [33]. In addition, oxyapatites which have only oxygen ion instead of OH^- ion are used for solid oxide fuel cell (SOFC) applications [34].

Some of the apatite formulas and their application areas are given in Table 2.1. As seen from the examples, apatites are promising materials for a wide range of applications, so it is essential to study their crystal structures.

Table 2.1 Examples of apatite formula and their corresponding applications [2, 33, 35, 36, 37, 38].

Apatite formula	Application
$Ca_{10-x}[(PO_4)_{6-2x}(CO_3)_{2x}]F_2$ $Ca_{10-x}[(PO_4)_{6-2x}(CO_3)_{2x}](OH)_2$ $Ca_{10-x}[(PO_4)_{6-2x}(CO_3)_{2x}]CO_3$ $Ca_{10-x}[(PO_4)_{6-x}(HPO_4)_x](OH)_{2-x}$	Biological apatites
$Pb_5(AsO_4)_3Cl$ $Pb_5(AsO_4)_3OH$ $Ca_5(AsO_4)_3F$	Detoxification of water, wastes and soil
$Ca_8Nd_2(SiO_4)_6O_2$	Disposal of nuclear wastes
$La_{9.33}(SiO_4)_6O_2$ $La_{8.65}Sr_{1.35}(SiO_4)_6O_{2.32}$	Solid oxide fuel cell (SOFC)

2.2 Doping of Various Ions to Apatites

Apatite group has the general formula $A_5(BO_4)_3C$ where A,B,C are the elements given in the Table 2.2. Apatites are able to accept a large amount of elements into their crystal structure. Substitutions by various ions can cause a significant change in the properties of apatites which affect the lattice parameters, morphology, crystallinity, solubility, and thermal properties [39].

Table 2.2 Possible ion substitutions for apatites [2, 33, 40].

Atom Site	Elements
A	K^+, Na^+, Mn^{2+}, Ni^{2+}, Cu^{2+}, Co^{2+}, Sr^{2+}, Ba^{2+}, Pb^{2+}, Cd^{2+} Y^{3+}, La^{3+} Fe^{2+}, Zn^{2+}, Mg^{2+}, Ca^{2+}, Ce^{3+}
B	As, P, Si, V, Cr
C	F, Cl, O, OH, Br

2.2.1 Biological Apatites

Biological apatite crystal structure accepts K^+, Mg^{2-}, Na^+, CO_3^{2-} and F^- ions which are essential for the proper functioning of bone. However, it also accepts ions like Pb^{2+} which are harmful for the body [41]. Typical contents of inorganic components of enamel, dentine and bone are given in Table 2.3.

Biological apatite is incorporated about 4-6 wt% carbonate ions which can substitute either phosphate ions (B-type) or hydroxyl ions (A-type). Carbonate substitution is particularly important, because higher carbonate content causes higher dissolution, reduced crystallinity and smaller grain size [1, 3]. B-type substitution dominates for young people while A-type substitution dominates for older people [42].

Table 2.3 Typical contents of mineral part of enamel, dentine and bone as weight percents [8].

Component	Enamel	Dentine	Bone
Ca	37.6	40.3	36.6
P	18.3	18.6	17.1
CO_2	3.0	4.8	4.8
Na	0.7	0.1	1.0
K	0.05	0.07	0.07
Mg	0.2	1.1	0.6
Sr	0.03	0.04	0.05
Cl	0.4	0.27	0.1
F	0.01	0.07	0.1
Ca/P molar	1.59	1.67	1.65

2.3 Hydroxyapatite

Among the apatites, hydroxyapatite (HAp, $Ca_{10}(PO_4)_6(OH)_2$) is one of the most promising candidates for bone related applications, because its structure and composition are similar to those of the bone mineral. In addition, HAp forms very strong bonds between bone and implant. However, like other ceramics, HAp is brittle. Therefore it cannot be used for load bearing applications in its pure state [43]. Various ions seen in Table 2.2 can be substituted into the structure of HAp to eliminate the undesirable properties.

Geological apatite end-member with hydroxyl group is called hydroxylapatite and it has the same stoichiometric structure of synthetic hydroxyapatite, however these structures are shown to be different from bone apatite by X-ray diffraction studies [2].

Investigation of apatite crystal structure will reveal details that will be useful for biomedical applications and other applications like detoxification of wastes. Crystal structure of HAp is a good starting point for this research which focuses on determination of hexagonal lattice parameters. Crystal structure of HAp can be either hexagonal or monoclinic [44].

2.3.1 Hexagonal Structure

Hexagonal HAp belongs to the space group $P6_3/m$ with lattice parameters a=b=9.4225 Å and c=6.8850 Å and it has two formula units per unit cell [45]. Calcium ions at site one, Ca(I), are coordinated by nine oxygen atoms forming a polyhedron while Ca(II) are coordinated by five oxygen atoms and one hydroxyl group forming an octahedron. Coordination number of Ca(II) ion is seven, one of them being a weak bond to another oxygen [46]. Hydroxyl ions centre in columns paralel to c-axis which pass through the centers of calcium triangles which are on the mirror planes at z=1/4 and z=3/4 [47]. Atomic positions of HAp structure and number of atoms per unit cell are seen in Table 2.4. Atomic structure based on the values in Table 2.4 show the complexity of the structure. Atomic arrangements and symmetries are seen in Figures 2.1 and 2.2.

Table 2.4 Atomic positions of hydroxyapatite structure [49].

Atom	Number of atoms per unit cell	x	y	z
Ca (I)	4	0.333	0.667	0.001
Ca (II)	6	0.246	0.993	0.250
P	6	0.400	0.369	0.250
O(I)	6	0.329	0.484	0.250
O(II)	6	0.589	0.466	0.250
O(III)	12	0.348	0.259	0.073
OH	2	0.000	0.000	0.250

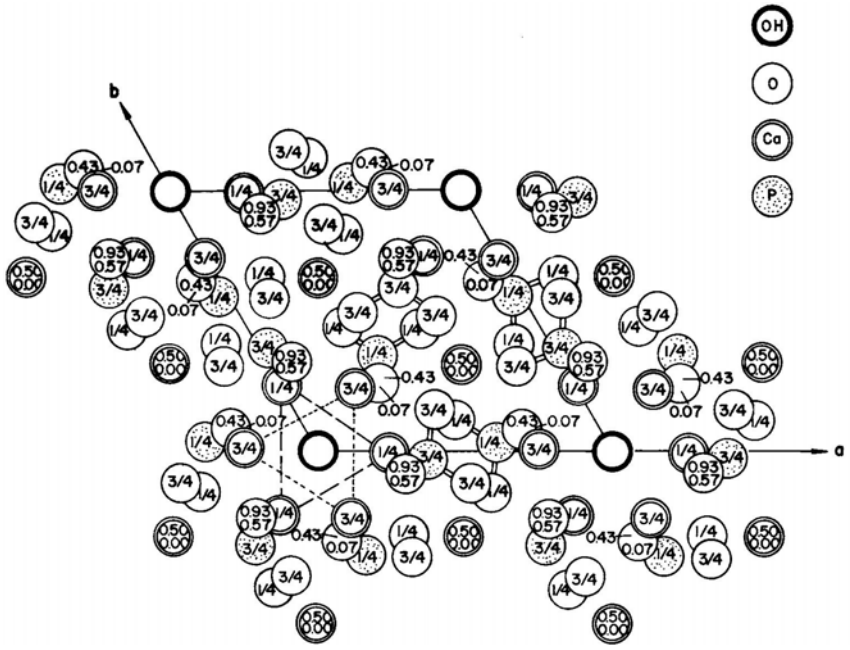

Figure 2.1 Hydroxyapatite structure projected down to the c-axis onto the basal plane [48, 49].

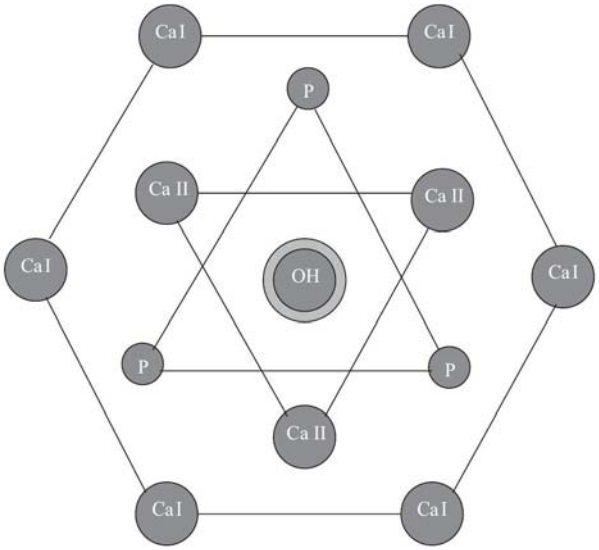

Figure 2.2 Sketch of the hydroxyapatite crystal structure with Ca(I) and Ca(II) sites [50].

In Figure 2.1, hydroxyl ions lie on the corners of the plane at equal intervals along columns perpendicular to the plane and surrounded by six calcium ions out of ten in a hexagonal arrangement [48]. Arrangement of calcium and hydroxyl ions in addition to phosphorous ions are given in greater detail in Figure 2.2. Oxygen ions are not shown in Figure 2.2, because they are located at the outer part of the hexagonal arrangement and showing them would make the figure crowded.

2.3.2 Monoclinic Structure

HAp with monoclinic structure belongs to the space group $P2_1/b$ with lattice parameters a=9.4114 Å, b~2a, c=6.8814 Å. This crystal structure of HAp forms only when it is virtually stoichiometric and when it is annealed at high temperatures [51]. For this reason, hexagonal crystal structure is generally observed for HAp.

The main difference between monoclinic and hexagonal HAp is the ordering of the hydroxyl ions. Monoclinic HAp has the ordering of hydroxyl ions like O-H, O-H, O-H, whereas hexagonal HAp has O-H, H-O, O-H, H-O order in hydroxyl columns [52].

2.4 Physical Modelling Methods

Physical modelling methods are based on theories and laws that describe the physical nature of the problem [10]. Most common physical modelling methods used for engineering and scientific purposes are molecular dynamics method, ab-initio method and finite element method.

The aim of molecular dynamics (MD) simulations is to reveal the structural and microscopic interactions between molecules. MD simulations helps to gain a

knowledge of transport coefficients, time-dependent responses to disturbances, rheological properties and spectra [53]. Basic principle of MD simulations is to break the total interatomic interaction into two-body, three-body and many-body systems. However, this model causes some problems such as innumerable different interatomic interactions that must be parametrized for many atom or molecule systems and qualitative changes of bonding pattern during simulation. To overcome these difficulties “ab initio molecular dynamics” techniques have been researched [54]. MD simulations are currently being used for the investigation of substitutions in HAp and interfacial molecular interactions of apatites [3,14].

Electronic structure problem of very large solid state systems were started being solved with the application of density functional theory in molecular dynamics and it was realized that electron wave function parameters can be treated as dynamic variables and the electron structure problem can be solved by the application of steepest descent method to classical Newtonian equations of motion. This calculation is called ab-initio molecular dynamics and it made new methods available to study on nuclear dynamics and pathway determination of chemical reactions [55]. Ab-initio method is also called first-principles method and it is used for biomaterials research such as investigation of substitutions in apatites and deposition of ions [1,11,12].

Finite Element Method is mainly used to solve equilibrium, eigenvalue and propagation problems. In this method, the actual continuum is represented as an assemblage of smaller parts which are called finite elements. These elements are interconnected at specified joints called nodal points and these nodes are usually on the boundaries of the element. The variation of the field variables like stress, temperature, pressure and velocity inside a finite element can be approximated by functions which are called interpolation models in terms of the values of the field

variables at the nodes. When field equations which are usually in the form of matrix equations are solved, the nodal values of the field variables will be found. These steps cause interpolation models to define the field variable on the whole range of the assemblage [56].

2.5 Statistical Modelling Methods

Physical modelling methods are not capable of modelling some real problems because of the lack of understanding of their mechanisms and complex interactions between a large number of variables. For these problems statistical modelling methods are applied. With statistical modelling methods, reaching accurate results without knowing all the mechanisms or variables is possible [16]. Most common statistical methods that are employed for biomaterials research are Monte Carlo method and artificial neural networks.

2.5.1 Monte Carlo Method

Monte Carlo Method is an efficient tool to understand the time-dependence of a model if this dependence does not follow ordinary physical rules but continues in a stochastic manner. This condition is satisfied by generating samples of random numbers for simulation. Motion of individual atoms, fluids and systems of large amounts of interacting particles can be given as common monte carlo method examples. Main disadvantages of monte carlo method are very long simulation times and statistical errors at large scales [57].

There are various kinds of monte carlo simulations such as Classical MC, Quantum MC and Volumetric MC. These methods can be used in the field of nanoscience to simulate property calculations, phase transitions, self-assembly, charge distributions and similar physical phenomena [58].

2.5.2 Artificial Neural Networks

The principles of artificial neural networks(ANN) are based on biological neuron assembly [18]. ANNs are simpler forms of biological neural networks [19].

Biological neurons are made of three components which are dendrite, cell body and axon. Dendrites input signals to the cell body and axons output the signals processed by the cell body. Output signal of one neuron is passed to another neuron as input signal and further processed until the desired outcome is achieved [16]. Information processing mechanism of a biological neuron is shown in Figure 2.3.

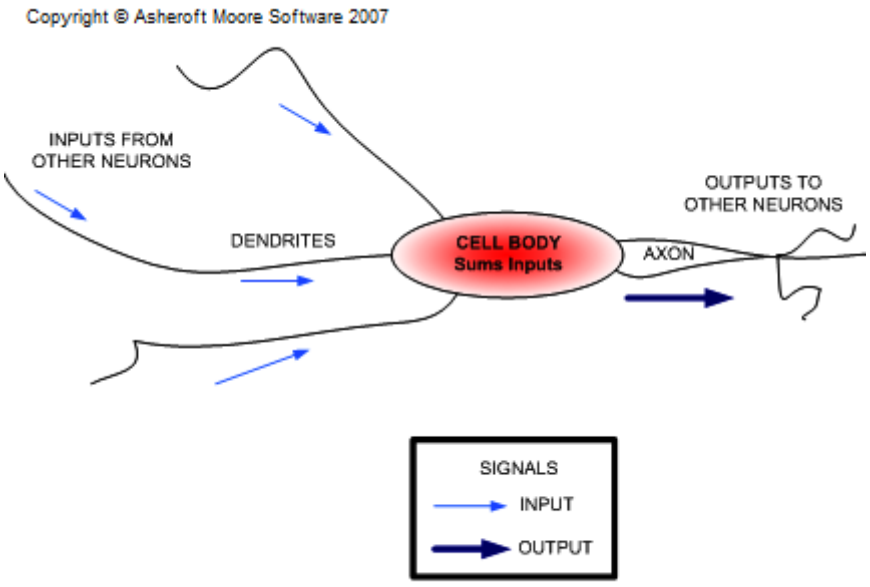

Figure 2.3 Sketch of a simple biological neural network [59].

ANNs operate using the principles of biological neuron assembly. ANNs are composed of an input layer, a hidden layer and an output layer. Input data is weighted and passed to the hidden layer and processed by an activation function. Than, data is passed to the output neuron and output is generated by using a proper training algorithm. There are also weight factors between the neurons of the hidden layer and between hidden layer and output layer. Learning is continued until optimum weights that represent the problem mathematically are found. Various problems can be solved by training the network with changing weight factors [24].

ANNs can be used to solve complex problems which cannot be solved by other mathematical methods, but a large and complex dataset with incomplete and noisy data should be present. In addition, input parameters should have a close relationship with output parameters [24].

Operation of a simple neural network can be seen in Figure 2.4 where X represents input and output data and W represents the corresponding weight factors.

There are several approaches such as gradient descent to minimize the error between target outputs and predicted outputs. Typically 60-80% of data is used for training the network while the rest is used for testing and validation purposes. Validation data is used to calculate the error after each epoch (one cycle of training data), preventing over-training. At the end of the training process, test data is used to check the predicting ability of the network on new data [60].

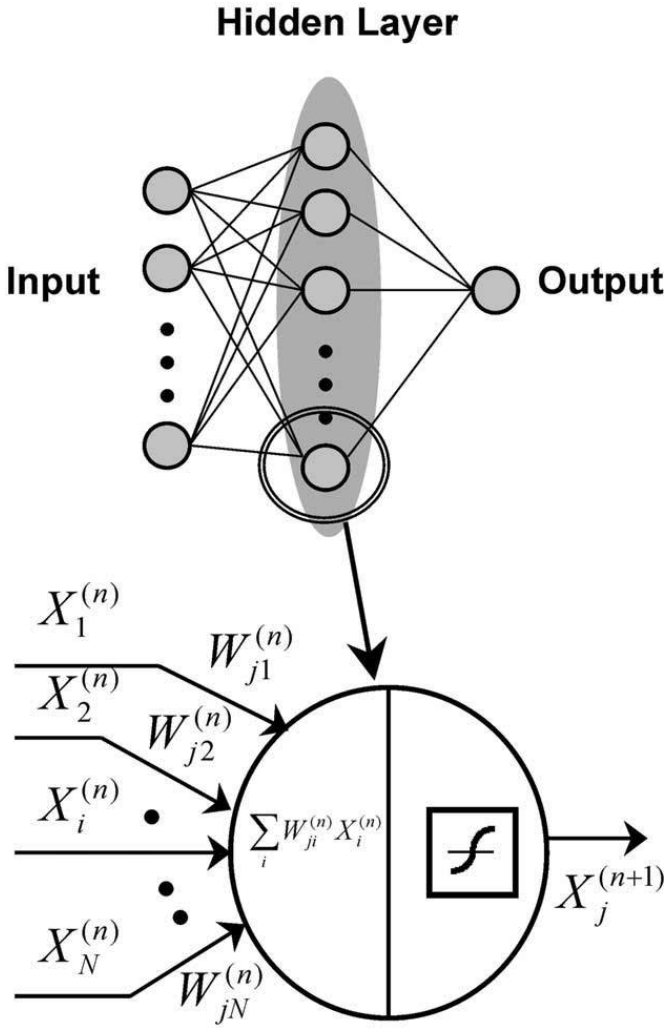

Figure 2.4 Sketch of a simple artificial neural network [24].

The need of more effective and reliable tools for information processing caused ANNs to be developed rapidly. ANNs are used for recognition, forecast, association and control purposes in diverse fields like finance, medicine, physics, military and engineering. In recent years, there is also an increase in the applications of ANNs in the field of materials science. This is mostly because ANNs only need experimental data to determine the relationships between the

quantities [25]. Another advantage of ANNs is the fact that they make no initial assumptions about input-output relationships like standart statistical regression techniques [61].

2.6 Applications of Neural Networks to Materials Science

There are numerous applications of neural networks in materials science. The most widely researched properties are physical and mechanical properties, because large databases give these properties as functions of input parameters such as percent chemicals added, time and temperature of processing. By using this method, many properties like stress, strain, hardness, toughness, fatigue, residual stress [18,19,27,62] and anything else that has a complex non-linear relationship with known inputs can be found without extensive theoretical and experimental studies. Percent chemicals added are input parameters that can be changed easily, so alloy design is particularly efficient with this method [17].

A few brief examples can be given for the the use of neural networks in materials science. One of them use welding speed and tool speed as inputs for the prediction of stir welding parameters of aluminum plates [104] while another one is to use Cu, Sn, Pb, Zn and Ni content as inputs to predict the mechanical properties of the Cu-Sn-Pb-Zn-Ni cast alloys [105]. Also, formulas are presented in these studies for the outputs of mechanical properties which show that neural networks can give brief formulas [107] by combining weights and biases of each processing unit with corresponding activation functions. However, produced formulas do not represent a physical relationship and sometimes they may be very long and confusing. Because of that, exact formulas for outputs are rarely used in the neural networks studies.

Another example study is the determination of interfacial properties between metal film and ceramic substrate with an adhesive layer [106]. This study is a good example of how finite element method can be combined with neural networks. Peel forces were found by using finite element method and used as input with bending curvature radius for the neural networks application to predict interfacial cohesive energy and separation strength for the film-substrate interface.

Neural networks is also a beneficial tool for predicting advanced mechanical properties of composites like dynamic mechanical properties as well as process optimization [24]. This is also true for biomaterials which can be any type of material in addition to composites and optimization of their properties for dynamic conditions is crucial [63]. In the past few decades, materials science based research is concentrating on nanotechnology, so atomic properties are becoming more important for developing reliable products. For example, structure and properties of nanocrystalline apatites are being researched to obtain properties similar to biological apatites [64]. Neural networks are also effective at predicting atomic properties like lattice parameters [9], so this method can also be used to predict physical and mechanical properties of nanomaterials, given that enough experimental data is obtained.

2.7 General Concepts of Neural Networks

Neural networks are complex systems and in order to use them effectively some general concepts like learning types, local minima, learning rate and overfitting must be understood clearly. Brief information related to these concepts is given below.

2.7.1 Learning Types

There are two types of neural networks learning models which are supervised learning and unsupervised learning. They are defined as follows [65]:

Supervised Learning: Inputs and their corresponding outputs are used for training the network by minimizing the error function. The network is trained by applying an input vector, calculating the output and comparing the calculated output with the real output value. The difference of the outputs are used to generate an error value and weights of the network are changed according to this value to minimize the error.

Unsupervised Learning: Neural Networks without known outputs are trained with unsupervised learning. This learning type is used to find an underlying structure of the data which is called **clusters**. This method is not commonly used in engineering applications.

Batch learning and online learning are also important concepts related to learning types and defined as follows [16]:

Batch Learning: Error is minimized by changing weights after the whole training set has been processed.

Online Learning: Weights are readjusted after each training data.

2.7.2 Local Minima and Learning Rate

Backpropagation uses gradient descent to minimize the error, however a network can reach a local minima easily and give false results. In this case the weights

should be re-initialized and training should be repeated to find the global minima [65].

Learning rate depends on the step size which tunes the change of weights after each cycle. Too small step size is extremely time consuming while large step sizes cause unstability of the network. A technique called **annealing** is used to overcome this problem by starting with large learning rates and decreasing it over time [65].

2.7.3 Overfitting

Multilayer feed-forward neural networks can approximate any relationship between inputs and outputs provided that there are sufficient number of neurons in the hidden layers. On the other hand, too many neurons causes over-fitting, meaning that the network memorized the training data without making generalization. To prevent this, the network should contain precisely enough neurons to represent the problem. To achieve this balance, two methods can be used which are **regularization** and **early stopping**. Regularization works by modifying the performance function while early stopping uses a **validation dataset** during training to determine the minimum value of the error [24].

2.8 Types of Neural Networks

There are three main neural networks present in the literature which are recurrent networks, multilayer feed-forward neural networks and local interaction based neural networks [66].

2.8.1. Recurrent Networks

A network is called recurrent network if there exists feedback links within. The signals in these networks can travel in both forward and backward directions and within the layers. The outputs depend on the previous state of the network, so by using this property previous events can be retained by the network for processing [67]. A sketch of this type of network is shown in Figure 2.5.

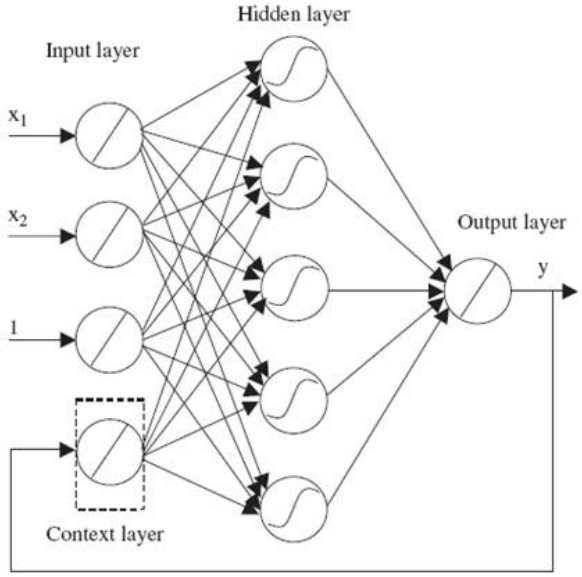

Figure 2.5 Recurrent neural network [69].

The most common example to recurrent networks is **Hopfield Neural Networks**. These networks are fully interconnected networks. Two types of Hopfield Neural Networks are present. In binary version, all neurons are connected to each other except the connection from a neuron to itself and in the continuous case, self connections are also allowed. This network is commonly used for image restoration and segmentation [66].

Learning of Hopfield Neural Networks is described below [66].

1. A pattern is represented by a N-dimensional vector $p = [p_1,p_2,\ldots,p_N]$ from the space $P = \{-1,1\}^N$.
2. $E = \{e^k : 1 \leq k \leq K\}$ is a subset of P representing the reference patterns where $e^k = [e_1^k, e_2^k,\ldots, e_N^k]$ determines the k^{th} example pattern.
3. Hopfield network learns by relating P to E. First weights w_{ij} are determined by using the following conditions;

$$w_{ij} = \begin{cases} \sum_{k=1}^{K} e_i^k e_j^k & if\ i \neq j \\ 0 & if\ i = j \end{cases} \tag{2.1}$$

4. An unknown pattern is presented to the network with the formula;

$$X_o(i) = p_i \quad , \quad 1 \leq i \leq N \tag{2.2}$$

Where X is the value or state of each neuron.

5. Iteration is made according to the propagation rule and activation function until state change stops at each node.

2.8.2 Multilayer Feedforward Neural Networks

Multilayer feed-forward neural networks work by non-linear mapping of inputs to outputs. **Multilayer perceptron (MLP)** and **radial-basis neural network** are the most common examples to these networks [66].

MLP consists of an input layer, one or more hidden layers and an output layer. The input vector is processed in the forward direction passing through each layer

[66]. The network can solve higher-order statistics with the addition of extra hidden layers. This ability of the network is beneficial when the number of inputs is large. The network is called **fully connected** if all neurons in each layer is connected to all neurons in the adjacent forward layer [67]. An example of a MLP network is presented in Figure 2.6.

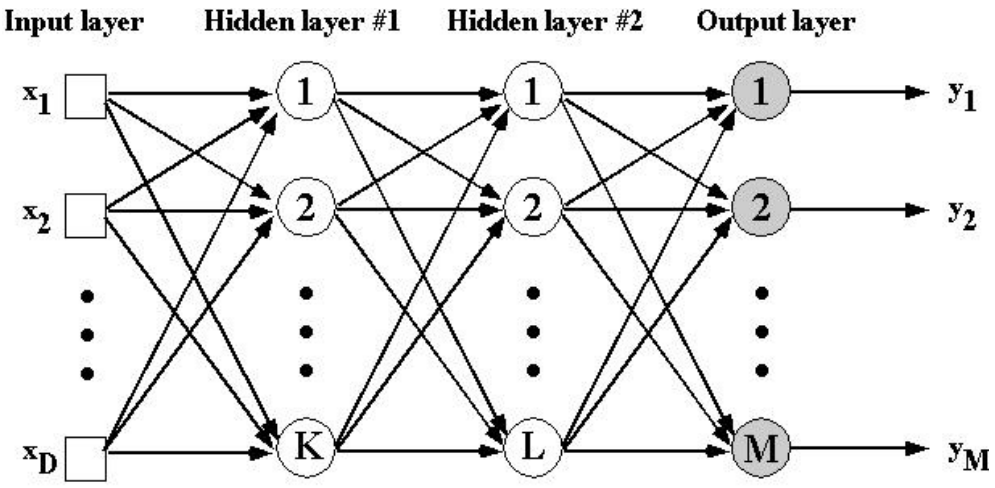

Figure 2.6 MLP Network with D,K,L and M being the number of units in each layer [68].

Radial basis neural networks (RBF) have a hybrid learning mechanism. They are composed of three layers with just one hidden layer. Hidden layer has self-organized learning type while supervised learning is applied to the output layer [66]. These networks can be used for problems where MLP networks work and they are easier to train [70]. Performance of these networks vary with the type of application, but RBF networks perform better when there is a large number of training vectors [71]. This is partly because MLP uses hyperplanes whereas RBF uses class separation for data classification [72]. Organization of a RBF network is shown in Figure 2.7 where u_j is the output of the j^{th} node in the hidden layer and w_{kj} is the weight connecting j^{th} node to k^{th} output.

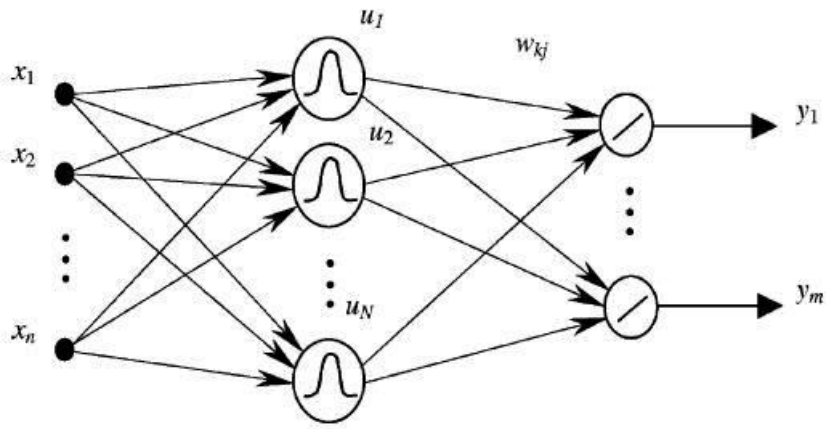

Figure 2.7 Radial basis neural network [102].

2.8.3 Local Interaction Based Neural Networks

Local interaction based neural networks use competitive learning to activate the correct output which is called the **winning neuron**. A common local interaction is found in **Kohonen Maps** [66].

Kohonen networks which are also known as self organizing maps are used when there is no previous data for the current problem. These networks learn without having previously known outputs by using both self-organizing and unsupervised learning. Inputs of the network are connected to every neuron and all neurons are connected to each other. Small random values are given to the weights and all neurons receive an input pattern. Then, the neuron with the largest output and its neighbours are given permission to adapt their weights. The output of each neuron is inhibitory to other ones and excitory to its neighbourhood which is known as lateral inhibition [73].

Most important property of these networks is they reduce the dimensions of data to one or two from higher dimensions for a more meaningful visualization [74].

Some applications of this technique include clustering of text documents [75] and color image segmentation [76]. The mapping procedure is shown in Figure 2.8.

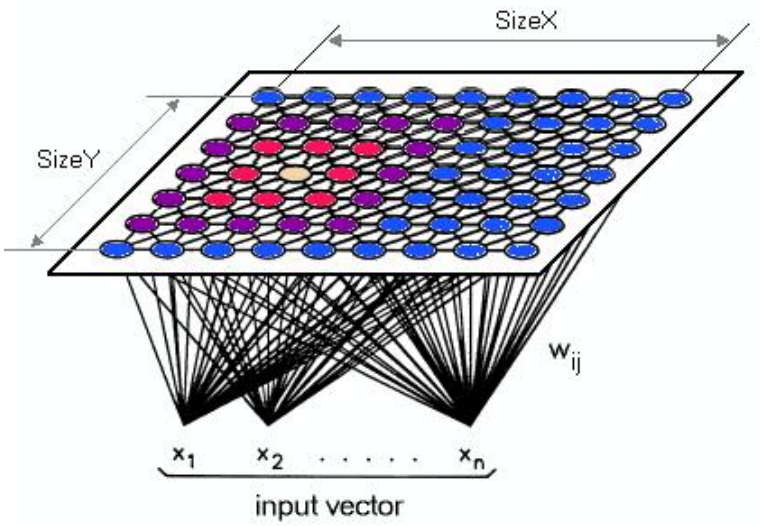

Figure 2.8 Self organizing maps [77].

2.9 Non-linear Activation Functions

Most commonly used non-linear activation functions can be listed as logistic, hyperbolic-tangent, gaussian, gaussian complement and sine functions. These are nonlinear, continuous functions that have upper and lower bounds. Continuity of these functions make them differentiable so delta-rule which is based on the change of the error with respect to the weighted sums, can be used to adjust the weights of the network in backpropagation of errors. In addition, these functions are bounded which means that even if inputs are very large, output will never reach large values [16]. Logistic and hyperbolic-tangent activation functions are shown in Figures 2.8 and 2.9, respectively. The activation functions mentioned above are briefly described [16] as follows:

Sigmoid functions are S-shaped functions. The most widely used one is the logistic function with a lower bound zero and upper bound one. The logistic function has the following mathematical formula:

$$y = L(u) = \frac{1}{1+e^{-u}} \tag{2.3}$$

where u is the input and L(u) is the output for input u.

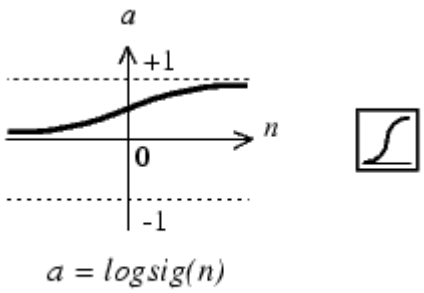

Figure 2.9 Log-sigmoid transfer function [78].

Hyperbolic tangent is also a commonly used function with the formula:

$$\tanh(u) = \frac{1+e^{-u}}{1-e^{-u}} \tag{2.4}$$

It has a lower bound of -1 and upper bound of 1.

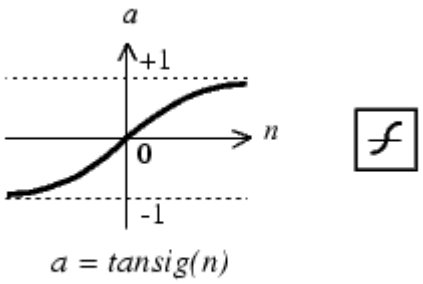

Figure 2.10 Tan-sigmoid transfer function [79].

Tan-sigmoid transfer function trains faster and leads to more accurate weights compared to log-sigmoid function, because it causes hidden units to have a mean value is close to zero which is desired to prevent ill conditioning of the network [80].

There are two types of gaussian functions. **Standard normal curve** has a symmetric bell shape with a range of [0,1]. As seen from the curve in Figure 2.10, it is highly sensitive to values around the center and much less sensitive to values at the tails. This function is more sensitive to the weighted inputs that are close to zero. It has the formula [16]:

$$y = e^{-u^2} \tag{2.5}$$

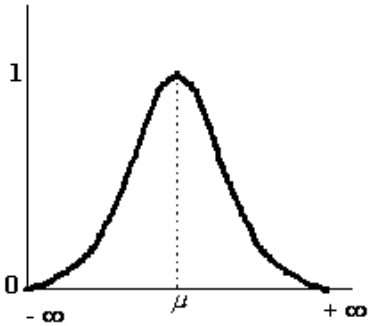

Figure 2.11 Gaussian transfer function [81].

Gaussian complement is the inverted gaussian function so it is more sensitive at the tails. This function is more sensitive to the weighted inputs that are at edges. It has the formula [16]:

$$y = 1 - e^{-u^2} \tag{2.6}$$

There are many activation functions for different purposes and details of these functions are given in reference [82].

CHAPTER 3

METHODS

In this study, neural networks was used to predict the hexagonal lattice parameters of apatites from their average ionic radii. Neural networks was used because there was no ordinary mathematical solution to the problem encountered and large databases were available for training the network. Parameters of the network were defined and datasets were prepared for determining the hexagonal lattice parameters of apatites. To achieve this, datasets were prepared by using raw data collected from Joint Committee on Powder Diffraction Standards (JCPDS) database and literature which are given in Tables 3.1 and 3.2. Raw data includes crystal structure and hexagonal lattice parameter values. In Table 3.1, data taken from JCPDS database has two properties denoted with C and I. C means that the patterns have been indexed and I means that patterns have been calculated from single crystal data [85]. In addition, ionic radii of the elements were taken from a handbook [83].

After data were collected, several network parameters were identified such as type of the network, number of hidden layers, learning methods, and normalization functions. Hexagonal unit cell volumes were calculated according to the following formula [84]:

$$V = 2.589*a^2*c \quad (3.1)$$

where a and c are the lattice parameters of the hexagonal unit cell.

Table 3.1 Raw data collected from JCPDS database.

#	Apatite formula	Card Number	System	Quality	a = b (Å)	c (Å)
1*	$Ca_{4.03}Cd_{0.97}(PO_4)_3(OH)$	75-0425	hexagonal	C	9,391	6,837
2*	$Ca_{3.98}Cd_{1.02}(PO_4)_3F$	75-0446	hexagonal	C	9,379	6,834
3*	$Ca_{3.475}Cd_{1.525}(PO_4)_3F$	75-0622	hexagonal	C	9,36	6,812
4	$Ca_5(PO_4)_3(OH)$	09-0432	hexagonal	I	9,418	6,884
5	$Ca_{10}(PO_4)_6(OH)_2$	72-1243	hexagonal	C	9,432	6,881
6	$Ca_5(PO_4)_3(OH)$	73-0293	hexagonal	C	9,432	8,881
7	$Ca_5(PO_4)_3(OH)$	73-1731	hexagonal	C	9,4	6,93
8*	$Ca_{10}(PO_4)_6(OH)_2$	74-0565	hexagonal	C	9,424	6,879
9	$Ca_{10}(PO_4)_6(OH)_2$	74-0566	hexagonal	C	9,424	6,879
10	$Ca_{2.79}Pb_{2.21}(PO_4)_3(OH)$	79-0685	hexagonal	C	9,609	7,077
11	$Ca_{9.42}Sr_{0.18}H_{0.4}(PO_4)_6(OH)_{1.60}$	82-1429	hexagonal	C	9,392	6,89
12+	$Ca_{2.5}Pb_{7.5}(PO_4)_6(OH)_2$	84-0814	hexagonal	C	9,88	7,417
13	$Ca_5(PO_4)_3(OH)$	84-1998	hexagonal	C	9,4166	6,8745
14	$Ca_5(PO_4)_3(OH)$	86-0740	hexagonal	C	9,352	6,882
15*	$Ca_{8.98}Sr_{1.02}(PO_4)_6(OH)_2$	89-5631	hexagonal	C	9,4352	6,9087
16*	$Ca_{7.684}Sr_{2.316}(PO_4)_6(OH)_2$	89-5632	hexagonal	C	9,4955	6,9718
17*	$Ca_{3.616}Sr_{6.384}(PO_4)_6(OH)_2$	89-5633	hexagonal	C	9,6313	7,1246
18	$Ca_5(PO_4)_3F$	71-0880	hexagonal	C	9,363	6,878
19*	$Ca_5(PO_4)_3F$	71-0881	hexagonal	C	9,367	6,884
20+	$Ca_{9.3}Mn_{0.7}(PO_4)_6F_2$	77-1902	hexagonal	C	9,3323	6,8424
21*	$Ca_{9.37}Sr_{0.63}(PO_4)_6F_2$	79-1459	hexagonal	C	9,3902	6,9011
22	$Ca_5(PO_4)_3Cl$	33-0271	hexagonal	I	9,641	6,771
23+	$Mn_5(PO_4)_3Cl_{0.9}(OH)_{0.1}$	70-0892	hexagonal	C	9,532	6,199
24	$Cd_5(PO_4)_3Cl$	70-1298	hexagonal	C	9,633	6,484
25*	$Ca_5(PO_4)_3F_{0.17}Cl_{0.83}$	70-2066	hexagonal	C	9,6205	6,7761
26*	$Ca_5(PO_4)_3Cl$	73-1728	hexagonal	C	9,52	6,85
27*	$Ca_5(PO_4)_3Br$	74-0672	hexagonal	C	9,761	6,739
28+	$Sr_5(PO_4)_3F_{0.25}Br_{0.75}$	52-0671	hexagonal	I	9,8885	7,2344
29+	$Sr_{4.99}Eu_{0.01}(PO_4)_3Cl_{0.75}Br_{0.25}$	87-0121	hexagonal	C	9,8909	7,1934
30+	$Sr_{4.99}Eu_{0.01}(PO_4)_3Cl_{0.5}Br_{0.5}$	87-0122	hexagonal	C	9,9056	7,195
31+	$Sr_{4.99}Eu_{0.01}(PO_4)_3Cl_{0.25}Br_{0.75}$	87-0123	hexagonal	C	9,9934	7,202
32+	$Sr_{4.99}Eu_{0.01}(PO_4)_3Br$	87-0124	hexagonal	C	9,9636	7,2061
33*	$Sr_5(PO_4)_3Br$	89-5876	hexagonal	C	9,9641	7,207
34	$Sr_5(PO_4)_{2.99}(MnO_4)_{0.01}Cl$	24-1223	hexagonal	I	9,891	7,205
35	$Sr_5(PO_4)_3Cl_{0.75}F_{0.25}$	50-1741	hexagonal	I	9,8697	7,1966
36*	$Sr_5(PO_4)_3Cl$	70-1007	hexagonal	C	9,859	7,206

Table 3.1 (continued)

#	Apatite formula	Card Number	System	Quality	a = b (Å)	c (Å)
37+	$Ca_{2.6}\ Sr_{2.4}\ (PO_4)_3\ Cl$	73-0855	hexagonal	C	9,737	7,022
38+	$Ca_{4.6}\ Sr_{0.4}\ (PO_4)_3\ Cl$	73-0856	hexagonal	C	9,653	6,777
39+	$Ca_{4.9}\ Sr_{0.1}\ (PO_4)_3\ Cl$	73-0857	hexagonal	C	9,643	6,766
40	$Sr_5\ (PO_4)_3\ Cl$	83-0973	hexagonal	C	9,8774	7,189
41+	$Sr_5\ (PO_4)_3\ F_{0.5}\ Br_{0.5}$	52-0670	hexagonal	C	9,7623	7,2699
42+	$Sr_5\ (PO_4)_3\ F_{0.75}\ Br_{0.25}$	52-0669	hexagonal	C	9,7186	7,2853
43+	$Sr_{2.54}\ Ca_{2.45}\ Eu_{0.01}\ (PO_4)_3\ Cl$	85-1952	hexagonal	C	9,754	7,0061
44+	$Sr_{4.99}\ Eu_{0.01}\ (PO_4)_3\ Cl$	87-0120	hexagonal	C	9,878	7,1893
45+	$Sr_{4.99}\ Eu_{0.01}\ (PO_4)_3\ Cl_{0.75}\ F_{0.25}$	89-0046	hexagonal	C	9,8697	7,1966
46+	$Sr_{4.99}\ Eu_{0.01}\ (PO_4)_3\ Cl_{0.5}\ F_{0.5}$	89-0047	hexagonal	C	9,8042	7,2357
47+	$Sr_{4.99}\ Eu_{0.01}\ (PO_4)_3\ F_{0.75}\ Cl_{0.25}$	89-0048	hexagonal	C	9,7357	7,2769
48	$Pb_5\ (PO_4)_3\ Cl$	19-0701	hexagonal	I	9,987	7,33
49	$Na_2\ Nd_2\ Pb_6\ (PO_4)_6\ Cl_2$	36-0577	hexagonal	I	9,78	7,18
50	$Pb_5\ (PO_4)_3\ Cl$	73-1729	hexagonal	C	9,95	7,31
51	$Pb_5\ (PO_4)_3\ Cl$	79-1214	hexagonal	C	9,9981	7,344
52+	$Ca_{2.1}\ Pb_{7.9}\ (PO_4)_6\ Cl_2$	84-0815	hexagonal	C	9,99	7,276
53	$Pb_5\ (PO_4)_3\ Cl$	84-2045	hexagonal	C	9,9764	7,3511
54*	$Pb_5\ (PO_4)_3\ Cl$	89-4339	hexagonal	C	9,993	7,334
55	$Pb_5\ (PO_4)_3\ F$	23-0348	hexagonal	I	9,75	7,3
56+	$K_2\ Pb_6\ Eu_2\ (PO_4)_6\ F_2$	29-1008	hexagonal	I	9,7482	7,2655
57+	$K\ Pb_8\ Nd\ (PO_4)_6\ F_2$	29-1010	hexagonal	I	9,7768	7,2791
58+	$K_2\ Pb_6\ Nd_2\ (PO_4)_6\ F_2$	29-1011	hexagonal	I	9,7604	7,2754
59+	$Pb_6\ Eu_2\ Na_2\ (PO_4)_6\ F_2$	29-1223	hexagonal	I	9,655	7,058
60+	$Pb_8\ Eu\ Na\ (PO_4)_6\ F_2$	29-1224	hexagonal	I	9,73	7,176
61+	$Pb_6\ La_2\ Na_2\ (PO_4)_6\ F_2$	29-1225	hexagonal	I	9,721	7,15
62+	$Pb_4\ La_3\ Na_3\ (PO_4)_6\ F_2$	29-1226	hexagonal	I	9,725	7,158
63+	$Pb_6\ Nd_2\ Na_2\ (PO_4)_6\ F_2$	29-1227	hexagonal	I	9,661	7,067
64+	$Pb_4\ Nd_3\ Na_3\ (PO_4)_6\ F_2$	29-1228	hexagonal	I	9,616	7,029
65+	$Pb_8\ Nd\ Na\ (PO_4)_6\ F_2$	29-1229	hexagonal	I	9,741	7,198
66+	$Pb\ Y_2\ Na_2\ (PO_4)_6\ F_2$	29-1233	hexagonal	I	9,649	7,055
67+	$Pb_8\ Y\ Na\ (PO_4)_6\ F_2$	29-1234	hexagonal	I	9,712	7,17
68+	$Pb_6\ Bi_2\ Na_2\ (PO_4)_6\ F_2$	33-1256	hexagonal	I	9,6956	7,1826
69+	$Pb_{10}\ (PO_4)_6\ F_2$	52-1180	hexagonal	I	9,773	7,315
70+	$Pb_5\ (PO_4)_3\ F$	72-2221	hexagonal	C	9,76	7,3
71+	$Ca_{4.5}\ Pb_{5.5}\ (PO_4)_6\ F_2$	84-0816	hexagonal	C	9,759	7,291
72*	$Pb_5\ (PO_4)_3\ OH$	08-0259	hexagonal	I	9,877	7,427
73*	$Cd_5\ (PO_4)_3\ OH$	70-1207	hexagonal	C	9,335	6,664

Table 3.1 (continued)

#	Apatite formula	Card Number	System	Quality	a = b (Å)	c (Å)
74	$Ca_2\ Pb_3\ (AsO_4)_3\ Cl$	36-0396	hexagonal	I	10,14	7,185
75	$Ca_5\ (AsO_4)_3\ Cl$	38-0383	hexagonal	I	9,81	6,868
76*	$Ca_5\ (AsO_4)_3\ Cl$	87-1917	hexagonal	C	10,076	6,807
77*	$Ca_5\ (VO_4)_3\ (OH)$	70-1996	hexagonal	C	9,818	6,981
78	$Ca_5\ (VO_4)_3\ Cl$	23-0109	hexagonal	I	10,18	6,77
79	$Ca_5\ (CrO_4)_3\ OH$	18-0290	hexagonal	I	9,663	7,028
80*	$Ca_5\ (CrO_4)_3\ OH$	73-1599	hexagonal	C	9,683	7,01
81	$Sr_5\ (CrO_4)_3\ OH$	17-0835	hexagonal	I	10,01	7,435
82	$Ba_5\ (CrO_4)_3\ OH$	17-0834	hexagonal	I	10,42	7,855
83*	$Ba_5\ (CrO_4)_3\ OH$	73-0162	hexagonal	C	10,428	7,89
84	$Ba_5\ (AsO_4)_3\ Cl$	23-0046	hexagonal	I	10,54	7,73
85	$Ba_5\ (AsO_4)_3\ Cl$	31-0132	hexagonal	I	10,169	7,315
86	$Pb_5\ (AsO_4)_3\ OH$	24-0568	hexagonal	I	10,154	7,515
87	$Sr_5\ (AsO_4)_3\ OH$	28-1206	hexagonal	I	10,031	7,39
88	$Ca_5\ Sr_5\ (AsO_4)_6\ (OH)_2$	35-0323	hexagonal	I	9,95	7,3
89	$Sr_5\ (VO_4)_3\ OH$	28-1272	hexagonal	I	10,047	7,411
90	$Sr_5\ (VO_4)_3\ Br$	25-0918	hexagonal	I	10,27	7,33
91*	$Ba_5\ (PO_4)_3\ F$	71-1316	hexagonal	C	10,153	7,733
92+	$Ba_3\ La\ Na\ (PO_4)_3\ F$	71-1317	hexagonal	C	9,9392	7,4419
93+	$Ba_4\ Nd_3\ Na_3\ (PO_4)_6\ F_2$	71-1318	hexagonal	C	9,786	7,281
94	$Pb_5\ (PO_4)_3\ F$	72-2221	hexagonal	C	9,76	7,3
95*	$Sr_6\ Ca_4\ (PO_4)_6\ F_2$	72-2399	hexagonal	C	9,63	7,22
96+	$Ca_2\ Ba_3\ (PO_4)_3\ F$	77-0712	hexagonal	C	9,845	7,359
97*	$Sr_{7.3}\ Ca_{2.7}\ (PO_4)_6\ F_2$	78-1715	hexagonal	C	9,565	7,115
98+	$Ca_5\ (PO_4)_3\ F_{0.39}\ Cl_{0.33}\ (OH)_{0.28}$	80-1095	hexagonal	C	9,4615	6,8491
99	$Na\ Ca_2\ Sr\ Ce\ (PO_4)_3\ F$	89-8930	hexagonal	C	9,51	7,01
100*	$Cd_5\ (PO_4)_3\ Cl$	70-0087	hexagonal	C	9,625	6,504
101*	$Ca_5\ (PO_4)_3\ F_{0.41}\ Cl_{0.59}$	70-2278	hexagonal	C	9,5485	6,8237
102	$Ba_5\ (PO_4)_3\ Cl$	70-2318	hexagonal	C	10,284	7,651
103+	$Co\ Ca_4\ (PO_4)_3\ Cl$	84-1243	hexagonal	C	9,625	6,747
104+	$Sr_{2.54}\ Ba_{2.45}\ Eu_{0.01}\ (PO_4)_3\ Cl$	87-1515	hexagonal	C	10,0265	7,4099
105+	$Ba_{4.99}\ Eu_{0.01}\ (PO_4)_3\ Cl$	87-1516	hexagonal	C	10,2712	7,65
106+	$Sr_{4.99}\ Eu_{0.01}\ (PO_4)_3\ Cl$	89-0045	hexagonal	C	9,878	7,1893
107*	$Pb_5\ (AsO_4)_3\ Cl$	73-1730	hexagonal	C	10,24	7,43
108	$Pb_5\ (AsO_4)_3\ Cl$	76-0203	hexagonal	C	10,25	7,454
109	$Pb_5\ (AsO_4)_3\ Cl$	80-2103	hexagonal	C	10,211	7,4185
110+	$Ca_2\ Pb_3\ (AsO_4)_3\ Cl$	86-2319	hexagonal	C	10,14	7,185

Table 3.1 (continued)

#	Apatite formula	Card Number	System	Quality	a = b (Å)	c (Å)
111	$Pb_5 (VO_4)_3 Cl$	72-0396	hexagonal	C	10,331	7,343
112	$Pb_5 (VO_4)_3 Cl$	73-1732	hexagonal	C	10,31	7,34
113+	$Pb_5 (VO_4)_3 Cl$	84-2044	hexagonal	C	10,3174	7,3378
114	$Sr_{10} (CrO_4)_6 F_2$	80-1751	hexagonal	C	9,956	7,437
115*	$Sr_5(CrO_4)_3Cl$	76-2248	hexagonal	C	10,125	7,3280
116*	$Sr_5(PO_4)_3OH$	70-1511	hexagonal	C	9,745	7,2650
117*	$Ba_5(PO_4)_3OH$	78-1141	hexagonal	C	10,1904	7,7210
118	$Ca_{4.33}Sr_{0.51}La_{0.16}(PO_4)_3(OH)_{0.5} F_{0.5}$	74-2348	hexagonal	C	9,35	6,85

***** Indicates data used for training the network.
+ Indicates data used for testing the network.

Meaning of the quality marks [85]:

I = Indexed pattern , C = Patterns calculated from single crystal data

Table 3.2 Raw data collected from literature.

	Apatite formula	System	a = b (Å)	c (Å)	References
1+	$Ca_{10} (PO_4)_{5.84} (SiO_4)_{0.16} (OH)_{1.84}$	hexagonal	9,4082	6,8828	[86]
2	$Ca_5 (PO_4)_3 F$	hexagonal	9,3718	6,8876	[35]
3+	$Na\ Y_9 (SiO_4)_6 O_2$	hexagonal	9,334	6,759	
4	$Ca_{10} (PO_4)_6 (OH)_2$	hexagonal	9,416	6,888	[87]
5+	$Ca_{10} (VO_4) (PO_4)_5 (OH)_2$	hexagonal	9,467	6,904	
6+	$Ca_{10} (VO_4)_2 (PO_4)_4 (OH)_2$	hexagonal	9,535	6,927	
7+	$Ca_{10} (VO_4)_3 (PO_4)_3 (OH)_2$	hexagonal	9,586	6,943	
8+	$Ca_{10} (VO_4)_4 (PO_4)_2 (OH)_2$	hexagonal	9,649	6,986	
9+	$Ca_{10} (VO_4)_5 (PO_4) (OH)_2$	hexagonal	9,695	6,986	
10	$Ca_{10} (VO4)_6 (OH)_2$	hexagonal	9,717	7,007	
11	$Sr_5 (PO_4)_3 Zn_{0.15} (O)_{0.3} (OH)_{0.7}$	hexagonal	9,7499	7,3066	[88]
12	$Sr_5 (PO_4)_3 Ni_{0.2} (O)_{0.4} (OH)_{0.6}$	hexagonal	9,7722	7,2962	
13	$Sr_5 (PO_4)_3 Co_{0.2} (O)_{0.5} (OH)_{0.4}$	hexagonal	9,7507	7,2988	
14	$Pb_5 (VO_4)_3 Cl$	hexagonal	10,311	7,358	[89]

Table 3.2 (continued)

	Apatite formula	System	a = b (Å)	c (Å)	References
15	$Ca_5 (VO_4)_3 Cl$	hexagonal	10,15	6,7938	[90]
16	$Sr_5 (VO_4)_3 Cl$	hexagonal	10,2073	7,3067	
17	$Ba_5 (VO_4)_3 Cl$	hexagonal	10,5468	7,7437	
18*	$Sr_5 (PO_4)_3 F$	hexagonal	9,7174	7,2851	[91]
19	$Sr_{10} (PO_4)_6 O$	hexagonal	9,767	7,289	
20	$Sr_{10} (PO_4)_6 F_2$	hexagonal	9,719	7,286	
21+	$Sr_9 La (PO_4)_5 (SiO_4) F_2$	hexagonal	9,723	7,282	
22+	$Sr_8 La_2 (PO_4)_4 (SiO_4)_2 F_2$	hexagonal	9,727	7,277	
23+	$Sr_6 La_4 (PO_4)_2 (SiO_4)_4 F_2$	hexagonal	9,732	7,27	
24+	$Sr_4 La_6 (SiO_4)_6 F_2$	hexagonal	9,737	7,265	
25+	$Sr_{10} (PO_4)_6 O$	hexagonal	9,753	7,276	
26+	$Sr_9 La (PO_4)_5 (SiO_4) O$	hexagonal	9,756	7,272	
27+	$Sr_8 La_2 (PO_4)_4 (SiO_4)_2 O$	hexagonal	9,761	7,267	
28+	$Sr_6 La_4 (PO_4)_2 (SiO_4)_4 O$	hexagonal	9,768	7,258	
29+	$Sr_4 La_6 (SiO_4)_6 O$	hexagonal	9,771	7,255	
30	$Ca_{10} (PO_4)_6 F_2$	hexagonal	9,363	6,878	[92]
31	$Sr_{10} (PO_4)_6 F_2$	hexagonal	9,712	7,285	
32	$Pb_{10} (PO_4)_6 F_2$	hexagonal	9,76	7,3	
33	$Ba_{10} (PO_4)_6 F_2$	hexagonal	10,153	7,733	
34	$Ca_{10} (PO_4)_6 Cl_2$	hexagonal	9,59	6,766	
35	$Sr_{10} (PO_4)_6 Cl_2$	hexagonal	9,877	7,189	
36	$Pb_{10} (PO_4)_6 Cl_2$	hexagonal	9,998	7,344	
37*	$Ba_{10} (PO_4)_6 Cl_2$	hexagonal	10,284	7,651	
38	$Ca_{10} (PO_4)_6 Br_2$	hexagonal	9,761	6,739	
39	$Sr_{10} (PO_4)_6 Br_2$	hexagonal	9,964	7,207	
40+	$Pb_{10} (PO_4)_6 Br_2$	hexagonal	10,062	7,359	
41	$Ca_{10} (PO_4)_6 (OH)_2$	hexagonal	9,41339	6,88181	[93]
42+	$Ca_{10} (PO_4)_{5.83} (SiO_4)_{0.17} (OH)_{1.83}$	hexagonal	9,41763	6,88545	
43+	$Ca_{10} (PO_4)_{5.65} (SiO_4)_{0.35} (OH)_{1.65}$	hexagonal	9,41869	6,88683	
44+	$Ca_{10} (PO_4)_{5.48} (SiO_4)_{0.52} (OH)_{1.48}$	hexagonal	9,42158	6,89155	
45+	$Ca_{10} (PO_4)_{5.30} (SiO_4)_{0.70} (OH)_{1.30}$	hexagonal	9,42332	6,89703	

* Indicates data used for training the network.
+ Indicates data used for testing the network.

3.1 Lattice Parameter Calculations of Different Apatite Forms

Apatites can be in different forms like single crystal, powder or sintered bulk form. Different forms of this material group can cause a deviation in x-ray diffraction peaks, so lattice parameters are also changed by some amount.

For example, x-ray diffraction peak positions for dried and sintered hydroxyapatites are seen in Appendix A. Peaks of sintered HAp are sharp and narrow indicating that grain sizes are larger than 100nm while dried HAp shows only one very wide peak because of very small particles [97]. This difference causes slight shifts in XRD peak positions result in changes in lattice parameters of apatites.

In this work, lattice parameters of various apatites were predicted, but it was essential to present how lattice parameters of powder or sintered bulk forms of apatites were calculated. One method for this calculation is to use successive approximations. For this calculation, $\frac{a}{c}$ ratio and (hkl) values should be obtained from a reference such as JCPDS cards and (hkl) values should be matched with the 2θ values of the experimental data. Then, lattice parameters can be calculated using the following formula [101]:

$$a_o = \frac{\lambda}{2\sin\theta}\sqrt{\frac{4}{3}(h^2 + hk + k^2) + (\frac{a}{c})^2 l^2} \tag{3.2}$$

$$c_o = \frac{\lambda}{2\sin\theta}\sqrt{\frac{4}{3}(\frac{c}{a})^2 (h^2 + hk + k^2) + l^2} \tag{3.3}$$

where;

a_o, c_o = calculated lattice parameters,

λ = x-ray wavelength,

θ = Bragg angle for corresponding plane (hkl),

$\frac{a}{c}$ = last calculated ratio in successive approximation.

If $\frac{4}{3}(h^2 + hk + k^2)$ was larger than $(\frac{a}{c})^2 l^2$, a_o was calculated. If the opposite was true, c_o was calculated. Then averages of each parameter were taken and used for next calculation. Iteration procedure was repeated until the lattice parameter values remained constant. This approach minimized the errors caused by unknown axial ratio. An example of calculation of hydroxyapatite lattice parameters can be found in Appendix B.

3.2 Type of the Network and Parameters

Firstly, MLP model with supervised learning and batch training was used because of its high non-linear regression performance. A single hidden layer with different numbers of processing units and various learning methods were experimented to achieve the highest network performance. Sigmoid transfer functions for the hidden layer and linear function for the output layer were used.

3.3 Experimented Learning Methods

Some neural networks algorithms are more frequently used and the reason for this incident is their efficient error determination for a large number of problems encountered. Some of these algorithms use first-order derivatives while others use second-order derivatives of error functions to determine the delta value which is used to adjust the weights of the network. By this way, it becomes possible to solve problems of different complexities [16]. In this work, backpropagation,

steepest-descent, gauss-newton and levenberg-marquardt learning methods were used as well as generalization methods such as early-stopping and generalization.

3.3.1 Backpropagation Algorithm

Backpropagation algorithm is one of the most commonly used algorithms for neural networks. Mean squared error (MSE) and gradient descent are the methods used by backpropagation algorithm for feedforward networks. This algorithm is useful for finding the network's weight gradient $\nabla\eta(w)$ easily [94]. Weights are updated to new weights W^* as shown in Equation 3.4.

$$W^* = W - p\nabla\eta(w) \tag{3.4}$$

where **η** is the MSE and **p** is the step size and a positive value. The following formulas were used to perform gradient descent with a differentiable error function:

$$S_i = \sum_{j=0}^{i-1} W_{i,j} u_j \tag{3.5}$$

$$u_i = f(S_i) = \frac{1}{1+e^{-s_i}} \tag{3.6}$$

where;
S_i = Weighted sums
u_i = Activations for each unit

It is also important to compute the following value while using this algorithm.

$$\delta_i = -\frac{\partial \eta}{\partial S_i} \tag{3.7}$$

Backpropagation algorithm can be given briefly as follows:

1. A small step size is chosen and small initial weights are given to all units.
2. Next training example E with a correct output C is taken.
3. An input to output pass is made to calculate S_i and u_i for each cell.
4. An output to input pass is made to calculate:

$$f'(S_i) = u_i(1-u_i) \tag{3.8}$$

$$\delta_i = \begin{cases} (C_i - u_i) f'(S_i) & \textit{if } u_i \textit{ is an output unit} \\ (\sum_{m:m>i} w_{m,i}\delta_m) f'(S_i) & \textit{for other units} \end{cases} \tag{3.9}$$

5. Update weights with the formula $w_{i,j}^{*} = w_{i,j} + p\delta_i u_j$ (3.10)

Steps 2-5 were repeated until MSE reached a very small value [94].

3.3.2 Steepest Descent Method

This method also uses error reduction along the negative gradient of the error surface like the backpropagation method. However, the learning rate (ε) is changed during training while it is fixed for backpropagation method. Faster convergence of the network is possible by changing the rate. Learning rate is given an initial value and doubled in each step. MSE is calculated in each step and if the value does not decrease, learning rate is halved until MSE decreases. When the learning rate is determined, final weights are adjusted and ε is doubled to start a new step. This process is repeated until ε falls below a certain limit (ε_{min}) or decrease between consecutive errors is smaller than a certain level (E_{min}). The formula related to these limits are as follows:

$$\frac{E(W_m) - E(W_{m+1})}{E(W_m)} \leq E_{\min} \qquad \varepsilon < \varepsilon_{\min} \tag{3.11}$$

$E(W_m)$ and $E(W_{m+1})$ are the errors for consecutive epochs [16].

3.3.3 Gauss-Newton Method

The second derivative of the error function with respect to a weight is used for this method [16].

$$d^s = \frac{\partial^2 E}{\partial w^2} \tag{3.12}$$

where d^s is the second derivative.

Weight change for the epoch m is denoted by;

$$\Delta w_m = -\varepsilon \frac{d_m}{d_m^s} \tag{3.13}$$

After each epoch, ε is reset to 1 and accepted if there is a decrease in MSE. If there is no decrease, ε is halved until a decrease is achieved. The learning ends according to the formula;

$$\frac{E(w_m) - E(w_{m+1})}{E(w_m)} \leq E_{\min} \qquad \varepsilon < \varepsilon_{\min} \tag{3.14}$$

Details of weight change are as follows [16]:

$$w_m = w_{m-1} - \varepsilon R d_m \tag{3.15}$$

where;

R = inverse of the second derivative of error.

d_m = sum of the error gradient for each weight across all patterns.

The whole set of second derivatives for all weights in a matrix form is represented by **Hessian matrix** denoted by **H**.

$$R = \frac{1}{H} \tag{3.16}$$

The MSE (E) is:

$$E = \frac{1}{N}\sum_{i=1}^{N}(t_i - z_i(x_i, w_i))^2 \tag{3.17}$$

where;

t_i = target output; z_i = network output; x_i = inputs; w_i = weights; N = number of input patterns.

The second derivative of the error gives;

$$H = \frac{\partial^2 E}{\partial w_i \partial w_j} = \frac{2}{N}\sum_{i=1}^{N}\left\{(t_i - z_i)(\frac{-\partial^2 z_i}{\partial w_i \partial w_j}) + (\frac{-\partial z_i}{\partial w_i})(\frac{-\partial z_i}{\partial w_j})\right\} \tag{3.18}$$

The first part of the equation is not taken into consideration because of computational instability when H is inverted to find R, so the equation becomes;

$$H = \frac{\partial^2 E}{\partial w_i \partial w_j} \approx \frac{2}{N}\sum_{i=1}^{N}\left\{(\frac{-\partial z_i}{\partial w_i})(\frac{-\partial z_i}{\partial w_j})\right\} \tag{3.19}$$

3.3.4 Levenberg-Marquardt Method

This method is essential for complex problems that are hard to solve with other methods. Learning rate ε is replaced with the term $\mathbf{e}^{\lambda}$ where e is the natural logarithm and λ is a random number. This term is added to the second derivative. This term results in a smaller error and increased stability for the solution. Weights are adjusted according to the formula;

$$\Delta w_m = -\frac{d_m}{d_m^s + e^{\lambda}} \tag{3.20}$$

It is known that the value of **R** for a network with single weight is equal to;

$$R = \frac{1}{d_m^s + e^{\lambda}} \tag{3.21}$$

and Hessian matrix is changed to;

$$H' = H + e^{\lambda} I \tag{3.22}$$

where;
I = Identity matrix so,

$$\Delta w_m = -\frac{d_m}{(H_m + e^{\lambda} I)} \tag{3.23}$$

λ is given an initial value and incrementally decreased in each step. If MSE does not decrease, λ is increased until another decrease in the error takes place. Learning is ended according to the following criteria;

$$\lambda > 10\Delta\lambda + \max[H] \tag{3.24}$$

$$\frac{E(w_m) - E(w_{m+1})}{E(w_m)} \leq E_{\min} \tag{3.25}$$

where max[H] is the max. eigenvalue of the Hessian matrix [16].

3.3.5 Details of Generalization

Performance function of most of the networks is MSE, but generalization can be improved by modifying the performance function with mean square of weights and biases. By using this new performance function, weights and biases are minimized, so network performance increases. Modified performance function is shown in the following formula [71]:

$$\text{msereg} = \gamma\ \text{mse} + (1- \gamma)\text{msw} \tag{3.26}$$

where, γ = Performance ratio

$$msw = \frac{1}{n}\sum_{j=1}^{n} w_j^2 \tag{3.27}$$

Performance ratio is hard to optimize so it is crucial to automatically find the best performance ratio. To do this, bayesian regularization method can be used. Most important property of this method is that it is possible to reveal how many network parameters (weights and biases) are being effectively used. This algorithm is especially useful when inputs and targets fall in the range of [-1,1] or scaled to fit this range [71].

CHAPTER 4

RESULTS AND DISCUSSION

4.1 Dataset Preparation

In this research, neural network method was used for the prediction of lattice parameters of apatites taken from the JCPDS database and the literature. There were also applications of neural networks for the prediction of lattice parameters of other materials [9,108] and one of them was a study on the same subject. Previous work on this subject [9] combined pattern recognition methods with neural networks to determine lattice parameters of apatites. Pattern recognition method was used to validate the reliability of the predictions. Our study concentrated only on neural networks, because reliability of predictions were validated by large test datasets involving both stoichiometric and non-stoichiometric apatites which showed the maximum prediction capabilities of the network and was not influenced by boundary condition errors caused by pattern recognition method. In addition, learning methods were investigated throughly to obtain the most precise results. After the neural network was created, lattice parameters of apatites with a maximum of triple substitutions at each site and non-stoichiometric apatites were compared with the results taken from the neural network and the amount of deviation from real values were observed.

Data shown in Tables 3.1 and 3.2 were reorganized by removing duplicate and unreliable data to prevent inconsistencies in network performance. Previous works showed that lattice parameters of apatites depend strongly on the average ionic radii of A, B and C sites [9]. Therefore, to calculate average ionic radii of each site, weights were given to A, B and C sites, all sites accepting up to triple

substitutions. These apatites, their ionic radii and weights of ions at each site are given in Table 4.1. In this table, A1, A2, A3, B1, B2, B3, C1, C2, C3 represent ionic radii of each element in the same order given in each formula while wA1, wA2, wA3, wB1, wB2, wB3, wC1, wC2, wC3 represent the weights of each element which were simply the number of moles of ions per apatite formula and these weights were also in the same order of each element in the apatite formula.

By using the values in Table 4.1, average ionic radii of each site were calculated by multiplying each ionic radii with its weight, adding these values and dividing the total value by the total weight of A, B and C sites, separately. Results are given in Table 4.2 with their corresponding lattice parameters a and c. Average ionic radii of A, B and C sites and lattice parameters in Table 4.2 were used for the neural networks application as inputs and outputs, respectively. Example calculation of average ionic radii for the first data of Table 4.1 is given as follows:

$$\text{Average radii A} = \frac{(wA1 * A1) + (wA2 * A2) + (wA3 * A3)}{(wA1 + wA2 + wA3)} \tag{4.1}$$

$$\text{Average radii A} = \frac{(4.03 * 1) + (0.97 * 0.95) + (0 * 0)}{(4.03 + 0.97 + 0)} = 0.9903 \text{ Å}$$

$$\text{Average radii B} = \frac{(wB1 * B1) + (wB2 * B2) + (wB3 * B3)}{(wB1 + wB2 + wB3)} \tag{4.2}$$

$$\text{Average radii B} = \frac{(3 * 0.38) + (0 * 0) + (0 * 0)}{(3 + 0 + 0)} = 0.38 \text{ Å}$$

$$\text{Average radii C} = \frac{(wC1 * C1) + (wC2 * C2) + (wC3 * C3)}{(wC1 + wC2 + wC3)} \tag{4.3}$$

$$\text{Average radii C} = \frac{(1 * 1.37) + (0 * 0) + (0 * 0)}{(1 + 0 + 0)} = 1.37 \text{ Å}$$

Datasets prepared by using Table 4.2 showed that the number of data should be kept as small as possible to prevent large deviations of results and overfitting. After some trial and error, a refined dataset was prepared for neural networks application with the addition of two extra data [95,96] as seen in Table 4.3.

Table 4.1 Ionic radii and weights of ions of apatites.

#		Ionic Radii									Weights of Ions								
	Apatite formula	**A1**	**A2**	**A3**	**B1**	**B2**	**B3**	**C1**	**C2**	**C3**	**wA1**	**wA2**	**wA3**	**wB1**	**wB2**	**wB3**	**wC1**	**wC2**	**wC3**
1	$Ca_{4.03}\ Cd_{0.97}\ (PO_4)_3\ (OH)$	1	0,95	0	0,38	0	0	1,37	0	0	4,03	0,97	0	3	0	0	1	0	0
2	$Ca_{3.98}\ Cd_{1.02}\ (PO_4)_3\ F$	1	0,95	0	0,38	0	0	1,33	0	0	3,98	1,02	0	3	0	0	1	0	0
3	$Ca_{3.475}\ Cd_{1.525}\ (PO_4)_3\ F$	1	0,95	0	0,38	0	0	1,33	0	0	3,475	1,525	0	3	0	0	1	0	0
4	$Ca_{10}\ (PO_4)_6\ (OH)_2$	1	0	0	0,38	0	0	1,37	0	0	10	0	0	6	0	0	2	0	0
5	$Ca_{2.5}\ Pb_{7.5}\ (PO_4)_6\ (OH)_2$	1	1,19	0	0,38	0	0	1,37	0	0	2,5	7,5	0	6	0	0	2	0	0
6	$Ca_{8.98}\ Sr_{1.02}\ (PO_4)_6\ (OH)_2$	1	1,18	0	0,38	0	0	1,37	0	0	8,98	1,02	0	6	0	0	2	0	0
7	$Ca_{7.684}\ Sr_{2.316}\ (PO_4)_6\ (OH)_2$	1	1,18	0	0,38	0	0	1,37	0	0	7,684	2,316	0	6	0	0	2	0	0
8	$Ca_{3.616}\ Sr_{6.384}\ (PO_4)_6\ (OH)_2$	1	1,18	0	0,38	0	0	1,37	0	0	3,616	6,384	0	6	0	0	2	0	0
9	$Ca_5\ (PO_4)_3\ F$	1	0	0	0,38	0	0	1,33	0	0	5	0	0	3	0	0	1	0	0
10	$Ca_{9.3}\ Mn_{0.7}\ (PO_4)_6\ F_2$	1	0,83	0	0,38	0	0	1,33	0	0	9,3	0,7	0	6	0	0	2	0	0
11	$Ca_{9.37}\ Sr_{0.63}\ (PO_4)_6\ F_2$	1	1,18	0	0,38	0	0	1,33	0	0	9,37	0,63	0	6	0	0	2	0	0
12	$Mn_5\ (PO_4)_3\ Cl_{0.9}\ (OH)_{0.1}$	0,83	0	0	0,38	0	0	1,81	1,37	0	5	0	0	3	0	0	0,9	0,1	0
13	$Cd_5\ (PO_4)_3\ Cl$	0,95	0	0	0,38	0	0	1,81	0	0	5	0	0	3	0	0	1	0	0
14	$Ca_5\ (PO_4)_3\ F_{0.17}\ Cl_{0.83}$	1	0	0	0,38	0	0	1,33	1,81	0	5	0	0	3	0	0	0,17	0,83	0
15	$Ca_5\ (PO_4)_3\ Cl$	1	0	0	0,38	0	0	1,81	0	0	5	0	0	3	0	0	1	0	0
16	$Ca_5\ (PO_4)_3\ Br$	1	0	0	0,38	0	0	1,96	0	0	5	0	0	3	0	0	1	0	0
17	$Sr_5\ (PO_4)_3\ F_{0.75}\ Br_{0.25}$	1,18	0	0	0,38	0	0	1,33	1,96	0	5	0	0	3	0	0	0,75	0,25	0
18	$Sr_5\ (PO_4)_3\ F_{0.5}\ Br_{0.5}$	1,18	0	0	0,38	0	0	1,33	1,96	0	5	0	0	3	0	0	0,5	0,5	0
19	$Sr_5\ (PO_4)_3\ F_{0.25}\ Br_{0.75}$	1,18	0	0	0,38	0	0	1,33	1,96	0	5	0	0	3	0	0	0,25	0,75	0
20	$Sr_{4.99}\ Eu_{0.01}\ (PO_4)_3\ Cl_{0.75}\ Br_{0.25}$	1,18	1,17	0	0,38	0	0	1,81	1,96	0	4,99	0,01	0	3	0	0	0,75	0,25	0
21	$Sr_{4.99}\ Eu_{0.01}\ (PO_4)_3\ Cl_{0.5}\ Br_{0.5}$	1,18	1,17	0	0,38	0	0	1,81	1,96	0	4,99	0,01	0	3	0	0	0,5	0,5	0
22	$Sr_{4.99}\ Eu_{0.01}\ (PO_4)_3\ Cl_{0.25}\ Br_{0.75}$	1,18	1,17	0	0,38	0	0	1,81	1,96	0	4,99	0,01	0	3	0	0	0,25	0,75	0
23	$Sr_{4.99}\ Eu_{0.01}\ (PO_4)_3\ Br$	1,18	1,17	0	0,38	0	0	1,96	0	0	4,99	0,01	0	3	0	0	1	0	0

Table 4.1 (continued)

#		Ionic Radii									Weights of Ions								
	Apatite formula	**A1**	**A2**	**A3**	**B1**	**B2**	**B3**	**C1**	**C2**	**C3**	**wA1**	**wA2**	**wA3**	**wB1**	**wB2**	**wB3**	**wC1**	**wC2**	**wC3**
24	$Sr_5 (PO_4)_3 Br$	1,18	0	0	0,38	0	0	1,96	0	0	5	0	0	3	0	0	1	0	0
25	$Sr_5 (PO_4)_3 Cl$	1,18	0	0	0,38	0	0	1,81	0	0	5	0	0	3	0	0	1	0	0
26	$Ca_{2.6} Sr_{2.4} (PO_4)_3 Cl$	1	1,18	0	0,38	0	0	1,81	0	0	2,6	2,4	0	3	0	0	1	0	0
27	$Ca_{4.6} Sr_{0.4} (PO_4)_3 Cl$	1	1,18	0	0,38	0	0	1,81	0	0	4,6	0,4	0	3	0	0	1	0	0
28	$Ca_{4.9} Sr_{0.1} (PO_4)_3 Cl$	1	1,18	0	0,38	0	0	1,81	0	0	4,9	0,1	0	3	0	0	1	0	0
29	$Sr_{4.99} Eu_{0.01} (PO_4)_3 Cl$	1,18	1,17	0	0,38	0	0	1,81	0	0	4,99	0,01	0	3	0	0	1	0	0
30	$Sr_{2.54} Ca_{2.45} Eu_{0.01} (PO_4)_3 Cl$	1,18	1	1,17	0,38	0	0	1,81	0	0	2,54	2,45	0,01	3	0	0	1	0	0
31	$Sr_{4.99} Eu_{0.01} (PO_4)_3 Cl_{0.75} F_{0.25}$	1,18	1,17	0	0,38	0	0	1,81	1,33	0	4,99	0,01	0	3	0	0	0,75	0,25	0
32	$Sr_{4.99} Eu_{0.01} (PO_4)_3 Cl_{0.5} F_{0.5}$	1,18	1,17	0	0,38	0	0	1,81	1,33	0	4,99	0,01	0	3	0	0	0,5	0,5	0
33	$Sr_{4.99} Eu_{0.01} (PO_4)_3 Cl_{0.25} F_{0.75}$	1,18	1,17	0	0,38	0	0	1,81	1,33	0	4,99	0,01	0	3	0	0	0,25	0,75	0
34	$Ca_{2.1} Pb_{7.9} (PO_4)_6 Cl_2$	1	1,19	0	0,38	0	0	1,81	0	0	2,1	7,9	0	6	0	0	2	0	0
35	$Pb_5 (PO_4)_3 Cl$	1,19	0	0	0,38	0	0	1,81	0	0	5	0	0	3	0	0	1	0	0
36	$K_2 Pb_6 Eu_2 (PO_4)_6 F_2$	1,38	1,19	0,95	0,38	0	0	1,33	0	0	2	6	2	6	0	0	2	0	0
37	$K Pb_8 Nd (PO_4)_6 F_2$	1,38	1,19	0,98	0,38	0	0	1,33	0	0	1	8	1	6	0	0	2	0	0
38	$K_2 Pb_6 Nd_2 (PO_4)_6 F_2$	1,38	1,19	0,98	0,38	0	0	1,33	0	0	2	6	2	6	0	0	2	0	0
39	$Pb_6 Eu_2 Na_2 (PO_4)_6 F_2$	1,19	0,95	1,02	0,38	0	0	1,33	0	0	6	2	2	6	0	0	2	0	0
40	$Pb_8 Eu Na (PO_4)_6 F_2$	1,19	0,95	1,02	0,38	0	0	1,33	0	0	8	1	1	6	0	0	2	0	0
41	$Pb_6 La_2 Na_2 (PO_4)_6 F_2$	1,19	1,03	1,02	0,38	0	0	1,33	0	0	6	2	2	6	0	0	2	0	0
42	$Pb_4 La_3 Na_3 (PO_4)_6 F_2$	1,19	1,03	1,02	0,38	0	0	1,33	0	0	4	3	3	6	0	0	2	0	0
43	$Pb_6 Nd_2 Na_2 (PO_4)_6 F_2$	1,19	0,98	1,02	0,38	0	0	1,33	0	0	6	2	2	6	0	0	2	0	0
44	$Pb_4 Nd_3 Na_3 (PO_4)_6 F_2$	1,19	0,98	1,02	0,38	0	0	1,33	0	0	4	3	3	6	0	0	2	0	0
45	$Pb_8 Nd Na (PO_4)_6 F_2$	1,19	0,98	1,02	0,38	0	0	1,33	0	0	8	1	1	6	0	0	2	0	0
46	$Pb Y_2 Na_2 (PO_4)_6 F_2$	1,19	0,9	1,02	0,38	0	0	1,33	0	0	1	2	2	6	0	0	2	0	0

Table 4.1 (continued)

#		Ionic Radii									Weights of Ions								
	Apatite formula	**A1**	**A2**	**A3**	**B1**	**B2**	**B3**	**C1**	**C2**	**C3**	**wA1**	**wA2**	**wA3**	**wB1**	**wB2**	**wB3**	**wC1**	**wC2**	**wC3**
47	Pb_8 Y Na $(PO_4)_6$ F_2	1,19	0,9	1,02	0,38	0	0	1,33	0	0	8	1	1	6	0	0	2	0	0
48	Pb_6 Bi_2 Na_2 $(PO_4)_6$ F_2	1,19	1,03	1,02	0,38	0	0	1,33	0	0	6	2	2	6	0	0	2	0	0
49	Pb_{10} $(PO_4)_6$ F_2	1,19	0	0	0,38	0	0	1,33	0	0	10	0	0	6	0	0	2	0	0
50	$Ca_{4.5}$ $Pb_{5.5}$ $(PO_4)_6$ F_2	1	1,19	0	0,38	0	0	1,33	0	0	4,5	5,5	0	6	0	0	2	0	0
51	Pb_5 $(PO_4)_3$ OH	1,19	0	0	0,38	0	0	1,37	0	0	5	0	0	3	0	0	1	0	0
52	Cd_5 $(PO_4)_3$ OH	0,95	0	0	0,38	0	0	1,37	0	0	5	0	0	3	0	0	1	0	0
53	Ca_5 $(AsO_4)_3$ Cl	1	0	0	0,46	0	0	1,81	0	0	5	0	0	3	0	0	1	0	0
54	Ca_5 $(VO_4)_3$ (OH)	1	0	0	0,54	0	0	1,37	0	0	5	0	0	3	0	0	1	0	0
55	Ca_5 $(CrO_4)_3$ OH	1	0	0	0,55	0	0	1,37	0	0	5	0	0	3	0	0	1	0	0
56	Ba_5 $(CrO_4)_3$ OH	1,35	0	0	0,55	0	0	1,37	0	0	5	0	0	3	0	0	1	0	0
57	Ba_5 $(PO_4)_3$ F	1,35	0	0	0,38	0	0	1,33	0	0	5	0	0	3	0	0	1	0	0
58	Ba_3 La Na $(PO_4)_3$ F	1,35	1,03	1,02	0,38	0	0	1,33	0	0	3	1	1	3	0	0	1	0	0
59	Ba_4 Nd_3 Na_3 $(PO_4)_6$ F_2	1,35	0,98	1,02	0,38	0	0	1,33	0	0	4	3	3	6	0	0	2	0	0
60	Pb_5 $(PO_4)_3$ F	1,19	0	0	0,38	0	0	1,33	0	0	5	0	0	3	0	0	1	0	0
61	Sr_6 Ca_4 $(PO_4)_6$ F_2	1,18	1	0	0,38	0	0	1,33	0	0	6	4	0	6	0	0	2	0	0
62	Ca_2 Ba_3 $(PO_4)_3$ F	1	1,35	0	0,38	0	0	1,33	0	0	2	3	0	3	0	0	1	0	0
63	$Sr_{7.3}$ $Ca_{2.7}$ $(PO_4)_6$ F_2	1,18	1	0	0,38	0	0	1,33	0	0	7,3	2,7	0	6	0	0	2	0	0
64	Ca_5 $(PO_4)_3$ $F_{0.39}$ $Cl_{0.33}$ $(OH)_{0.28}$	1	0	0	0,38	0	0	1,33	1,81	1,37	5	0	0	3	0	0	0,39	0,33	0,28
65	Ca_5 $(PO_4)_3$ $F_{0.29}$ $Cl_{0.47}$ $(OH)_{0.24}$	1	0	0	0,38	0	0	1,33	1,81	1,37	5	0	0	3	0	0	0,29	0,47	0,24
66	Cd_5 $(PO_4)_3$ Cl	0,95	0	0	0,38	0	0	1,81	0	0	5	0	0	3	0	0	1	0	0
67	Ca_5 $(PO_4)_3$ $F_{0.41}$ $Cl_{0.59}$	1	0	0	0,38	0	0	1,33	1,81	0	5	0	0	3	0	0	0,41	0,59	0
68	Ba_5 $(PO_4)_3$ Cl	1,35	0	0	0,38	0	0	1,81	0	0	5	0	0	3	0	0	1	0	0
69	Co Ca_4 $(PO_4)_3$ Cl	0,65	1	0	0,38	0	0	1,81	0	0	1	4	0	3	0	0	1	0	0

Table 4.1 (continued)

#		Ionic Radii									Weights of Ions								
	Apatite formula	**A1**	**A2**	**A3**	**B1**	**B2**	**B3**	**C1**	**C2**	**C3**	**wA1**	**wA2**	**wA3**	**wB1**	**wB2**	**wB3**	**wC1**	**wC2**	**wC3**
70	$Sr_{2.54}\ Ba_{2.45}\ Eu_{0.01}\ (PO_4)_3\ Cl$	1,18	1,35	1,17	0,38	0	0	1,81	0	0	2,54	2,45	0,01	3	0	0	1	0	0
71	$Ba_{4.99}\ Eu_{0.01}\ (PO_4)_3\ Cl$	1,35	1,17	0	0,38	0	0	1,81	0	0	4,99	0,01	0	3	0	0	1	0	0
72	$Sr_{4.99}\ Eu_{0.01}\ (PO_4)_3\ Cl$	1,18	1,17	0	0,38	0	0	1,81	0	0	4,99	0,01	0	3	0	0	1	0	0
73	$Pb_5\ (AsO_4)_3\ Cl$	1,19	0	0	0,46	0	0	1,81	0	0	5	0	0	3	0	0	1	0	0
74	$Ca_2\ Pb_3\ (AsO_4)_3\ Cl$	1	1,19	0	0,46	0	0	1,81	0	0	2	3	0	3	0	0	1	0	0
75	$Pb_5\ (VO_4)_3\ Cl$	1,19	0	0	0,54	0	0	1,81	0	0	5	0	0	3	0	0	1	0	0
76	$Sr_{10}\ (CrO_4)_6\ F_2$	1,18	0	0	0,55	0	0	1,33	0	0	10	0	0	6	0	0	2	0	0
77	$Ca_{10}\ (VO_4)\ (PO_4)_5\ (OH)_2$	1	0	0	0,54	0,38	0	1,37	0	0	10	0	0	1	5	0	2	0	0
78	$Ca_{10}\ (VO_4)_2\ (PO_4)_4\ (OH)_2$	1	0	0	0,54	0,38	0	1,37	0	0	10	0	0	2	4	0	2	0	0
79	$Ca_{10}\ (VO_4)_3\ (PO_4)_3\ (OH)_2$	1	0	0	0,54	0,38	0	1,37	0	0	10	0	0	3	3	0	2	0	0
80	$Ca_{10}\ (VO_4)_4\ (PO_4)_2\ (OH)_2$	1	0	0	0,54	0,38	0	1,37	0	0	10	0	0	4	2	0	2	0	0
81	$Ca_{10}\ (VO_4)_5\ (PO_4)\ (OH)_2$	1	0	0	0,54	0,38	0	1,37	0	0	10	0	0	5	1	0	2	0	0
82	$Ca_{10}\ (VO_4)_6\ (OH)_2$	1	0	0	0,54	0	0	1,37	0	0	10	0	0	6	0	0	2	0	0
83	$Sr_5\ (PO_4)_3\ F$	1,18	0	0	0,38	0	0	1,33	0	0	5	0	0	3	0	0	1	0	0
84	$Pb_{10}\ (PO_4)_6\ Br_2$	1,19	0	0	0,38	0	0	1,96	0	0	10	0	0	6	0	0	2	0	0
85	$Ca_{10}\ (PO_4)_{5.83}\ (SiO_4)_{0.17}\ (OH)_{1.83}$	1	0	0	0,38	0,4	0	1,37	0	0	10	0	0	5,83	0,17	0	1,83	0	0
86	$Ca_{10}\ (PO_4)_{5.65}\ (SiO_4)_{0.35}\ (OH)_{1.65}$	1	0	0	0,38	0,4	0	1,37	0	0	10	0	0	5,65	0,35	0	1,65	0	0
87	$Ca_{10}\ (PO_4)_{5.48}\ (SiO_4)_{0.52}\ (OH)_{1.48}$	1	0	0	0,38	0,4	0	1,37	0	0	10	0	0	5,48	0,52	0	1,48	0	0
88	$Ca_{10}\ (PO_4)_{5.30}\ (SiO_4)_{0.70}\ (OH)_{1.30}$	1	0	0	0,38	0,4	0	1,37	0	0	10	0	0	5,3	0,7	0	1,3	0	0
89	$Ca_{10}\ (PO_4)_{5.84}\ (SiO_4)_{0.16}\ (OH)_{1.84}$	1	0	0	0,38	0,4	0	1,37	0	0	10	0	0	5,84	0,16	0	1,84	0	0
90	$Na\ Y_9\ (SiO_4)_6\ O_2$	1,02	0,9	0	0,4	0	0	1,4	0	0	1	9	0	6	0	0	2	0	0
91	$Sr_9\ La\ (PO_4)_5\ (SiO_4)\ F_2$	1,18	1,03	0	0,38	0,4	0	1,33	0	0	9	1	0	5	1	0	2	0	0
92	$Sr_8\ La_2\ (PO_4)_4\ (SiO_4)_2\ F_2$	1,18	1,03	0	0,38	0,4	0	1,33	0	0	8	2	0	4	2	0	2	0	0

Table 4.1 (continued)

#		Ionic Radii									Weights of Ions								
	Apatite formula	**A1**	**A2**	**A3**	**B1**	**B2**	**B3**	**C1**	**C2**	**C3**	**wA1**	**wA2**	**wA3**	**wB1**	**wB2**	**wB3**	**wC1**	**wC2**	**wC3**
93	$Sr_6\ La_4\ (PO_4)_2\ (SiO_4)_4\ F_2$	1,18	1,03	0	0,38	0,4	0	1,33	0	0	6	4	0	2	4	0	2	0	0
94	$Sr_4\ La_6\ (SiO_4)_6\ F_2$	1,18	1,03	0	0,4	0	0	1,33	0	0	4	6	0	6	0	0	2	0	0
95	$Sr_{10}\ (PO_4)_6\ O$	1,18	0	0	0,38	0	0	1,4	0	0	10	0	0	6	0	0	1	0	0
96	$Sr_9\ La\ (PO_4)_5\ (SiO_4)\ O$	1,18	1,03	0	0,38	0,4	0	1,4	0	0	9	1	0	5	1	0	1	0	0
97	$Sr_8\ La_2\ (PO_4)_4\ (SiO_4)_2\ O$	1,18	1,03	0	0,38	0,4	0	1,4	0	0	8	2	0	4	2	0	1	0	0
98	$Sr_6\ La_4\ (PO_4)_2\ (SiO_4)_4\ O$	1,18	1,03	0	0,38	0,4	0	1,4	0	0	6	4	0	2	4	0	1	0	0
99	$Sr_4\ La_6\ (SiO_4)_6\ O$	1,18	1,03	0	0,4	0	0	1,4	0	0	4	6	0	6	0	0	1	0	0
100	$Sr_5\ (PO_4)_3\ OH$	1,18	0	0	0,38	0	0	1,37	0	0	5	0	0	3	0	0	1	0	0
101	$Ba_5\ (PO_4)_3\ OH$	1,35	0	0	0,38	0	0	1,37	0	0	5	0	0	3	0	0	1	0	0
102	$Sr_5\ (CrO_4)_3\ Cl$	1,18	0	0	0,55	0	0	1,81	0	0	5	0	0	3	0	0	1	0	0

Table 4.2 Average ionic radii of each site of apatites and their corresponding a and c values.

#	Apatite formula	Average Radii A	Average Radii B	Average Radii C	a (Å)	c (Å)
1	$Ca_{4.03}\ Cd_{0.97}\ (PO_4)_3\ (OH)$	0,9903	0,38	1,37	9,391	6,837
2	$Ca_{3.98}\ Cd_{1.02}\ (PO_4)_3\ F$	0,9898	0,38	1,33	9,379	6,834
3	$Ca_{3.475}\ Cd_{1.525}\ (PO_4)_3\ F$	0,98475	0,38	1,33	9,36	6,812
4	$Ca_{10}\ (PO_4)_6\ (OH)_2$	1	0,38	1,37	9,424	6,879
5	$Ca_{2.5}\ Pb_{7.5}\ (PO_4)_6\ (OH)_2$	1,1425	0,38	1,37	9,88	7,417
6	$Ca_{8.98}\ Sr_{1.02}\ (PO_4)_6\ (OH)_2$	1,01836	0,38	1,37	9,4352	6,9087
7	$Ca_{7.684}\ Sr_{2.316}\ (PO_4)_6\ (OH)_2$	1,041688	0,38	1,37	9,4955	6,9718
8	$Ca_{3.616}\ Sr_{6.384}\ (PO_4)_6\ (OH)_2$	1,114912	0,38	1,37	9,6313	7,1246
9	$Ca_5\ (PO_4)_3\ F$	1	0,38	1,33	9,367	6,884
10	$Ca_{9.3}\ Mn_{0.7}\ (PO_4)_6\ F_2$	0,9881	0,38	1,33	9,3323	6,8424
11	$Ca_{9.37}\ Sr_{0.63}\ (PO_4)_6\ F_2$	1,01134	0,38	1,33	9,3902	6,9011
12	$Mn_5\ (PO_4)_3\ Cl_{0.9}\ (OH)_{0.1}$	0,83	0,38	1,766	9,532	6,199
13	$Cd_5\ (PO_4)_3\ Cl$	0,95	0,38	1,81	9,633	6,484
14	$Ca_5\ (PO_4)_3\ F_{0.17}\ Cl_{0.83}$	1	0,38	1,7284	9,6205	6,7761
15	$Ca_5\ (PO_4)_3\ Cl$	1	0,38	1,81	9,52	6,85
16	$Ca_5\ (PO_4)_3\ Br$	1	0,38	1,96	9,761	6,739
17	$Sr_5\ (PO_4)_3\ F_{0.75}\ Br_{0.25}$	1,18	0,38	1,4875	9,7186	7,2853
18	$Sr_5\ (PO_4)_3\ F_{0.5}\ Br_{0.5}$	1,18	0,38	1,645	9,7623	7,2699
19	$Sr_5\ (PO_4)_3\ F_{0.25}\ Br_{0.75}$	1,18	0,38	1,8025	9,8885	7,2344
20	$Sr_{4.99}\ Eu_{0.01}\ (PO_4)_3\ Cl_{0.75}\ Br_{0.25}$	1,17998	0,38	1,8475	9,8909	7,1934
21	$Sr_{4.99}\ Eu_{0.01}\ (PO_4)_3\ Cl_{0.5}\ Br_{0.5}$	1,17998	0,38	1,885	9,9056	7,195
22	$Sr_{4.99}\ Eu_{0.01}\ (PO_4)_3\ Cl_{0.25}\ Br_{0.75}$	1,17998	0,38	1,9225	9,9934	7,202
23	$Sr_{4.99}\ Eu_{0.01}\ (PO_4)_3\ Br$	1,17998	0,38	1,96	9,9636	7,2061
24	$Sr_5\ (PO_4)_3\ Br$	1,18	0,38	1,96	9,9641	7,207
25	$Sr_5\ (PO_4)_3\ Cl$	1,18	0,38	1,81	9,859	7,206
26	$Ca_{2.6}\ Sr_{2.4}\ (PO_4)_3\ Cl$	1,0864	0,38	1,81	9,737	7,022
27	$Ca_{4.6}\ Sr_{0.4}\ (PO_4)_3\ Cl$	1,0144	0,38	1,81	9,653	6,777
28	$Ca_{4.9}\ Sr_{0.1}\ (PO_4)_3\ Cl$	1,0036	0,38	1,81	9,643	6,766
29	$Sr_{4.99}\ Eu_{0.01}\ (PO_4)_3\ Cl$	1,17998	0,38	1,81	9,878	7,1893
30	$Sr_{2.54}\ Ca_{2.45}\ Eu_{0.01}\ (PO_4)_3\ Cl$	1,09178	0,38	1,81	9,754	7,0061
31	$Sr_{4.99}\ Eu_{0.01}\ (PO_4)_3\ Cl_{0.75}\ F_{0.25}$	1,17998	0,38	1,69	9,8697	7,1966
32	$Sr_{4.99}\ Eu_{0.01}\ (PO_4)_3\ Cl_{0.5}\ F_{0.5}$	1,17998	0,38	1,57	9,8042	7,2357
33	$Sr_{4.99}\ Eu_{0.01}\ (PO_4)_3\ Cl_{0.25}\ F_{0.75}$	1,17998	0,38	1,45	9,7357	7,2769
34	$Ca_{2.1}\ Pb_{7.9}\ (PO_4)_6\ Cl_2$	1,1501	0,38	1,81	9,99	7,276
35	$Pb_5\ (PO_4)_3\ Cl$	1,19	0,38	1,81	9,9764	7,3511

Table 4.2 (continued)

#	Apatite formula	Average Radii A	Average Radii B	Average Radii C	a (Å)	c (Å)
36	$K_2\ Pb_6\ Eu_2\ (PO_4)_6\ F_2$	1,18	0,38	1,33	9,7482	7,2655
37	$K\ Pb_8\ Nd\ (PO_4)_6\ F_2$	1,188	0,38	1,33	9,7768	7,2791
38	$K_2\ Pb_6\ Nd_2\ (PO_4)_6\ F_2$	1,186	0,38	1,33	9,7604	7,2754
39	$Pb_6\ Eu_2\ Na_2\ (PO_4)_6\ F_2$	1,108	0,38	1,33	9,655	7,058
40	$Pb_8\ Eu\ Na\ (PO_4)_6\ F_2$	1,149	0,38	1,33	9,73	7,176
41	$Pb_6\ La_2\ Na_2\ (PO_4)_6\ F_2$	1,124	0,38	1,33	9,721	7,15
42	$Pb_4\ La_3\ Na_3\ (PO_4)_6\ F_2$	1,091	0,38	1,33	9,725	7,158
43	$Pb_6\ Nd_2\ Na_2\ (PO_4)_6\ F_2$	1,114	0,38	1,33	9,661	7,067
44	$Pb_4\ Nd_3\ Na_3\ (PO_4)_6\ F_2$	1,076	0,38	1,33	9,616	7,029
45	$Pb_8\ Nd\ Na\ (PO_4)_6\ F_2$	1,152	0,38	1,33	9,741	7,198
46	$Pb\ Y_2\ Na_2\ (PO_4)_6\ F_2$	1,006	0,38	1,33	9,649	7,055
47	$Pb_8\ Y\ Na\ (PO_4)_6\ F_2$	1,144	0,38	1,33	9,712	7,17
48	$Pb_6\ Bi_2\ Na_2\ (PO_4)_6\ F_2$	1,124	0,38	1,33	9,6956	7,1826
49	$Pb_{10}\ (PO_4)_6\ F_2$	1,19	0,38	1,33	9,773	7,315
50	$Ca_{4.5}\ Pb_{5.5}\ (PO_4)_6\ F_2$	1,1045	0,38	1,33	9,759	7,291
51	$Pb_5\ (PO_4)_3\ OH$	1,19	0,38	1,37	9,877	7,427
52	$Cd_5\ (PO_4)_3\ OH$	0,95	0,38	1,37	9,335	6,664
53	$Ca_5\ (AsO_4)_3\ Cl$	1	0,46	1,81	10,076	6,807
54	$Ca_5\ (VO_4)_3\ (OH)$	1	0,54	1,37	9,818	6,981
55	$Ca_5\ (CrO_4)_3\ OH$	1	0,55	1,37	9,683	7,01
56	$Ba_5\ (CrO_4)_3\ OH$	1,35	0,55	1,37	10,428	7,89
57	$Ba_5\ (PO_4)_3\ F$	1,35	0,38	1,33	10,153	7,733
58	$Ba_3\ La\ Na\ (PO_4)_3\ F$	1,22	0,38	1,33	9,9392	7,4419
59	$Ba_4\ Nd_3\ Na_3\ (PO_4)_6\ F_2$	1,14	0,38	1,33	9,786	7,281
60	$Pb_5\ (PO_4)_3\ F$	1,19	0,38	1,33	9,76	7,3
61	$Sr_6\ Ca_4\ (PO_4)_6\ F_2$	1,108	0,38	1,33	9,63	7,22
62	$Ca_2\ Ba_3\ (PO_4)_3\ F$	1,21	0,38	1,33	9,845	7,359
63	$Sr_{7.3}\ Ca_{2.7}\ (PO_4)_6\ F_2$	1,1314	0,38	1,33	9,565	7,115
64	$Ca_5\ (PO_4)_3\ F_{0.39}\ Cl_{0.33}\ (OH)_{0.28}$	1	0,38	1,4996	9,4615	6,8491
65	$Ca_5\ (PO_4)_3\ F_{0.29}\ Cl_{0.47}\ (OH)_{0.24}$	1	0,38	1,5652	9,4877	6,8224
66	$Cd_5\ (PO_4)_3\ Cl$	0,95	0,38	1,81	9,625	6,504
67	$Ca_5\ (PO_4)_3\ F_{0.41}\ Cl_{0.59}$	1	0,38	1,6132	9,5485	6,8237
68	$Ba_5\ (PO_4)_3\ Cl$	1,35	0,38	1,81	10,284	7,651
69	$Co\ Ca_4\ (PO_4)_3\ Cl$	0,93	0,38	1,81	9,625	6,747
70	$Sr_{2.54}\ Ba_{2.45}\ Eu_{0.01}\ (PO_4)_3\ Cl$	1,26328	0,38	1,81	10,0265	7,4099
71	$Ba_{4.99}\ Eu_{0.01}\ (PO_4)_3\ Cl$	1,34964	0,38	1,81	10,2712	7,65

Table 4.2 (continued)

#	Apatite formula	Average Radii A	Average Radii B	Average Radii C	a (Å)	c (Å)
72	$Sr_{4.99}\ Eu_{0.01}\ (PO_4)_3\ Cl$	1,17998	0,38	1,81	9,878	7,1893
73	$Pb_5\ (AsO_4)_3\ Cl$	1,19	0,46	1,81	10,211	7,4185
74	$Ca_2\ Pb_3\ (AsO_4)_3\ Cl$	1,114	0,46	1,81	10,14	7,185
75	$Pb_5\ (VO_4)_3\ Cl$	1,19	0,54	1,81	10,3174	7,3378
76	$Sr_{10}\ (CrO_4)_6\ F_2$	1,18	0,55	1,33	9,956	7,437
77	$Ca_{10}\ (VO_4)\ (PO_4)_5\ (OH)_2$	1	0,40667	1,37	9,467	6,904
78	$Ca_{10}\ (VO_4)_2\ (PO_4)_4\ (OH)_2$	1	0,43333	1,37	9,535	6,927
79	$Ca_{10}\ (VO_4)_3\ (PO_4)_3\ (OH)_2$	1	0,46	1,37	9,586	6,943
80	$Ca_{10}\ (VO_4)_4\ (PO_4)_2\ (OH)_2$	1	0,48667	1,37	9,649	6,986
81	$Ca_{10}\ (VO_4)_5\ (PO_4)\ (OH)_2$	1	0,51333	1,37	9,695	6,986
82	$Ca_{10}\ (VO_4)_6\ (OH)_2$	1	0,54	1,37	9,717	7,007
83	$Sr_5\ (PO_4)_3\ F$	1,18	0,38	1,33	9,7174	7,2851
84	$Pb_{10}\ (PO_4)_6\ Br_2$	1,19	0,38	1,96	10,062	7,359
85	$Ca_{10}\ (PO_4)_{5.83}\ (SiO_4)_{0.17}\ (OH)_{1.83}$	1	0,38057	1,37	9,41763	6,88545
86	$Ca_{10}\ (PO_4)_{5.65}\ (SiO_4)_{0.35}\ (OH)_{1.65}$	1	0,38117	1,37	9,41869	6,88683
87	$Ca_{10}\ (PO_4)_{5.48}\ (SiO_4)_{0.52}\ (OH)_{1.48}$	1	0,38173	1,37	9,42158	6,89155
88	$Ca_{10}\ (PO_4)_{5.30}\ (SiO_4)_{0.70}\ (OH)_{1.30}$	1	0,38233	1,37	9,42332	6,89703
89	$Ca_{10}\ (PO_4)_{5.84}\ (SiO_4)_{0.16}\ (OH)_{1.84}$	1	0,38053	1,37	9,4082	6,8828
90	$Na\ Y_9\ (SiO_4)_6\ O_2$	0,912	0,4	1,4	9,334	6,759
91	$Sr_9\ La\ (PO_4)_5\ (SiO_4)\ F_2$	1,165	0,38333	1,33	9,723	7,282
92	$Sr_8\ La_2\ (PO_4)_4\ (SiO_4)_2\ F_2$	1,15	0,38667	1,33	9,727	7,277
93	$Sr_6\ La_4\ (PO_4)_2\ (SiO_4)_4\ F_2$	1,12	0,39333	1,33	9,732	7,27
94	$Sr_4\ La_6\ (SiO_4)_6\ F_2$	1,09	0,4	1,33	9,737	7,265
95	$Sr_{10}\ (PO_4)_6\ O$	1,18	0,38	1,4	9,753	7,276
96	$Sr_9\ La\ (PO_4)_5\ (SiO_4)\ O$	1,165	0,38333	1,4	9,756	7,272
97	$Sr_8\ La_2\ (PO_4)_4\ (SiO_4)_2\ O$	1,15	0,38667	1,4	9,761	7,267
98	$Sr_6\ La_4\ (PO_4)_2\ (SiO_4)_4\ O$	1,12	0,39333	1,4	9,768	7,258
99	$Sr_4\ La_6\ (SiO_4)_6\ O$	1,09	0,4	1,4	9,771	7,255
100	$Sr_5\ (PO_4)_3\ OH$	1,18	0,38	1,37	9,745	7,265
101	$Ba_5\ (PO_4)_3\ OH$	1,35	0,38	1,37	10,1904	7,721
102	$Sr_5\ (CrO_4)_3\ Cl$	1,18	0,55	1,81	10,125	7,328

Table 4.3 Refined dataset for neural networks application.

#	Apatite formula	Average Radii A	Average Radii B	Average Radii C	a (Å)	c (Å)
1	$Ca_5 (PO_4)_3 OH$	1	0,38	1,37	9,424	6,879
2	$Ca_5 (VO_4)_3 (OH)$	1	0,54	1,37	9,818	6,981
3	$Ca_5 (CrO_4)_3 OH$	1	0,55	1,37	9,683	7,01
4	$Ca_5 (PO_4)_3 F$	1	0,38	1,33	9,367	6,884
5	$Ca_5 (PO_4)_3 Cl$	1	0,38	1,81	9,52	6,85
6	$Ca_5 (AsO_4)_3 Cl$	1	0,46	1,81	10,076	6,807
7	$Ca_5 (PO_4)_3 Br$	1	0,38	1,96	9,761	6,739
8	$Cd_5 (PO_4)_3 OH$	0,95	0,38	1,37	9,335	6,664
9	$Cd_5 (PO_4)_3 Cl$	0,95	0,38	1,81	9,625	6,504
10	$Sr_5 (PO_4)_3 Cl$	1,18	0,38	1,81	9,859	7,206
11	$Sr_5 (CrO_4)_3 Cl$	1,18	0,55	1,81	10,125	7,328
12	$Sr_5 (PO_4)_3 Br$	1,18	0,38	1,96	9,9641	7,207
13	$Sr_5 (PO_4)_3 OH$	1,18	0,38	1,37	9,745	7,265
14	$Sr_5 (PO_4)_3 F$	1,18	0,38	1,33	9,7174	7,2851
15	$Pb_5 (PO_4)_3 Cl$	1,19	0,38	1,81	9,993	7,334
16	$Pb_5 (AsO_4)_3 Cl$	1,19	0,46	1,81	10,24	7,43
17	$Pb_5 (PO_4)_3 OH$	1,19	0,38	1,37	9,877	7,427
18	$Ba_5 (PO_4)_3 OH$	1,35	0,38	1,37	10,1904	7,721
19	$Ba_5 (PO_4)_3 F$	1,35	0,38	1,33	10,153	7,733
20	$Ba_5 (PO_4)_3 Cl$	1,35	0,38	1,81	10,284	7,651
21	$Ba_5 (CrO_4)_3 OH$	1,35	0,55	1,37	10,428	7,89
22	$Ca_{7.684} Sr_{2.316} (PO_4)_6 (OH)_2$	1,041688	0,38	1,37	9,4955	6,9718
23	$Ca_{3.616} Sr_{6.384} (PO_4)_6 (OH)_2$	1,114912	0,38	1,37	9,6313	7,1246
24	$Ca_{8.98} Sr_{1.02} (PO_4)_6 (OH)_2$	1,01836	0,38	1,37	9,4352	6,9087
25	$Ca_{4.03} Cd_{0.97} (PO_4)_3 (OH)$	0,9903	0,38	1,37	9,391	6,837
26	$Ca_{3.98} Cd_{1.02} (PO_4)_3 F$	0,9898	0,38	1,33	9,379	6,834
27	$Ca_{3.475} Cd_{1.525} (PO_4)_3 F$	0,98475	0,38	1,33	9,36	6,812
28	$Ca_5 (PO_4)_3 F_{0.41} Cl_{0.59}$	1	0,38	1,6132	9,5485	6,8237
29	$Sr_6 Ca_4 (PO_4)_6 F_2$	1,108	0,38	1,33	9,63	7,22
30	$Sr_{7.3} Ca_{2.7} (PO_4)_6 F_2$	1,1314	0,38	1,33	9,565	7,115
31	$Ca_{9.37} Sr_{0.63} (PO_4)_6 F_2$	1,01134	0,38	1,33	9,3902	6,9011
32	$Ca_5 (PO_4)_3 F_{0.17} Cl_{0.83}$	1	0,38	1,7284	9,6205	6,7761
33	$Ca_5 (AsO_4)_3 F$	1	0,46	1,33	9,75	6,92
34	$Ca_5 (AsO_4)_3 OH$	1	0,46	1,37	9,7	6,93

4.2 Simulation

Matlab Neural Network Toolbox Version 4 was used to create the network. After training the network with different learning types and neurons for the MLP network, it was seen that all learning types except resilient backpropagation (RP) and gradient descent with momentum and adaptive learning rate backpropagation (GDX) resulted in correlation coefficients, indicators of better fit as they become close to one, higher than 0.99. However, prediction results were not equally successful. Levenberg-marquardt backpropagation (LM), scaled conjugate gradient backpropagation (SCG) and bayesian regularization (BR) methods were all successful, but only BR resulted in both high correlation coefficient and very consistent prediction capabilities. BR used LM method with a modified performance function to minimize the errors. Results were improved compared to ordinary LM method because effectively used weights and biases were found by the algorithm, leading to a more efficient generalization of the non-linear relationship between ionic radii and hexagonal lattice parameters of apatites. Training parameters for each learning method are given in Table 4.4.

Table 4.4 Training parameters for each learning method

	Number of neurons in the hidden layer	Activation function for hidden layer	Activation function for output layer	Epoch	Train goal (MSE)
BR	4	tansig	purelin	1000	-
GDX	7	tansig	purelin	5000	1e-3
LM	4	tansig	purelin	400	15e-4
RP	6	tansig	purelin	5000	1e-3
SCG	7	tansig	purelin	3000	177e-5 1e-3 (for c)

Matlab codes for simulations are given in Appendix C. For BR method, one hidden layer with four processing elements were used with tansig function for the hidden layer and purelin function for the output layer. For the other methods, the same functions and processing elements were used which varied between four and seven processing elements. Learning algorithms were sensitive to the number of processing units, providing best weights and biases without using too many processing units in the hidden layer. Large numbers of these units may increase the complexity of the network and generate large errors. Sketch of the neural network which was trained with BR is given in Figure 4.1.

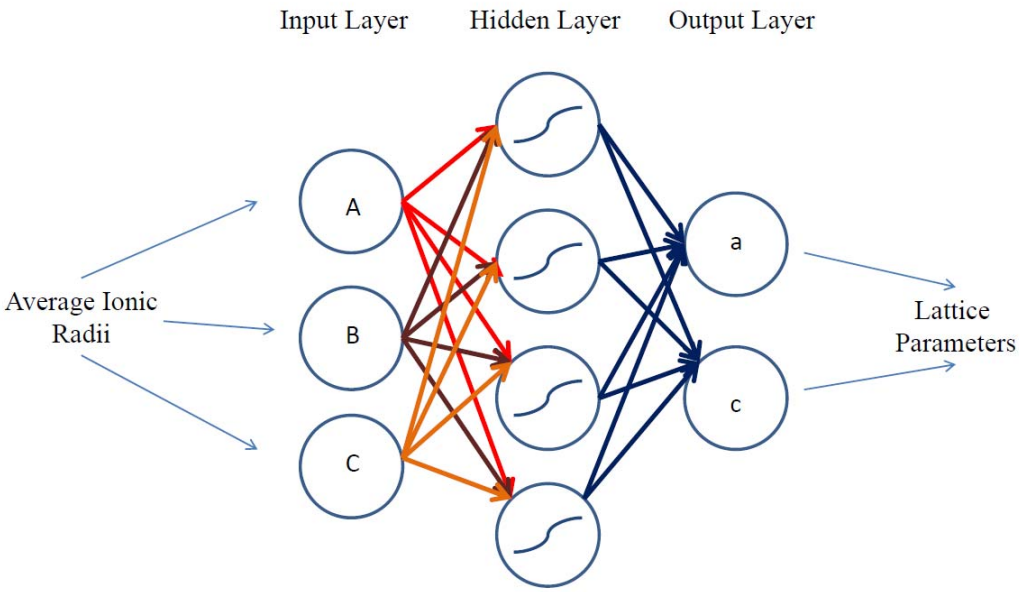

Figure 4.1 Sketch of the network trained with BR method

Post-analysis results for simulations are given in Tables 4.5 and 4.6 for lattice parameters a and c, respectively. Post-analysis of the network revealed three important parameters which were slope (m), y-intercept (b) and correlation coefficient between outputs and targets (r). Linear correlation analysis was done

to determine the success of matching experimental and predicted output values. **m** and **r** were wanted as high as possible while the opposite was needed for **b**. This demand arised from the fact that if experimental outputs were the same as predicted outputs, their ratio would become unity which is the highest value for slope and graph of experimental outputs versus predicted outputs passes from the origin which gives the lowest value for y-intercept. It was seen in Tables 4.5 and 4.6 that **b** values were unacceptable for RP and GDX methods in addition to low **r** values for both lattice parameters.

Table 4.5 Post-analysis results for lattice parameter a.

Learning method	Slope (m)	y-intercept (b)	Correlation coefficient (r)	Coefficient of determination (r^2)
GDX	0.9658	0.3319	0.9828	0.966
LM	0.9799	0.1951	0.9916	0.983
RP	0.9401	0.5831	0.9698	0.94
SCG	0.9795	0.1991	0.9901	0.98
BR	0.9801	0.1942	0.9910	0.982

Table 4.6 Post-analysis results for lattice parameter c.

Learning method	Slope (m)	y-intercept (b)	Correlation coefficient (r)	Coefficient of determination (r^2)
GDX	0.9476	0.3711	0.9728	0.946
LM	0.9871	0.0910	0.9930	0.986
RP	0.9577	0.3000	0.9785	0.958
SCG	0.9898	0.0720	0.9949	0.99
BR	0.9804	0.1392	0.9909	0.982

BR method generated extra parameters that did not exist for other learning methods because of its modified performance function. These parameters are shown in Figures 4.2 and 4.4. Training parameters of Bayesian learning for lattice parameter a are given in Figure 4.2. It was found that training ended after 143 epochs with 'maximum mu reached' notification. 'mu' means marquardt adjustment parameter and when the maximum was attained, the network was successfully trained by setting weights and biases to their best values and minimizing their number. Sum of squared errors (SSE) was 0.0545969 and sum of squared weights (SSW) was 93.8083 which means that BR method successfully minimized the modified error function. Tr-Blue label on the graph was used to show that training SSE was shown with a blue line. Effective number of parameters were found to be 11.6737 out of 21. This decrease caused less use of weights and biases, hence higher generalization performance was achieved.

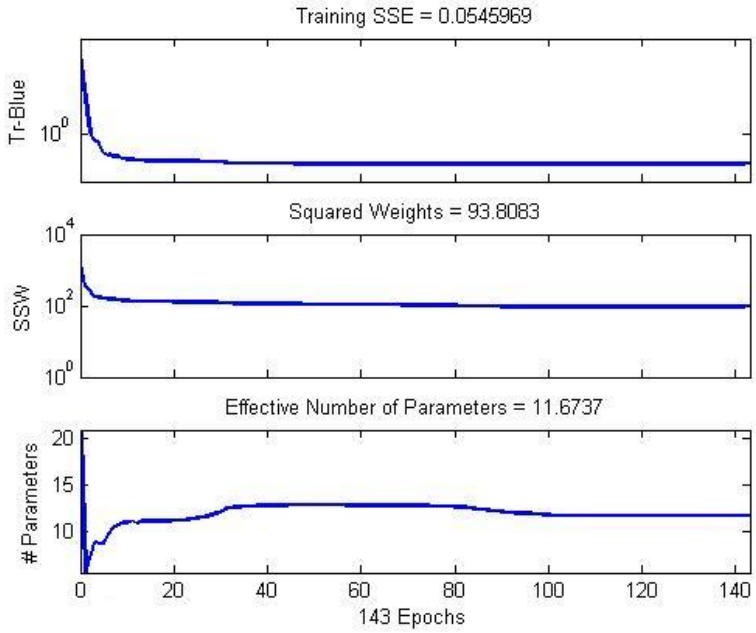

Figure 4.2 Training parameters of Bayesian learning for lattice parameter a.

Post-analysis results showed that the network was successfully trained for lattice parameter a and this can be seen better by examining Figure 4.3. In this figure, it was shown that linear correlation coefficient was 0.991 which means 98.2% prediction accuracy (r^2) was achieved for lattice parameter a of the training dataset. Horizontal axis with label (T) represented the target data, whereas vertical axis (A) represented predicted data. Best linear fit equation between the target and the predicted data is given above the graph.

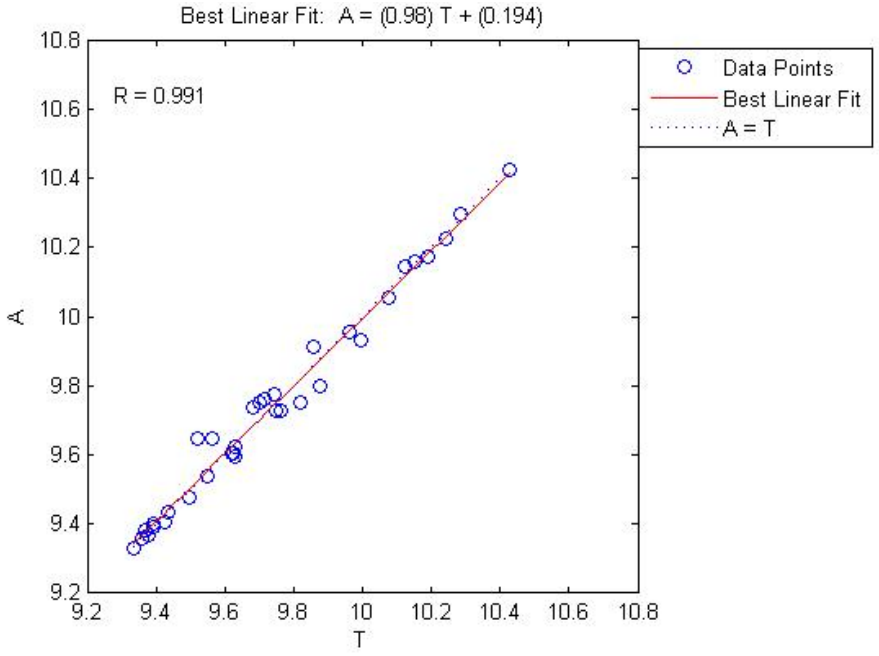

Figure 4.3 Linear correlation of outputs and targets for lattice parameter a.

Training parameters of Bayesian learning for lattice parameter c are given in Figure 4.4. At the end of 426 epochs, SSE was 0.06575 which was acceptable for precise prediction purposes. In addition, SSW was seen to decrease sharply at first few epochs and remained constant at 23.5184. Effective number of

parameters were determined as 8.60435 out of 21, so generalization success for lattice parameter c was ensured with these results.

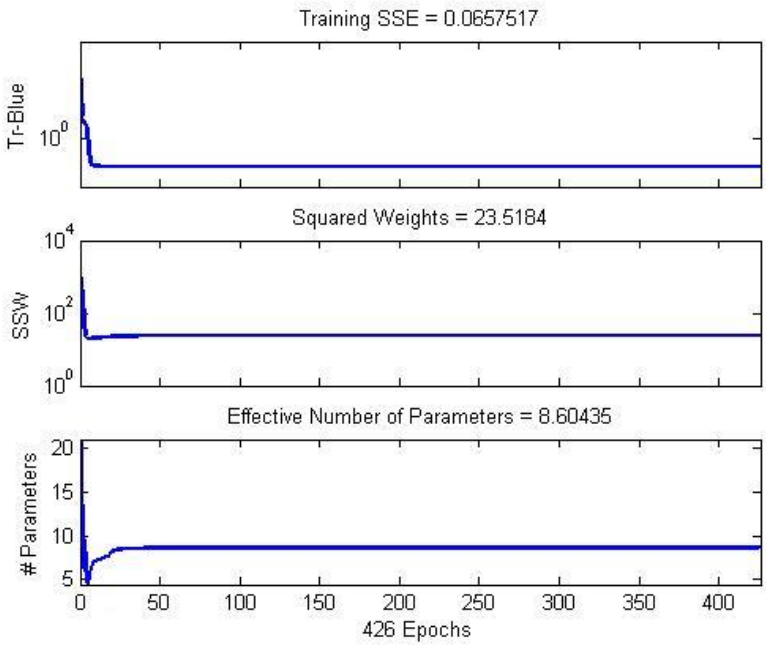

Figure 4.4 Training parameters of Bayesian learning for lattice parameter c.

Linear correlation of outputs and targets for lattice parameter c are given in Figure 4.5. Performance of the network was similar to the one that was used for prediction of lattice parameter a. Coefficient of determination was again 98.2% and large deviations of data points from the best line were not seen. Best linear fit was slightly shifted on the y-axis from 0.194 to 0.139.

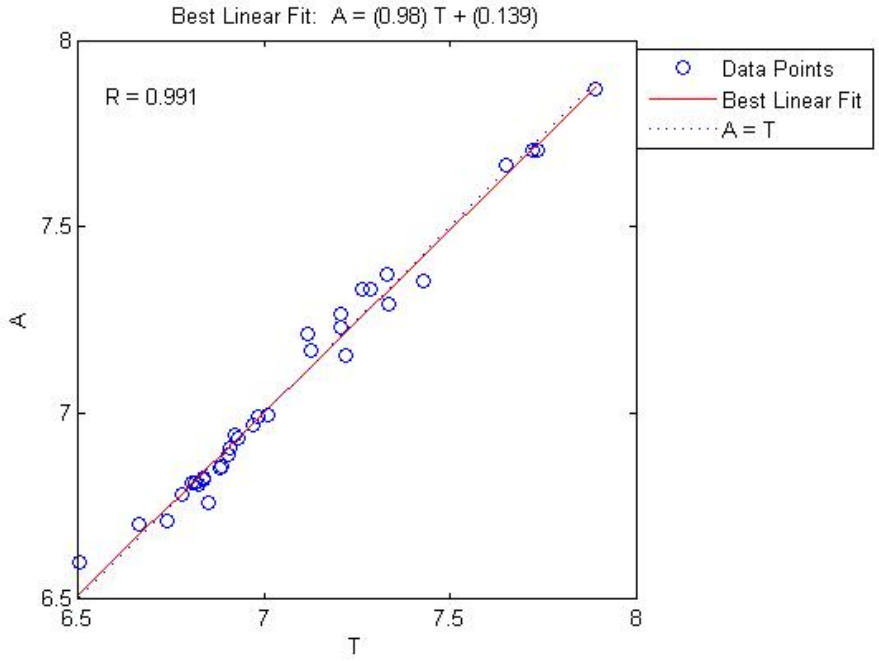

Figure 4.5 Linear correlation of outputs and targets for lattice parameter c.

Average percent errors of lattice parameters for the training dataset with each learning method are given in Table 4.7. It was seen that average errors of lattice parameters for BR were 0.299% for lattice parameter a and 0.472% for lattice parameter c which were quite small values for errors. LM and SCG methods produced slightly better results for lattice parameter c, and LM method was a little better for lattice parameter a, but it was shown in Tables 4.11 to 4.15 that BR method was more successful at predicting new apatites that were presented to the network. This was expected because of the decreases in SSE, SSW and number of parameters which serve as better generalization tools than standard performance functions used with other experimented methods. Because of this reason, prediction of new candidates were made by using BR.

Table 4.7 Average errors of lattice parameters for the training dataset.

Learning method	Average percent error for a	Average percent error for c
GDX	0.469	0.829
LM	0.293	0.371
RP	0.584	0.757
SCG	0.317	0.302
BR	0.299	0.472

Predicted outputs a and c and percent errors for the outputs generated by BR method are given in Table 4.8. It was seen that BR method was successful for training data ranging from 9.335 to 10.428 Å for **a** and from 6.504 to 7.89 Å for **c**. Maximum errors were found to be 1.320% and 1.476% for lattice parameters a and c, respectively.

Predicted and calculated hexagonal unit cell volumes of the apatites in Table 4.8 are presented in Table 4.9. Increase in errors for volume predictions was because errors from both of the lattice parameters were used for the calculations. Even in this situation, average percent error for volume was found to be 0.855% and highest error in the dataset was 3.097%. These values were accurate enough to be used in most of the real life applications.

Table 4.8 Average percent errors for the outputs generated by Bayesian learning.

	Apatite formula	Average Radii A	Average Radii B	Average Radii C	a (Å)	c (Å)	a output	c output	error%(a)	error%(c)
1	$Ca_5 (PO_4)_3 OH$	1	0,38	1,37	9,424	6,879	9,4037	6,8499	0,215	0,423
2	$Ca_5 (VO_4)_3 (OH)$	1	0,54	1,37	9,818	6,981	9,7524	6,9889	0,668	0,113
3	$Ca_5 (CrO_4)_3 OH$	1	0,55	1,37	9,683	7,01	9,7353	6,9945	0,540	0,221
4	$Ca_5 (PO_4)_3 F$	1	0,38	1,33	9,367	6,884	9,3817	6,855	0,157	0,421
5	$Ca_5 (PO_4)_3 Cl$	1	0,38	1,81	9,52	6,85	9,6457	6,7576	1,320	1,349
6	$Ca_5 (AsO_4)_3 Cl$	1	0,46	1,81	10,076	6,807	10,057	6,8122	0,189	0,076
7	$Ca_5 (PO_4)_3 Br$	1	0,38	1,96	9,761	6,739	9,7262	6,7111	0,357	0,414
8	$Cd_5 (PO_4)_3 OH$	0,95	0,38	1,37	9,335	6,664	9,3293	6,7003	0,061	0,545
9	$Cd_5 (PO_4)_3 Cl$	0,95	0,38	1,81	9,625	6,504	9,6019	6,6	0,240	1,476
10	$Sr_5 (PO_4)_3 Cl$	1,18	0,38	1,81	9,859	7,206	9,91	7,2671	0,517	0,848
11	$Sr_5 (CrO_4)_3 Cl$	1,18	0,55	1,81	10,125	7,328	10,144	7,3722	0,188	0,603
12	$Sr_5 (PO_4)_3 Br$	1,18	0,38	1,96	9,9641	7,207	9,9553	7,2315	0,088	0,340
13	$Sr_5 (PO_4)_3 OH$	1,18	0,38	1,37	9,745	7,265	9,7731	7,3304	0,288	0,900
14	$Sr_5 (PO_4)_3 F$	1,18	0,38	1,33	9,7174	7,2851	9,7597	7,3331	0,435	0,659
15	$Pb_5 (PO_4)_3 Cl$	1,19	0,38	1,81	9,993	7,334	9,9297	7,2928	0,633	0,562
16	$Pb_5 (AsO_4)_3 Cl$	1,19	0,46	1,81	10,24	7,43	10,226	7,3553	0,137	1,005
17	$Pb_5 (PO_4)_3 OH$	1,19	0,38	1,37	9,877	7,427	9,7969	7,3545	0,811	0,976
18	$Ba_5 (PO_4)_3 OH$	1,35	0,38	1,37	10,1904	7,721	10,175	7,707	0,151	0,181
19	$Ba_5 (PO_4)_3 F$	1,35	0,38	1,33	10,153	7,733	10,159	7,7079	0,059	0,325
20	$Ba_5 (PO_4)_3 Cl$	1,35	0,38	1,81	10,284	7,651	10,296	7,668	0,117	0,222
21	$Ba_5 (CrO_4)_3 OH$	1,35	0,55	1,37	10,428	7,89	10,423	7,8724	0,048	0,223
22	$Ca_{7.684} Sr_{2.316} (PO_4)_6 (OH)_2$	1,041688	0,38	1,37	9,4955	6,9718	9,4762	6,9692	0,203	0,037

Table 4.8 (continued)

	Apatite formula	Average Radii A	Average Radii B	Average Radii C	a (Å)	c (Å)	a output	c output	error%(a)	error%(c)
23	$Ca_{3.616}\ Sr_{6.384}\ (PO_4)_6\ (OH)_2$	1,114912	0,38	1,37	9,6313	7,1246	9,6244	7,1669	0,072	0,594
24	$Ca_{8.98}\ Sr_{1.02}\ (PO_4)_6\ (OH)_2$	1,01836	0,38	1,37	9,4352	6,9087	9,4345	6,9031	0,007	0,081
25	$Ca_{4.03}\ Cd_{0.97}\ (PO_4)_3\ (OH)$	0,9903	0,38	1,37	9,391	6,837	9,3881	6,8215	0,031	0,227
26	$Ca_{3.98}\ Cd_{1.02}\ (PO_4)_3\ F$	0,9898	0,38	1,33	9,379	6,834	9,3647	6,8252	0,152	0,129
27	$Ca_{3.475}\ Cd_{1.525}\ (PO_4)_3\ F$	0,98475	0,38	1,33	9,36	6,812	9,3566	6,8103	0,036	0,025
28	$Ca_5\ (PO_4)_3\ F_{0.41}\ Cl_{0.59}$	1	0,38	1,6132	9,5485	6,8237	9,5379	6,8072	0,111	0,242
29	$Sr_6\ Ca_4\ (PO_4)_6\ F_2$	1,108	0,38	1,33	9,63	7,22	9,5936	7,1525	0,378	0,935
30	$Sr_{7.3}\ Ca_{2.7}\ (PO_4)_6\ F_2$	1,1314	0,38	1,33	9,565	7,115	9,646	7,2127	0,847	1,373
31	$Ca_{9.37}\ Sr_{0.63}\ (PO_4)_6\ F_2$	1,01134	0,38	1,33	9,3902	6,9011	9,4012	6,8878	0,117	0,193
32	$Ca_5\ (PO_4)_3\ F_{0.17}\ Cl_{0.83}$	1	0,38	1,7284	9,6205	6,7761	9,6012	6,7798	0,201	0,055
33	$Ca_5\ (AsO_4)_3\ F$	1	0,46	1,33	9,75	6,92	9,7251	6,9385	0,255	0,267
34	$Ca_5\ (AsO_4)_3\ OH$	1	0,46	1,37	9,7	6,93	9,7503	6,931	0,519	0,014
							Average Percent Errors of Outputs:		0,299	0,472

Table 4.9 Comparison of calculated and predicted unit cell volumes for data in Table 4.8.

	Apatite formula	a (Å)	c (Å)	a output	c output	Vol. (unit cell)	Vol. (predicted)	Error % for volumes
1	$Ca_5 (PO_4)_3 OH$	9,424	6,879	9,4037	6,8499	1581,7	1568,2	0,852
2	$Ca_5 (VO_4)_3 (OH)$	9,818	6,981	9,7524	6,9889	1742,2	1720,9	1,220
3	$Ca_5 (CrO_4)_3 OH$	9,683	7,01	9,7353	6,9945	1701,6	1716,3	0,860
4	$Ca_5 (PO_4)_3 F$	9,367	6,884	9,3817	6,855	1563,8	1562,1	0,108
5	$Ca_5 (PO_4)_3 Cl$	9,52	6,85	9,6457	6,7576	1607,3	1627,8	1,273
6	$Ca_5 (AsO_4)_3 Cl$	10,076	6,807	10,057	6,8122	1789,2	1783,8	0,301
7	$Ca_5 (PO_4)_3 Br$	9,761	6,739	9,7262	6,7111	1662,3	1643,7	1,123
8	$Cd_5 (PO_4)_3 OH$	9,335	6,664	9,3293	6,7003	1503,5	1509,8	0,422
9	$Cd_5 (PO_4)_3 Cl$	9,625	6,504	9,6019	6,6	1560,0	1575,4	0,990
10	$Sr_5 (PO_4)_3 Cl$	9,859	7,206	9,91	7,2671	1813,4	1847,7	1,894
11	$Sr_5 (CrO_4)_3 Cl$	10,125	7,328	10,144	7,3722	1944,9	1964,0	0,981
12	$Sr_5 (PO_4)_3 Br$	9,9641	7,207	9,9553	7,2315	1852,5	1855,5	0,163
13	$Sr_5 (PO_4)_3 OH$	9,745	7,265	9,7731	7,3304	1786,2	1812,7	1,483
14	$Sr_5 (PO_4)_3 F$	9,7174	7,2851	9,7597	7,3331	1781,0	1808,4	1,537
15	$Pb_5 (PO_4)_3 Cl$	9,993	7,334	9,9297	7,2928	1896,1	1861,7	1,818
16	$Pb_5 (AsO_4)_3 Cl$	10,24	7,43	10,226	7,3553	2017,1	1991,3	1,276
17	$Pb_5 (PO_4)_3 OH$	9,877	7,427	9,7969	7,3545	1875,8	1827,5	2,576
18	$Ba_5 (PO_4)_3 OH$	10,1904	7,721	10,175	7,707	2075,8	2065,8	0,483
19	$Ba_5 (PO_4)_3 F$	10,153	7,733	10,159	7,7079	2063,8	2059,5	0,207
20	$Ba_5 (PO_4)_3 Cl$	10,284	7,651	10,296	7,668	2095,0	2104,5	0,456
21	$Ba_5 (CrO_4)_3 OH$	10,428	7,89	10,423	7,8724	2221,3	2214,2	0,319
22	$Ca_{7.684} Sr_{2.316} (PO_4)_6 (OH)_2$	9,4955	6,9718	9,4762	6,9692	1627,5	1620,3	0,443

Table 4.9 (continued)

	Apatite formula	a (Å)	c (Å)	a output	c output	Vol. (unit cell)	Vol. (predicted)	Error % for volumes
23	$Ca_{3.616}\ Sr_{6.384}\ (PO_4)_6\ (OH)_2$	9,6313	7,1246	9,6244	7,1669	1711,0	1718,7	0,450
24	$Ca_{8.98}\ Sr_{1.02}\ (PO_4)_6\ (OH)_2$	9,4352	6,9087	9,4345	6,9031	1592,3	1590,8	0,096
25	$Ca_{4.03}\ Cd_{0.97}\ (PO_4)_3\ (OH)$	9,391	6,837	9,3881	6,8215	1561,1	1556,6	0,288
26	$Ca_{3.98}\ Cd_{1.02}\ (PO_4)_3\ F$	9,379	6,834	9,3647	6,8252	1556,4	1549,7	0,433
27	$Ca_{3.475}\ Cd_{1.525}\ (PO_4)_3\ F$	9,36	6,812	9,3566	6,8103	1545,1	1543,6	0,098
28	$Ca_5\ (PO_4)_3\ F_{0.41}\ Cl_{0.59}$	9,5485	6,8237	9,5379	6,8072	1610,7	1603,3	0,463
29	$Sr_6\ Ca_4\ (PO_4)_6\ F_2$	9,63	7,22	9,5936	7,1525	1733,5	1704,3	1,682
30	$Sr_{7.3}\ Ca_{2.7}\ (PO_4)_6\ F_2$	9,565	7,115	9,646	7,2127	1685,3	1737,5	3,097
31	$Ca_{9.37}\ Sr_{0.63}\ (PO_4)_6\ F_2$	9,3902	6,9011	9,4012	6,8878	1575,4	1576,1	0,041
32	$Ca_5\ (PO_4)_3\ F_{0.17}\ Cl_{0.83}$	9,6205	6,7761	9,6012	6,7798	1623,7	1618,1	0,346
33	$Ca_5\ (AsO_4)_3\ F$	9,75	6,92	9,7251	6,9385	1703,1	1699,0	0,244
34	$Ca_5\ (AsO_4)_3\ OH$	9,7	6,93	9,7503	6,931	1688,1	1705,9	1,054
						Average percent error for volume:		0,855

4.3 Prediction Performance

Prediction dataset was taken from the literature to make sure that the network was generalized without overfitting and produced accurate results. Prediction of new apatite candidates by using BR method is presented in Table 4.10. Results obtained for both lattice parameters closely matched with the ones taken from the literature [9], but data between 54-66 (except 64) had the lattice parameter a, higher than 10 Å in this study. These data were smaller than 10 Å in the other work and thought as unreliable because of that, so there was a possibility that slightly better predictions were made in our work. In addition, unit cell volume of each apatite were calculated and can be seen in Table 4.10.

Table 4.10 Prediction of new apatite candidates by using Bayesian regularization.

#	Apatite formula	Average Radii A	Average Radii B	Average Radii C	a (Å)	c (Å)	Unit Cell Vol. (Å^3)
1	$Ba_5(AsO_4)_3F$	1,35	0,46	1,33	10,4437	7,7991	2202,3
2	$Ba_5(AsO_4)_3Cl$	1,35	0,46	1,81	10,5226	7,7364	2217,8
3	$Ba_5(AsO_4)_3Br$	1,35	0,46	1,96	10,5529	7,7035	2221,1
4	$Ba_5(AsO_4)_3OH$	1,35	0,46	1,37	10,4501	7,7964	2204,3
5	$Ba_5(CrO_4)_3F$	1,35	0,55	1,33	10,4295	7,8773	2218,4
6	$Ba_5(CrO_4)_3Br$	1,35	0,55	1,96	10,4300	7,7464	2181,7
7	$Ba_5(VO_4)_3Cl$	1,35	0,54	1,81	10,4321	7,7835	2193,0
8	$Ba_5(VO_4)_3Br$	1,35	0,54	1,96	10,4580	7,743	2192,5
9	$Ba_5(VO_4)_3OH$	1,35	0,54	1,37	10,4382	7,8652	2218,7
10	$Ca_5(AsO_4)_3Br$	1	0,46	1,96	10,1650	6,7571	1807,6
11	$Ca_5(CrO_4)_3F$	1	0,55	1,33	9,7106	7,0047	1710,1
12	$Ca_5(CrO_4)_3Cl$	1	0,55	1,81	10,0804	6,8469	1801,3
13	$Cd_5(AsO_4)_3F$	0,95	0,46	1,33	9,6724	6,7879	1644,1
14	$Cd_5(AsO_4)_3Cl$	0,95	0,46	1,81	10,0439	6,6527	1737,6
15	$Cd_5(AsO_4)_3OH$	0,95	0,46	1,37	9,7018	6,7796	1652,1
16	$Cd_5(CrO_4)_3F$	0,95	0,55	1,33	9,6744	6,8521	1660,4
17	$Cd_5(CrO_4)_3Cl$	0,95	0,55	1,81	10,0963	6,6859	1764,5
18	$Cd_5(CrO_4)_3OH$	0,95	0,55	1,37	9,7046	6,8411	1668,1

Table 4.10 (continued)

#	Apatite formula	Average Radii A	Average Radii B	Average Radii C	a (Å)	c (Å)	Unit Cell Vol. (Å^3)
19	$Cd_5(PO_4)_3F$	0,95	0,38	1,33	9,3041	6,7061	1503,0
20	$Cd_5(VO_4)_3F$	0,95	0,54	1,33	9,6901	6,8464	1664,4
21	$Cd_5(VO_4)_3Cl$	0,95	0,54	1,81	10,1087	6,6835	1768,2
22	$Cd_5(VO_4)_3OH$	0,95	0,54	1,37	9,7204	6,8357	1672,2
23	$Pb_5(AsO_4)_3F$	1,19	0,46	1,33	10,0646	7,4461	1952,8
24	$Pb_5(AsO_4)_3Br$	1,19	0,46	1,96	10,2919	7,312	2005,2
25	$Pb_5(AsO_4)_3OH$	1,19	0,46	1,37	10,0748	7,4414	1955,5
26	$Pb_5(CrO_4)_3F$	1,19	0,55	1,33	10,0204	7,5197	1954,8
27	$Pb_5(CrO_4)_3Cl$	1,19	0,55	1,81	10,1538	7,3988	1974,9
28	$Pb_5(CrO_4)_3Br$	1,19	0,55	1,96	10,2350	7,3462	1992,4
29	$Pb_5(CrO_4)_3OH$	1,19	0,55	1,37	10,0236	7,5124	1954,1
30	$Pb_5(PO_4)_3F$	1,19	0,38	1,33	9,7836	7,3572	1823,2
31	$Pb_5(PO_4)_3Br$	1,19	0,38	1,96	9,9731	7,2578	1868,9
32	$Pb_5(VO_4)_3F$	1,19	0,54	1,33	10,0385	7,5129	1960,1
33	$Pb_5(VO_4)_3Br$	1,19	0,54	1,96	10,2575	7,3438	2000,5
34	$Pb_5(VO_4)_3OH$	1,19	0,54	1,37	10,0426	7,5059	1959,9
35	$Sr_5(AsO_4)_3F$	1,18	0,46	1,33	10,0423	7,4219	1937,8
36	$Sr_5(AsO_4)_3Cl$	1,18	0,46	1,81	10,2115	7,3292	1978,6
37	$Sr_5(AsO_4)_3Br$	1,18	0,46	1,96	10,2803	7,2853	1993,4
38	$Sr_5(AsO_4)_3OH$	1,18	0,46	1,37	10,0530	7,417	1940,7
39	$Sr_5(CrO_4)_3F$	1,18	0,55	1,33	9,9980	7,4951	1939,7
40	$Sr_5(CrO_4)_3Br$	1,18	0,55	1,96	10,2286	7,3189	1982,5
41	$Sr_5(CrO_4)_3OH$	1,18	0,55	1,37	10,0022	7,4877	1939,4
42	$Sr_5(VO_4)_3F$	1,18	0,54	1,33	10,0162	7,4884	1945,0
43	$Sr_5(VO_4)_3Cl$	1,18	0,54	1,81	10,1669	7,3688	1972,0
44	$Sr_5(VO_4)_3Br$	1,18	0,54	1,96	10,2506	7,3166	1990,4
45	$Sr_5(VO_4)_3OH$	1,18	0,54	1,37	10,0212	7,4812	1945,1
46	$Mn_5(AsO_4)_3F$	0,83	0,46	1,33	9,6098	6,3967	1529,4
47	$Mn_5(AsO_4)_3F$	0,83	0,46	1,37	9,6479	6,3869	1539,2
48	$Mn_5(CrO_4)_3F$	0,83	0,55	1,33	9,6604	6,4572	1560,2
49	$Mn_5(CrO_4)_3OH$	0,83	0,55	1,37	9,7020	6,4447	1570,6
50	$Mn_5(PO_4)_3F$	0,83	0,38	1,33	9,1750	6,319	1377,2
51	$Mn_5(PO_4)_3Cl$	0,83	0,38	1,81	9,5388	6,1937	1459,1
52	$Mn_5(PO_4)_3OH$	0,83	0,38	1,37	9,2074	6,3117	1385,3
53	$Mn_5(VO_4)_3F$	0,83	0,54	1,33	9,6723	6,4519	1562,7
54	$Mn_5(VO_4)_3OH$	0,83	0,54	1,37	9,7137	6,4397	1573,1

Table 4.10 (continued)

#	Apatite formula	Average Radii A	Average Radii B	Average Radii C	a (Å)	c (Å)	Unit Cell Vol. (Å^3)
55	$Ca_5(CrO_4)_3Br$	1	0,55	1,96	10,2164	6,7828	1832,9
56	$Ca_5(VO_4)_3Br$	1	0,54	1,96	10,2289	6,7813	1837,0
57	$Cd_5(AsO_4)_3Br$	0,95	0,46	1,96	10,1596	6,595	1762,4
58	$Cd_5(CrO_4)_3Br$	0,95	0,55	1,96	10,2410	6,6195	1797,4
59	$Cd_5(VO_4)_3Br$	0,95	0,54	1,96	10,2506	6,618	1800,4
60	$Mn_5(AsO_4)_3Cl$	0,83	0,46	1,81	10,0531	6,2433	1633,6
61	$Mn_5(AsO_4)_3Br$	0,83	0,46	1,96	10,1784	6,1807	1657,8
62	$Mn_5(CrO_4)_3Cl$	0,83	0,55	1,81	10,1749	6,275	1681,9
63	$Mn_5(CrO_4)_3Br$	0,83	0,55	1,96	10,3308	6,205	1714,5
64	$Mn_5(PO_4)_3Br$	0,83	0,38	1,96	9,6395	6,1388	1476,8
65	$Mn_5(VO_4)_3Cl$	0,83	0,54	1,81	10,1806	6,2727	1683,2
66	$Mn_5(VO_4)_3Br$	0,83	0,54	1,96	10,3332	6,2034	1714,9

Another dataset was prepared by taking the unused data from Table 4.2 to see the performance of the neural network on different compositions of apatites. This dataset consisted the data that contained pure apatites as well as double and triple substituted apatites with different ionic charges. Lattice parameters of these apatites were determined from experimental results and it was useful to test the network on this dataset for both verifying the accuracy of this method and examining the effect of substitutions and charge differences in the experimental studies. Results for BR method can be seen in Table 4.11. Even on this challenging test, by using 67 data the network generated errors of 0.570% and 0.792% for lattice parameters a and c, respectively. Highest errors were 2.663% for **a** and 3.142% for **c**. With these results, BR method proved to be highly reliable for the prediction of lattice parameters of stoichiometric apatites regardless of multiple substitutions and charge differences of ions at each site. Also high prediction accuracy was observed for a few slightly non-stoichiometric apatites.

Comparison of calculated and predicted unit cell volumes of apatites found in Table 4.11 are given in Table 4.12. Average error for the dataset was 1.542%, but there were rather large errors for a few data, the highest one being 7.708%. This test showed that volume prediction for heavily substituted apatites with different ionic charges may lead to inaccurate results that were unreliable for scientific applications.

Same predictions that are shown in Table 4.11 were also made with other successful learning methods for a comparison and can be seen in Tables 4.13 and 4.14 for LM and SCG methods, respectively. Results were close to BR method with slightly less prediction accuracy and individual distribution of errors were small for most data but rather large for a few data with a maximum of 2.841% for **a** and 4.285% for **c** with LM method and 2.684% for **a** and 5.556% for **c** with SCG method. Most accurate results were obtained with BR but this method performs better with small training datasets and in the [-1,1] data range [71], so other methods may also give better results for large datasets with different data ranges. While considering which learning method to choose, it is also important to consider computer memory requirements. LM and other learning methods that use second order derivatives for error determination are faster than algorithms that use first order derivatives but they also use more memory [71]. In this study, training dataset was rather small so memory usage was not a constraint. However, slower methods must be considered for similar applications with large datasets and many input variables even if they give less accurate results to end the training of the network at a reasonable time.

Comparison of lattice parameters and volume predictions by using Tables 4.11-4.14 are given in Table 4.15. It was clearly seen that BR method gave the most accurate results while other methods generated close but less accurate outputs.

Lattice parameters and volumes of some possible apatite compounds that were not presented before in the literature were predicted and the results are given in Table 4.16. It was not checked if these apatites were thermodynamically stable, so results were given as if they exist. Ag, Fe, Mg, Co and Zn ions were substituted for site A and other sites were repeated as before which was P, V, Cr and As substitution for site B and OH, F, Cl and Br substitution for site C. Ions at site A were chosen because they are commonly used in materials science, so data obtained by using them may be useful in a variety of applications.

Finally, lattice parameter and volume prediction of some approximately calculated apatite formulas by using data from relevant literature are given in Tables 4.17 and 4.18, respectively. The formulas in these tables were calculated by examining the relevant journals and deciding which sites may be substituted in certain amounts of specific ions. These formulas were not guaranteed to be true and error margins of some of them were ignored, but their results gave clues about the accuracy of the calculated formula by comparing predicted and experimental lattice parameters. In addition, the trained network can be used for predicting the reliability of formulas found by experimental methods by comparing them with predicted lattice parameters. Accurate results could be found even without providing exact stoichiometric data but it should be noted that shift of the peaks caused slight deviations of lattice parameters of unsintered and sintered specimens [97], so the amount of deviation should be considered while evaluating the results and calculated whenever possible.

It was shown in Table 4.17 that prediction performance of non-stoichiometric apatites were less successful and error may increase in some situations as in one example of reference [103] because of the insufficient accuracy of the formula determination. The reason of decreased prediction accuracy for some non-stoichiometric apatites may be because of point defects like vacancies, additional

interstitial and substitutional atoms and differences in charge balance of the solid associated with these defects. In addition, trained network cannot determine the maximum amount of ions that can be doped into each apatite, so maximum doping amount and the role of extra ions in the lattice may change prediction results especially for non-stoichiometric apatites. Also, training dataset for the neural network contains a rather limited variety of probabilities for site B, causing prediction harder for non-stoichiometric data with complex B sites. Results from reference [41] lead to high errors but the errors were acknowledged by the authors to be high in their study. The reason was probably because of some calculation error in XRD spectras which were not shown in the mentioned reference.

Table 4.11 Prediction of both pure apatites and apatites with multiple substitutions with different ionic charges with BR method.

	Apatite formula	Average Radii A	Average Radii B	Average Radii C	a	c	a output	c output	error% (a)	error% (c)
1	$Pb_5 (PO_4)_3 F$	1,19	0,38	1,33	9,76	7,3	9,7836	7,3572	0,242	0,784
2	$Ca_{9.3} Mn_{0.7} (PO_4)_6 F_2$	0,9881	0,38	1,33	9,3323	6,8424	9,362	6,8202	0,318	0,324
3	$Mn_5 (PO_4)_3 Cl_{0.9} (OH)_{0.1}$	0,83	0,38	1,766	9,532	6,199	9,508	6,2085	0,252	0,153
4	$Sr_5 (PO_4)_3 F_{0.75} Br_{0.25}$	1,18	0,38	1,4875	9,7186	7,2853	9,8112	7,3195	0,953	0,469
5	$Sr_5 (PO_4)_3 F_{0.5} Br_{0.5}$	1,18	0,38	1,645	9,7623	7,2699	9,86	7,298	1,001	0,387
6	$Sr_5 (PO_4)_3 F_{0.25} Br_{0.75}$	1,18	0,38	1,8025	9,8885	7,2344	9,9078	7,2687	0,195	0,474
7	$Sr_{4.99} Eu_{0.01} (PO_4)_3 Cl_{0.75} Br_{0.25}$	1,17998	0,38	1,8475	9,8909	7,1934	9,9213	7,2588	0,307	0,909
8	$Sr_{4.99} Eu_{0.01} (PO_4)_3 Cl_{0.5} Br_{0.5}$	1,17998	0,38	1,885	9,9056	7,195	9,9326	7,2501	0,273	0,766
9	$Sr_{4.99} Eu_{0.01} (PO_4)_3 Cl_{0.25} Br_{0.75}$	1,17998	0,38	1,9225	9,9934	7,202	9,944	7,241	0,494	0,542
10	$Sr_{4.99} Eu_{0.01} (PO_4)_3 Br$	1,17998	0,38	1,96	9,9636	7,2061	9,9553	7,2314	0,083	0,351
11	$Ca_{2.6} Sr_{2.4} (PO_4)_3 Cl$	1,0864	0,38	1,81	9,737	7,022	9,751	7,0134	0,144	0,122
12	$Ca_{4.6} Sr_{0.4} (PO_4)_3 Cl$	1,0144	0,38	1,81	9,653	6,777	9,6606	6,8017	0,079	0,364
13	$Ca_{4.9} Sr_{0.1} (PO_4)_3 Cl$	1,0036	0,38	1,81	9,643	6,766	9,6494	6,7687	0,066	0,040
14	$Sr_{4.99} Eu_{0.01} (PO_4)_3 Cl$	1,17998	0,38	1,81	9,878	7,1893	9,91	7,267	0,324	1,081
15	$Sr_{2.54} Ca_{2.45} Eu_{0.01} (PO_4)_3 Cl$	1,09178	0,38	1,81	9,754	7,0061	9,7589	7,0287	0,050	0,323
16	$Sr_{4.99} Eu_{0.01} (PO_4)_3 Cl_{0.75} F_{0.25}$	1,17998	0,38	1,69	9,8697	7,1966	9,8737	7,2904	0,041	1,303
17	$Sr_{4.99} Eu_{0.01} (PO_4)_3 Cl_{0.5} F_{0.5}$	1,17998	0,38	1,57	9,8042	7,2357	9,8369	7,3092	0,334	1,016
18	$Sr_{4.99} Eu_{0.01} (PO_4)_3 Cl_{0.25} F_{0.75}$	1,17998	0,38	1,45	9,7357	7,2769	9,7992	7,3234	0,652	0,639
19	$Ca_{2.1} Pb_{7.9} (PO_4)_6 Cl_2$	1,1501	0,38	1,81	9,99	7,276	9,8542	7,1887	1,359	1,200
20	$K_2 Pb_6 Eu_2 (PO_4)_6 F_2$	1,18	0,38	1,33	9,7482	7,2655	9,7597	7,3331	0,118	0,930
21	$K Pb_8 Nd (PO_4)_6 F_2$	1,188	0,38	1,33	9,7768	7,2791	9,7788	7,3524	0,020	1,007

Table 4.11 (continued)

	Apatite formula	Average Radii A	Average Radii B	Average Radii C	a	c	a output	c output	error% (a)	error% (c)
22	$K_2\ Pb_6\ Nd_2\ (PO_4)_6\ F_2$	1,186	0,38	1,33	9,7604	7,2754	9,774	7,3476	0,139	0,992
23	$Pb_6\ Eu_2\ Na_2\ (PO_4)_6\ F_2$	1,108	0,38	1,33	9,655	7,058	9,5936	7,1525	0,636	1,339
24	$Pb_8\ Eu\ Na\ (PO_4)_6\ F_2$	1,149	0,38	1,33	9,73	7,176	9,6865	7,257	0,447	1,129
25	$Pb_6\ La_2\ Na_2\ (PO_4)_6\ F_2$	1,124	0,38	1,33	9,721	7,15	9,6292	7,1938	0,944	0,613
26	$Pb_4\ La_3\ Na_3\ (PO_4)_6\ F_2$	1,091	0,38	1,33	9,725	7,158	9,5568	7,1078	1,730	0,701
27	$Pb_6\ Nd_2\ Na_2\ (PO_4)_6\ F_2$	1,114	0,38	1,33	9,661	7,067	9,6069	7,1681	0,560	1,431
28	$Pb_4\ Nd_3\ Na_3\ (PO_4)_6\ F_2$	1,076	0,38	1,33	9,616	7,029	9,5252	7,0677	0,944	0,551
29	$Pb_8\ Nd\ Na\ (PO_4)_6\ F_2$	1,152	0,38	1,33	9,741	7,198	9,6935	7,2645	0,488	0,924
30	$Pb\ Y_2\ Na_2\ (PO_4)_6\ F_2$	1,006	0,38	1,33	9,649	7,055	9,392	6,8724	2,663	2,588
31	$Pb_8\ Y\ Na\ (PO_4)_6\ F_2$	1,144	0,38	1,33	9,712	7,17	9,6749	7,2445	0,382	1,039
32	$Pb_6\ Bi_2\ Na_2\ (PO_4)_6\ F_2$	1,124	0,38	1,33	9,6956	7,1826	9,6292	7,1938	0,685	0,156
33	$Pb_{10}\ (PO_4)_6\ F_2$	1,19	0,38	1,33	9,773	7,315	9,7836	7,3572	0,108	0,577
34	$Ca_{4.5}\ Pb_{5.5}\ (PO_4)_6\ F_2$	1,1045	0,38	1,33	9,759	7,291	9,5859	7,1434	1,774	2,024
35	$Ba_3\ La\ Na\ (PO_4)_3\ F$	1,22	0,38	1,33	9,9392	7,4419	9,856	7,4277	0,837	0,191
36	$Ba_4\ Nd_3\ Na_3\ (PO_4)_6\ F_2$	1,14	0,38	1,33	9,786	7,281	9,6657	7,2345	1,229	0,639
37	$Ca_{2.5}\ Pb_{7.5}\ (PO_4)_6\ (OH)_2$	1,1425	0,38	1,37	9,88	7,417	9,6859	7,2376	1,965	2,419
38	$Ca_2\ Ba_3\ (PO_4)_3\ F$	1,21	0,38	1,33	9,845	7,359	9,8318	7,4044	0,134	0,617
39	$Ca_5\ (PO_4)_3\ F_{0.39}\ Cl_{0.33}\ (OH)_{0.28}$	1	0,38	1,4996	9,4615	6,8491	9,4751	6,8297	0,144	0,283
40	$Ca_5\ (PO_4)_3\ F_{0.29}\ Cl_{0.47}\ (OH)_{0.24}$	1	0,38	1,5652	9,4877	6,8224	9,5114	6,8173	0,250	0,075
41	$Co\ Ca_4\ (PO_4)_3\ Cl$	0,93	0,38	1,81	9,625	6,747	9,5875	6,535	0,390	3,142
42	$Sr_{2.54}\ Ba_{2.45}\ Eu_{0.01}\ (PO_4)_3\ Cl$	1,26328	0,38	1,81	10,0265	7,4099	10,087	7,4728	0,603	0,849

Table 4.11 (continued)

	Apatite formula	Average Radii A	Average Radii B	Average Radii C	a	c	a output	c output	error% (a)	error% (c)
43	$Ba_{4.99}\ Eu_{0.01}\ (PO_4)_3\ Cl$	1,34964	0,38	1,81	10,2712	7,65	10,295	7,6672	0,232	0,225
44	$Sr_{4.99}\ Eu_{0.01}\ (PO_4)_3\ Cl$	1,17998	0,38	1,81	9,878	7,1893	9,91	7,267	0,324	1,081
45	$Ca_2\ Pb_3\ (AsO_4)_3\ Cl$	1,114	0,46	1,81	10,14	7,185	10,133	7,1501	0,069	0,486
46	$Pb_5\ (VO_4)_3\ Cl$	1,19	0,54	1,81	10,3174	7,3378	10,177	7,3954	1,361	0,785
47	$Ca_{10}\ (VO_4)\ (PO_4)_5\ (OH)_2$	1	0,407	1,37	9,467	6,904	9,5646	6,8795	1,031	0,355
48	$Ca_{10}\ (VO_4)_2\ (PO_4)_4\ (OH)_2$	1	0,433	1,37	9,535	6,927	9,679	6,9065	1,510	0,296
49	$Ca_{10}\ (VO_4)_3\ (PO_4)_3\ (OH)_2$	1	0,46	1,37	9,586	6,943	9,7503	6,931	1,714	0,173
50	$Ca_{10}\ (VO_4)_4\ (PO_4)_2\ (OH)_2$	1	0,487	1,37	9,649	6,986	9,7827	6,9529	1,386	0,474
51	$Ca_{10}\ (VO_4)_5\ (PO_4)\ (OH)_2$	1	0,513	1,37	9,695	6,986	9,7816	6,9722	0,893	0,198
52	$Pb_{10}\ (PO_4)_6\ Br_2$	1,19	0,38	1,96	10,062	7,359	9,9731	7,2578	0,884	1,375
53	$Ca_{10}\ (PO_4)_{5.83}\ (SiO_4)_{0.17}\ (OH)_{1.83}$	1	0,381	1,37	9,41763	6,88545	9,4076	6,8506	0,107	0,506
54	$Ca_{10}\ (PO_4)_{5.65}\ (SiO_4)_{0.35}\ (OH)_{1.65}$	1	0,381	1,37	9,41869	6,88683	9,4117	6,8513	0,074	0,516
55	$Ca_{10}\ (PO_4)_{5.48}\ (SiO_4)_{0.52}\ (OH)_{1.48}$	1	0,382	1,37	9,42158	6,89155	9,4156	6,8519	0,063	0,575
56	$Ca_{10}\ (PO_4)_{5.30}\ (SiO_4)_{0.70}\ (OH)_{1.30}$	1	0,382	1,37	9,42332	6,89703	9,4197	6,8526	0,038	0,644
57	$Ca_{10}\ (PO_4)_{5.84}\ (SiO_4)_{0.16}\ (OH)_{1.84}$	1	0,381	1,37	9,4082	6,8828	9,4074	6,8506	0,009	0,468
58	$Na\ Y_9\ (SiO_4)_6\ O_2$	0,912	0,4	1,4	9,334	6,759	9,442	6,5979	1,157	2,383
59	$Sr_9\ La\ (PO_4)_5\ (SiO_4)\ F_2$	1,165	0,383	1,33	9,723	7,282	9,7436	7,3008	0,212	0,258
60	$Sr_8\ La_2\ (PO_4)_4\ (SiO_4)_2\ F_2$	1,15	0,387	1,33	9,727	7,277	9,7277	7,2677	0,007	0,128
61	$Sr_6\ La_4\ (PO_4)_2\ (SiO_4)_4\ F_2$	1,12	0,393	1,33	9,732	7,27	9,6968	7,1997	0,362	0,967
62	$Sr_4\ La_6\ (SiO_4)_6\ F_2$	1,09	0,4	1,33	9,737	7,265	9,668	7,1289	0,709	1,873
63	$Sr_{10}\ (PO_4)_6\ O$	1,18	0,38	1,4	9,753	7,276	9,783	7,328	0,308	0,715

Table 4.11 (continued)

	Apatite formula	Average Radii A	Average Radii B	Average Radii C	a	c	a output	c output	error% (a)	error% (c)
64	$Sr_9\ La\ (PO_4)_5\ (SiO_4)\ O$	1,165	0,383	1,4	9,756	7,272	9,7676	7,2952	0,119	0,319
65	$Sr_8\ La_2\ (PO_4)_4\ (SiO_4)_2\ O$	1,15	0,386	1,4	9,761	7,267	9,7526	7,2617	0,086	0,073
66	$Sr_6\ La_4\ (PO_4)_2\ (SiO_4)_4\ O$	1,12	0,393	1,4	9,768	7,258	9,7239	7,1926	0,451	0,901
67	$Sr_4\ La_6\ (SiO_4)_6\ O$	1,09	0,4	1,4	9,771	7,255	9,6982	7,1208	0,745	1,850
					Average Percent Errors of Outputs:				0,570	0,792

Table 4.12 Comparison of the calculated and predicted volumes of apatites that are listed in Table 4.11.

	Apatite formula	a	c	a output	c output	Vol. (unit cell)	Vol. (predicted)	Vol. (error%)
1	$Pb_5\ (PO_4)3\ F$	9,76	7,3	9,7836	7,3572	1800,3	1823,2	1,272
2	$Ca_{9.3}\ Mn_{0.7}\ (PO_4)_6\ F_2$	9,3323	6,8424	9,362	6,8202	1542,8	1547,6	0,311
3	$Mn_5\ (PO_4)_3\ Cl_{0.9}\ (OH)_{0.1}$	9,532	6,199	9,508	6,2085	1458,2	1453,1	0,350
4	$Sr_5\ (PO_4)_3\ F_{0.75}\ Br_{0.25}$	9,7186	7,2853	9,8112	7,3195	1781,5	1824,1	2,393
5	$Sr_5\ (PO_4)_3\ F_{0.5}\ Br_{0.5}$	9,7623	7,2699	9,86	7,298	1793,8	1836,9	2,406
6	$Sr_5\ (PO_4)_3\ F_{0.25}\ Br_{0.75}$	9,8885	7,2344	9,9078	7,2687	1831,5	1847,3	0,867
7	$Sr_{4.99}\ Eu_{0.01}\ (PO_4)_3\ Cl_{0.75}\ Br_{0.25}$	9,8909	7,1934	9,9213	7,2588	1822,0	1849,8	1,530
8	$Sr_{4.99}\ Eu_{0.01}\ (PO_4)_3\ Cl_{0.5}\ Br_{0.5}$	9,9056	7,195	9,9326	7,2501	1827,8	1851,8	1,316
9	$Sr_{4.99}\ Eu_{0.01}\ (PO_4)_3\ Cl_{0.25}\ Br_{0.75}$	9,9934	7,202	9,944	7,241	1862,1	1853,8	0,450

Table 4.12 (continued)

	Apatite formula	a	c	a output	c output	Vol. (unit cell)	Vol. (predicted)	Vol. (error%)
10	$Sr_{4.99}\ Eu_{0.01}\ (PO_4)_3\ Br$	9,9636	7,2061	9,9553	7,2314	1852,1	1855,5	0,184
11	$Ca_{2.6}\ Sr_{2.4}\ (PO_4)_3\ Cl$	9,737	7,022	9,751	7,0134	1723,6	1726,5	0,165
12	$Ca_{4.6}\ Sr_{0.4}\ (PO_4)_3\ Cl$	9,653	6,777	9,6606	6,8017	1634,9	1643,5	0,523
13	$Ca_{4.9}\ Sr_{0.1}\ (PO_4)_3\ Cl$	9,643	6,766	9,6494	6,7687	1628,9	1631,7	0,173
14	$Sr_{4.99}\ Eu_{0.01}\ (PO_4)_3\ Cl$	9,878	7,1893	9,91	7,267	1816,2	1847,7	1,737
15	$Sr_{2.54}\ Ca_{2.45}\ Eu_{0.01}\ (PO_4)_3\ Cl$	9,754	7,0061	9,7589	7,0287	1725,7	1733,0	0,423
16	$Sr_{4.99}\ Eu_{0.01}\ (PO_4)_3\ Cl_{0.75}\ F_{0.25}$	9,8697	7,1966	9,8737	7,2904	1815,0	1840,1	1,386
17	$Sr_{4.99}\ Eu_{0.01}\ (PO_4)_3\ Cl_{0.5}\ F_{0.5}$	9,8042	7,2357	9,8369	7,3092	1800,7	1831,1	1,691
18	$Sr_{4.99}\ Eu_{0.01}\ (PO_4)_3\ Cl_{0.25}\ F_{0.75}$	9,7357	7,2769	9,7992	7,3234	1785,7	1820,6	1,956
19	$Ca_{2.1}\ Pb_{7.9}\ (PO_4)_6\ Cl_2$	9,99	7,276	9,8542	7,1887	1880,0	1807,3	3,868
20	$K_2\ Pb_6\ Eu_2\ (PO_4)_6\ F_2$	9,7482	7,2655	9,7597	7,3331	1787,5	1808,4	1,169
21	$K\ Pb_8\ Nd\ (PO_4)_6\ F_2$	9,7768	7,2791	9,7788	7,3524	1801,4	1820,3	1,048
22	$K_2\ Pb_6\ Nd_2\ (PO_4)_6\ F_2$	9,7604	7,2754	9,774	7,3476	1794,4	1817,3	1,274
23	$Pb_6\ Eu_2\ Na_2\ (PO_4)_6\ F_2$	9,655	7,058	9,5936	7,1525	1703,4	1704,3	0,054
24	$Pb_8\ Eu\ Na\ (PO_4)_6\ F_2$	9,73	7,176	9,6865	7,257	1758,9	1762,9	0,227
25	$Pb_6\ La_2\ Na_2\ (PO_4)_6\ F_2$	9,721	7,15	9,6292	7,1938	1749,3	1726,9	1,279
26	$Pb_4\ La_3\ Na_3\ (PO_4)_6\ F_2$	9,725	7,158	9,5568	7,1078	1752,7	1680,7	4,106
27	$Pb_6\ Nd_2\ Na_2\ (PO_4)_6\ F_2$	9,661	7,067	9,6069	7,1681	1707,7	1712,8	0,298
28	$Pb_4\ Nd_3\ Na_3\ (PO_4)_6\ F_2$	9,616	7,029	9,5252	7,0677	1682,7	1660,2	1,339
29	$Pb_8\ Nd\ Na\ (PO_4)_6\ F_2$	9,741	7,198	9,6935	7,2645	1768,3	1767,3	0,058
30	$Pb\ Y_2\ Na_2\ (PO_4)_6\ F_2$	9,649	7,055	9,392	6,8724	1700,6	1569,5	7,708
31	$Pb_8\ Y\ Na\ (PO_4)_6\ F_2$	9,712	7,17	9,6749	7,2445	1750,9	1755,6	0,269

Table 4.12 (continued)

	Apatite formula	a	c	a output	c output	Vol. (unit cell)	Vol. (predicted)	Vol. (error%)
32	$Pb_6\ Bi_2\ Na_2\ (PO_4)_6\ F_2$	9,6956	7,1826	9,6292	7,1938	1748,1	1726,9	1,211
33	$Pb_{10}\ (PO_4)_6\ F_2$	9,773	7,315	9,7836	7,3572	1808,8	1823,2	0,795
34	$Ca_{4.5}\ Pb_{5.5}\ (PO_4)_6\ F_2$	9,759	7,291	9,5859	7,1434	1797,8	1699,4	5,469
35	$Ba_3\ La\ Na\ (PO_4)_3\ F$	9,9392	7,4419	9,856	7,4277	1903,4	1868,0	1,855
36	$Ba_4\ Nd_3\ Na_3\ (PO_4)_6\ F_2$	9,786	7,281	9,6657	7,2345	1805,2	1749,9	3,067
37	$Ca_{2.5}\ Pb_{7.5}\ (PO_4)_6\ (OH)_2$	9,88	7,417	9,6859	7,2376	1874,5	1758,0	6,215
38	$Ca_2\ Ba_3\ (PO_4)_3\ F$	9,845	7,359	9,8318	7,4044	1846,6	1853,1	0,347
39	$Ca_5\ (PO_4)_3\ F_{0.39}\ Cl_{0.33}\ (OH)_{0.28}$	9,4615	6,8491	9,4751	6,8297	1587,4	1587,5	0,004
40	$Ca_5\ (PO_4)_3\ F_{0.29}\ Cl_{0.47}\ (OH)_{0.24}$	9,4877	6,8224	9,5114	6,8173	1590,0	1596,7	0,425
41	$Co\ Ca_4\ (PO_4)_3\ Cl$	9,625	6,747	9,5875	6,535	1618,2	1555,2	3,895
42	$Sr_{2.54}\ Ba_{2.45}\ Eu_{0.01}\ (PO_4)_3\ Cl$	10,0265	7,4099	10,087	7,4728	1928,6	1968,5	2,070
43	$Ba_{4.99}\ Eu_{0.01}\ (PO_4)_3\ Cl$	10,2712	7,65	10,295	7,6672	2089,5	2103,9	0,690
44	$Sr_{4.99}\ Eu_{0.01}\ (PO_4)_3\ Cl$	9,878	7,1893	9,91	7,267	1816,2	1847,7	1,737
45	$Ca_2\ Pb_3\ (AsO_4)_3\ Cl$	10,14	7,185	10,133	7,1501	1912,6	1900,7	0,623
46	$Pb_5\ (VO_4)_3\ Cl$	10,3174	7,3378	10,177	7,3954	2022,3	1983,0	1,939
47	$Ca_{10}\ (VO_4)\ (PO_4)_5\ (OH)_2$	9,467	6,904	9,5646	6,8795	1602,0	1629,4	1,710
48	$Ca_{10}\ (VO_4)_2\ (PO_4)_4\ (OH)_2$	9,535	6,927	9,679	6,9065	1630,5	1675,1	2,738
49	$Ca_{10}\ (VO_4)_3\ (PO_4)_3\ (OH)_2$	9,586	6,943	9,7503	6,931	1651,8	1705,9	3,278
50	$Ca_{10}\ (VO_4)_4\ (PO_4)_2\ (OH)_2$	9,649	6,986	9,7827	6,9529	1683,9	1722,7	2,303
51	$Ca_{10}\ (VO_4)_5\ (PO_4)\ (OH)_2$	9,695	6,986	9,7816	6,9722	1700,0	1727,1	1,593
52	$Pb_{10}\ (PO_4)_6\ Br_2$	10,062	7,359	9,9731	7,2578	1928,9	1868,9	3,110
53	$Ca_{10}\ (PO_4)_{5.83}\ (SiO_4)_{0.17}\ (OH)_{1.83}$	9,41763	6,88545	9,4076	6,8506	1581,1	1569,7	0,718

Table 4.12 (continued)

	Apatite formula	a	c	a output	c output	Vol. (unit cell)	Vol. (predicted)	Vol. (error%)
54	$Ca_{10}(PO_4)_{5.65}(SiO_4)_{0.35}(OH)_{1.65}$	9,41869	6,88683	9,4117	6,8513	1581,7	1571,2	0,664
55	$Ca_{10}(PO_4)_{5.48}(SiO_4)_{0.52}(OH)_{1.48}$	9,42158	6,89155	9,4156	6,8519	1583,8	1572,7	0,702
56	$Ca_{10}(PO_4)_{5.30}(SiO_4)_{0.70}(OH)_{1.30}$	9,42332	6,89703	9,4197	6,8526	1585,6	1574,2	0,721
57	$Ca_{10}(PO_4)_{5.84}(SiO_4)_{0.16}(OH)_{1.84}$	9,4082	6,8828	9,4074	6,8506	1577,3	1569,6	0,485
58	$Na\ Y_9(SiO_4)_6\ O_2$	9,334	6,759	9,442	6,5979	1524,6	1522,9	0,111
59	$Sr_9\ La(PO_4)_5(SiO_4)\ F_2$	9,723	7,282	9,7436	7,3008	1782,3	1794,5	0,683
60	$Sr_8\ La_2(PO_4)_4(SiO_4)_2\ F_2$	9,727	7,277	9,7277	7,2677	1782,6	1780,5	0,113
61	$Sr_6\ La_4(PO_4)_2(SiO_4)_4\ F_2$	9,732	7,27	9,6968	7,1997	1782,7	1752,7	1,682
62	$Sr_4\ La_6(SiO_4)_6\ F_2$	9,737	7,265	9,668	7,1289	1783,3	1725,2	3,259
63	$Sr_{10}(PO_4)_6\ O$	9,753	7,276	9,783	7,328	1791,8	1815,8	1,335
64	$Sr_9\ La(PO_4)_5(SiO_4)\ O$	9,756	7,272	9,7676	7,2952	1792,0	1802,0	0,558
65	$Sr_8\ La_2(PO_4)_4(SiO_4)_2\ O$	9,761	7,267	9,7526	7,2617	1792,6	1788,2	0,245
66	$Sr_6\ La_4(PO_4)_2(SiO_4)_4\ O$	9,768	7,258	9,7239	7,1926	1792,9	1760,8	1,794
67	$Sr_4\ La_6(SiO_4)_6\ O$	9,771	7,255	9,6982	7,1208	1793,3	1734,0	3,307
						Average percent error for volume:		1,542

Table 4.13 Prediction of both pure apatites and apatites with multiple substitutions with different ionic charges with LM method.

	Apatite formula	Average Radii A	Average Radii B	Average Radii C	a	c	a output	c output	error% (a)	error% (c)
1	$Pb_5 (PO_4)3 F$	1,19	0,38	1,33	9,76	7,3	9,7594	7,365	0,006	0,890
2	$Ca_{9.3} Mn_{0.7} (PO_4)_6 F_2$	0,9881	0,38	1,33	9,3323	6,8424	9,3456	6,8421	0,143	0,004
3	$Mn_5 (PO_4)_3 Cl_{0.9} (OH)_{0.1}$	0,83	0,38	1,766	9,532	6,199	9,4166	6,3632	1,211	2,649
4	$Sr_5 (PO_4)_3 F_{0.75} Br_{0.25}$	1,18	0,38	1,4875	9,7186	7,2853	9,9085	7,241	1,954	0,608
5	$Sr_5 (PO_4)_3 F_{0.5} Br_{0.5}$	1,18	0,38	1,645	9,7623	7,2699	9,9067	7,2038	1,479	0,909
6	$Sr_5 (PO_4)_3 F_{0.25} Br_{0.75}$	1,18	0,38	1,8025	9,8885	7,2344	9,9153	7,2228	0,271	0,160
7	$Sr_{4.99} Eu_{0.01} (PO_4)_3 Cl_{0.75} Br_{0.25}$	1,17998	0,38	1,8475	9,8909	7,1934	9,925	7,2294	0,345	0,500
8	$Sr_{4.99} Eu_{0.01} (PO_4)_3 Cl_{0.5} Br_{0.5}$	1,17998	0,38	1,885	9,9056	7,195	9,9346	7,234	0,293	0,542
9	$Sr_{4.99} Eu_{0.01} (PO_4)_3 Cl_{0.25} Br_{0.75}$	1,17998	0,38	1,9225	9,9934	7,202	9,9448	7,2378	0,486	0,497
10	$Sr_{4.99} Eu_{0.01} (PO_4)_3 Br$	1,17998	0,38	1,96	9,9636	7,2061	9,9553	7,2408	0,083	0,482
11	$Ca_{2.6} Sr_{2.4} (PO_4)_3 Cl$	1,0864	0,38	1,81	9,737	7,022	9,7575	7,0606	0,211	0,550
12	$Ca_{4.6} Sr_{0.4} (PO_4)_3 Cl$	1,0144	0,38	1,81	9,653	6,777	9,6538	6,8397	0,008	0,925
13	$Ca_{4.9} Sr_{0.1} (PO_4)_3 Cl$	1,0036	0,38	1,81	9,643	6,766	9,6395	6,7908	0,036	0,367
14	$Sr_{4.99} Eu_{0.01} (PO_4)_3 Cl$	1,17998	0,38	1,81	9,878	7,1893	9,9167	7,224	0,392	0,483
15	$Sr_{2.54} Ca_{2.45} Eu_{0.01} (PO_4)_3 Cl$	1,09178	0,38	1,81	9,754	7,0061	9,7659	7,0712	0,122	0,929
16	$Sr_{4.99} Eu_{0.01} (PO_4)_3 Cl_{0.75} F_{0.25}$	1,17998	0,38	1,69	9,8697	7,1966	9,9042	7,2063	0,350	0,135
17	$Sr_{4.99} Eu_{0.01} (PO_4)_3 Cl_{0.5} F_{0.5}$	1,17998	0,38	1,57	9,8042	7,2357	9,9158	7,2117	1,138	0,332
18	$Sr_{4.99} Eu_{0.01} (PO_4)_3 Cl_{0.25} F_{0.75}$	1,17998	0,38	1,45	9,7357	7,2769	9,8837	7,2604	1,520	0,227
19	$Ca_{2.1} Pb_{7.9} (PO_4)_6 Cl_2$	1,1501	0,38	1,81	9,99	7,276	9,8626	7,1718	1,275	1,432
20	$K_2 Pb_6 Eu_2 (PO_4)_6 F_2$	1,18	0,38	1,33	9,7482	7,2655	9,7357	7,3354	0,128	0,962
21	$K Pb_8 Nd (PO_4)_6 F_2$	1,188	0,38	1,33	9,7768	7,2791	9,7547	7,3591	0,226	1,099

Table 4.13 (continued)

	Apatite formula	Average Radii A	Average Radii B	Average Radii C	a	c	a output	c output	error% (a)	error% (c)
22	$K_2\ Pb_6\ Nd_2\ (PO_4)_6\ F_2$	1,186	0,38	1,33	9,7604	7,2754	9,7499	7,3532	0,108	1,069
23	$Pb_6\ Eu_2\ Na_2\ (PO_4)_6\ F_2$	1,108	0,38	1,33	9,655	7,058	9,5722	7,1304	0,858	1,026
24	$Pb_8\ Eu\ Na\ (PO_4)_6\ F_2$	1,149	0,38	1,33	9,73	7,176	9,6636	7,2434	0,682	0,939
25	$Pb_6\ La_2\ Na_2\ (PO_4)_6\ F_2$	1,124	0,38	1,33	9,721	7,15	9,6072	7,1726	1,171	0,316
26	$Pb_4\ La_3\ Na_3\ (PO_4)_6\ F_2$	1,091	0,38	1,33	9,725	7,158	9,536	7,0887	1,943	0,968
27	$Pb_6\ Nd_2\ Na_2\ (PO_4)_6\ F_2$	1,114	0,38	1,33	9,661	7,067	9,5852	7,1459	0,785	1,116
28	$Pb_4\ Nd_3\ Na_3\ (PO_4)_6\ F_2$	1,076	0,38	1,33	9,616	7,029	9,5051	7,0544	1,153	0,361
29	$Pb_8\ Nd\ Na\ (PO_4)_6\ F_2$	1,152	0,38	1,33	9,741	7,198	9,6704	7,2522	0,725	0,753
30	$Pb\ Y_2\ Na_2\ (PO_4)_6\ F_2$	1,006	0,38	1,33	9,649	7,055	9,3749	6,8961	2,841	2,252
31	$Pb_8\ Y\ Na\ (PO_4)_6\ F_2$	1,144	0,38	1,33	9,712	7,17	9,6521	7,2289	0,617	0,821
32	$Pb_6\ Bi_2\ Na_2\ (PO_4)_6\ F_2$	1,124	0,38	1,33	9,6956	7,1826	9,6072	7,1726	0,912	0,139
33	$Pb_{10}\ (PO_4)_6\ F_2$	1,19	0,38	1,33	9,773	7,315	9,7594	7,365	0,139	0,684
34	$Ca_{4.5}\ Pb_{5.5}\ (PO_4)_6\ F_2$	1,1045	0,38	1,33	9,759	7,291	9,5646	7,1216	1,992	2,323
35	$Ba_3\ La\ Na\ (PO_4)_3\ F$	1,22	0,38	1,33	9,9392	7,4419	9,8313	7,4507	1,086	0,118
36	$Ba_4\ Nd_3\ Na_3\ (PO_4)_6\ F_2$	1,14	0,38	1,33	9,786	7,281	9,643	7,2174	1,461	0,874
37	$Ca_{2.5}\ Pb_{7.5}\ (PO_4)_6\ (OH)_2$	1,1425	0,38	1,37	9,88	7,417	9,6968	7,1988	1,854	2,942
38	$Ca_2\ Ba_3\ (PO_4)_3\ F$	1,21	0,38	1,33	9,845	7,359	9,8073	7,4229	0,383	0,868
39	$Ca_5\ (PO_4)_3\ F_{0.39}\ Cl_{0.33}\ (OH)_{0.28}$	1	0,38	1,4996	9,4615	6,8491	9,5316	6,8249	0,741	0,353
40	$Ca_5\ (PO_4)_3\ F_{0.29}\ Cl_{0.47}\ (OH)_{0.24}$	1	0,38	1,5652	9,4877	6,8224	9,5407	6,8077	0,559	0,215
41	$Co\ Ca_4\ (PO_4)_3\ Cl$	0,93	0,38	1,81	9,625	6,747	9,5498	6,4933	0,781	3,760
42	$Sr_{2.54}\ Ba_{2.45}\ Eu_{0.01}\ (PO_4)_3\ Cl$	1,26328	0,38	1,81	10,0265	7,4099	10,085	7,404	0,583	0,080

Table 4.13 (continued)

	Apatite formula	Average Radii A	Average Radii B	Average Radii C	a	c	a output	c output	error% (a)	error% (c)
43	$Ba_{4.99}\ Eu_{0.01}\ (PO_4)_3\ Cl$	1,34964	0,38	1,81	10,2712	7,65	10,288	7,6556	0,164	0,073
44	$Sr_{4.99}\ Eu_{0.01}\ (PO_4)_3\ Cl$	1,17998	0,38	1,81	9,878	7,1893	9,9167	7,224	0,392	0,483
45	$Ca_2\ Pb_3\ (AsO_4)_3\ Cl$	1,114	0,46	1,81	10,14	7,185	10,165	7,311	0,247	1,754
46	$Pb_5\ (VO_4)_3\ Cl$	1,19	0,54	1,81	10,3174	7,3378	10,146	7,4005	1,661	0,854
47	$Ca_{10}\ (VO_4)\ (PO_4)_5\ (OH)_2$	1	0,407	1,37	9,467	6,904	9,4436	6,858	0,247	0,666
48	$Ca_{10}\ (VO_4)_2\ (PO_4)_4\ (OH)_2$	1	0,433	1,37	9,535	6,927	9,5875	6,8758	0,551	0,739
49	$Ca_{10}\ (VO_4)_3\ (PO_4)_3\ (OH)_2$	1	0,46	1,37	9,586	6,943	9,7275	6,9168	1,476	0,377
50	$Ca_{10}\ (VO_4)_4\ (PO_4)_2\ (OH)_2$	1	0,487	1,37	9,649	6,986	9,7785	6,9547	1,342	0,448
51	$Ca_{10}\ (VO_4)_5\ (PO_4)\ (OH)_2$	1	0,513	1,37	9,695	6,986	9,7765	6,9739	0,841	0,173
52	$Pb_{10}\ (PO_4)_6\ Br_2$	1,19	0,38	1,96	10,062	7,359	9,9684	7,2567	0,930	1,390
53	$Ca_{10}\ (PO_4)_{5.83}\ (SiO_4)_{0.17}\ (OH)_{1.83}$	1	0,381	1,37	9,41763	6,88545	9,4241	6,8647	0,069	0,301
54	$Ca_{10}\ (PO_4)_{5.65}\ (SiO_4)_{0.35}\ (OH)_{1.65}$	1	0,381	1,37	9,41869	6,88683	9,4233	6,8643	0,049	0,327
55	$Ca_{10}\ (PO_4)_{5.48}\ (SiO_4)_{0.52}\ (OH)_{1.48}$	1	0,382	1,37	9,42158	6,89155	9,4225	6,864	0,010	0,400
56	$Ca_{10}\ (PO_4)_{5.30}\ (SiO_4)_{0.70}\ (OH)_{1.30}$	1	0,382	1,37	9,42332	6,89703	9,4217	6,8637	0,017	0,483
57	$Ca_{10}\ (PO_4)_{5.84}\ (SiO_4)_{0.16}\ (OH)_{1.84}$	1	0,381	1,37	9,4082	6,8828	9,4242	6,8647	0,170	0,263
58	$Na\ Y_9\ (SiO_4)_6\ O_2$	0,912	0,4	1,4	9,334	6,759	9,3595	6,4694	0,273	4,285
59	$Sr_9\ La\ (PO_4)_5\ (SiO_4)\ F_2$	1,165	0,383	1,33	9,723	7,282	9,7016	7,3027	0,220	0,284
60	$Sr_8\ La_2\ (PO_4)_4\ (SiO_4)_2\ F_2$	1,15	0,386	1,33	9,727	7,277	9,6687	7,2694	0,599	0,104
61	$Sr_6\ La_4\ (PO_4)_2\ (SiO_4)_4\ F_2$	1,12	0,393	1,33	9,732	7,27	9,6077	7,2051	1,277	0,893
62	$Sr_4\ La_6\ (SiO_4)_6\ F_2$	1,09	0,4	1,33	9,737	7,265	9,554	7,1464	1,879	1,632
63	$Sr_{10}\ (PO_4)_6\ O$	1,18	0,38	1,4	9,753	7,276	9,8238	7,2905	0,726	0,199

Table 4.13 (continued)

	Apatite formula	Average Radii A	Average Radii B	Average Radii C	a	c	a output	c output	error% (a)	error% (c)
64	$Sr_9\ La\ (PO_4)_5\ (SiO_4)\ O$	1,165	0,383	1,4	9,756	7,272	9,7922	7,2571	0,371	0,205
65	$Sr_8\ La_2\ (PO_4)_4\ (SiO_4)_2\ O$	1,15	0,387	1,4	9,761	7,267	9,7623	7,2251	0,013	0,577
66	$Sr_6\ La_4\ (PO_4)_2\ (SiO_4)_4\ O$	1,12	0,393	1,4	9,768	7,258	9,7078	7,1679	0,616	1,241
67	$Sr_4\ La_6\ (SiO_4)_6\ O$	1,09	0,4	1,4	9,771	7,255	9,6611	7,1179	1,125	1,890
					Average Percent Errors of Outputs:				0,721	0,846

Table 4.14 Prediction of both pure apatites and apatites with multiple substitutions with different ionic charges with SCG method.

	Apatite formula	Average Radii A	Average Radii B	Average Radii C	a	c	a output	c output	error% (a)	error% (c)
1	$Pb_5\ (PO_4)3\ F$	1,19	0,38	1,33	9,76	7,3	9,7728	7,3276	0,131	0,378
2	$Ca_{9.3}\ Mn_{0.7}\ (PO_4)_6\ F_2$	0,9881	0,38	1,33	9,3323	6,8424	9,3644	6,8313	0,344	0,162
3	$Mn_5\ (PO_4)_3\ Cl_{0.9}\ (OH)_{0.1}$	0,83	0,38	1,766	9,532	6,199	9,4933	5,9849	0,406	3,454
4	$Sr_5\ (PO_4)_3\ F_{0.75}\ Br_{0.25}$	1,18	0,38	1,4875	9,7186	7,2853	9,8357	7,2887	1,205	0,047
5	$Sr_5\ (PO_4)_3\ F_{0.5}\ Br_{0.5}$	1,18	0,38	1,645	9,7623	7,2699	9,8963	7,2775	1,373	0,105
6	$Sr_5\ (PO_4)_3\ F_{0.25}\ Br_{0.75}$	1,18	0,38	1,8025	9,8885	7,2344	9,9341	7,2742	0,461	0,550
7	$Sr_{4.99}\ Eu_{0.01}\ (PO_4)_3\ Cl_{0.75}\ Br_{0.25}$	1,17998	0,38	1,8475	9,8909	7,1934	9,9416	7,2641	0,513	0,983
8	$Sr_{4.99}\ Eu_{0.01}\ (PO_4)_3\ Cl_{0.5}\ Br_{0.5}$	1,17998	0,38	1,885	9,9056	7,195	9,9471	7,2506	0,419	0,773
9	$Sr_{4.99}\ Eu_{0.01}\ (PO_4)_3\ Cl_{0.25}\ Br_{0.75}$	1,17998	0,38	1,9225	9,9934	7,202	9,9518	7,2315	0,416	0,410
10	$Sr_{4.99}\ Eu_{0.01}\ (PO_4)_3\ Br$	1,17998	0,38	1,96	9,9636	7,2061	9,9559	7,2061	0,077	0,000
11	$Ca_{2.6}\ Sr_{2.4}\ (PO_4)_3\ Cl$	1,0864	0,38	1,81	9,737	7,022	9,7562	7,0441	0,197	0,315

Table 4.14 (continued)

	Apatite formula	Average Radii A	Average Radii B	Average Radii C	a	c	a output	c output	error% (a)	error% (c)
12	$Ca_{4.6}\ Sr_{0.4}\ (PO_4)_3\ Cl$	1,0144	0,38	1,81	9,653	6,777	9,6562	6,8436	0,033	0,983
13	$Ca_{4.9}\ Sr_{0.1}\ (PO_4)_3\ Cl$	1,0036	0,38	1,81	9,643	6,766	9,6441	6,8038	0,011	0,559
14	$Sr_{4.99}\ Eu_{0.01}\ (PO_4)_3\ Cl$	1,17998	0,38	1,81	9,878	7,1893	9,9354	7,2729	0,581	1,163
15	$Sr_{2.54}\ Ca_{2.45}\ Eu_{0.01}\ (PO_4)_3\ Cl$	1,09178	0,38	1,81	9,754	7,0061	9,7651	7,0573	0,114	0,731
16	$Sr_{4.99}\ Eu_{0.01}\ (PO_4)_3\ Cl_{0.75}\ F_{0.25}$	1,17998	0,38	1,69	9,8697	7,1966	9,9091	7,279	0,399	1,145
17	$Sr_{4.99}\ Eu_{0.01}\ (PO_4)_3\ Cl_{0.5}\ F_{0.5}$	1,17998	0,38	1,57	9,8042	7,2357	9,8707	7,2774	0,678	0,576
18	$Sr_{4.99}\ Eu_{0.01}\ (PO_4)_3\ Cl_{0.25}\ F_{0.75}$	1,17998	0,38	1,45	9,7357	7,2769	9,8172	7,296	0,837	0,262
19	$Ca_{2.1}\ Pb_{7.9}\ (PO_4)_6\ Cl_2$	1,1501	0,38	1,81	9,99	7,276	9,8734	7,1994	1,167	1,053
20	$K_2\ Pb_6\ Eu_2\ (PO_4)_6\ F_2$	1,18	0,38	1,33	9,7482	7,2655	9,7475	7,3021	0,007	0,504
21	$K\ Pb_8\ Nd\ (PO_4)_6\ F_2$	1,188	0,38	1,33	9,7768	7,2791	9,7677	7,3225	0,093	0,596
22	$K_2\ Pb_6\ Nd_2\ (PO_4)_6\ F_2$	1,186	0,38	1,33	9,7604	7,2754	9,7626	7,3174	0,023	0,577
23	$Pb_6\ Eu_2\ Na_2\ (PO_4)_6\ F_2$	1,108	0,38	1,33	9,655	7,058	9,5767	7,1302	0,811	1,023
24	$Pb_8\ Eu\ Na\ (PO_4)_6\ F_2$	1,149	0,38	1,33	9,73	7,176	9,6711	7,2255	0,605	0,690
25	$Pb_6\ La_2\ Na_2\ (PO_4)_6\ F_2$	1,124	0,38	1,33	9,721	7,15	9,6124	7,1666	1,117	0,232
26	$Pb_4\ La_3\ Na_3\ (PO_4)_6\ F_2$	1,091	0,38	1,33	9,725	7,158	9,5406	7,0925	1,896	0,915
27	$Pb_6\ Nd_2\ Na_2\ (PO_4)_6\ F_2$	1,114	0,38	1,33	9,661	7,067	9,5899	7,1437	0,736	1,085
28	$Pb_4\ Nd_3\ Na_3\ (PO_4)_6\ F_2$	1,076	0,38	1,33	9,616	7,029	9,5104	7,0597	1,098	0,437
29	$Pb_8\ Nd\ Na\ (PO_4)_6\ F_2$	1,152	0,38	1,33	9,741	7,198	9,6783	7,2328	0,644	0,483
30	$Pb\ Y_2\ Na_2\ (PO_4)_6\ F_2$	1,006	0,38	1,33	9,649	7,055	9,39	6,8904	2,684	2,333
31	$Pb_8\ Y\ Na\ (PO_4)_6\ F_2$	1,144	0,38	1,33	9,712	7,17	9,6591	7,2135	0,545	0,607
32	$Pb_6\ Bi_2\ Na_2\ (PO_4)_6\ F_2$	1,124	0,38	1,33	9,6956	7,1826	9,6124	7,1666	0,858	0,223
33	$Pb_{10}\ (PO_4)_6\ F_2$	1,19	0,38	1,33	9,773	7,315	9,7728	7,3276	0,002	0,172

Table 4.14 (continued)

	Apatite formula	Average Radii A	Average Radii B	Average Radii C	a	c	a output	c output	error% (a)	error% (c)
34	$Ca_{4.5}\ Pb_{5.5}\ (PO_4)_6\ F_2$	1,1045	0,38	1,33	9,759	7,291	9,5691	7,1224	1,946	2,312
35	$Ba_3\ La\ Na\ (PO_4)_3\ F$	1,22	0,38	1,33	9,9392	7,4419	9,8489	7,4054	0,909	0,490
36	$Ba_4\ Nd_3\ Na_3\ (PO_4)_6\ F_2$	1,14	0,38	1,33	9,786	7,281	9,6496	7,204	1,394	1,058
37	$Ca_{2.5}\ Pb_{7.5}\ (PO_4)_6\ (OH)_2$	1,1425	0,38	1,37	9,88	7,417	9,6817	7,2124	2,007	2,759
38	$Ca_2\ Ba_3\ (PO_4)_3\ F$	1,21	0,38	1,33	9,845	7,359	9,8235	7,3792	0,218	0,274
39	$Ca_5\ (PO_4)_3\ F_{0.39}\ Cl_{0.33}\ (OH)_{0.28}$	1	0,38	1,4996	9,4615	6,8491	9,4991	6,8495	0,397	0,006
40	$Ca_5\ (PO_4)_3\ F_{0.29}\ Cl_{0.47}\ (OH)_{0.24}$	1	0,38	1,5652	9,4877	6,8224	9,5378	6,8268	0,528	0,064
41	$Co\ Ca_4\ (PO_4)_3\ Cl$	0,93	0,38	1,81	9,625	6,747	9,5771	6,3996	0,498	5,149
42	$Sr_{2.54}\ Ba_{2.45}\ Eu_{0.01}\ (PO_4)_3\ Cl$	1,26328	0,38	1,81	10,0265	7,4099	10,111	7,4709	0,843	0,823
43	$Ba_{4.99}\ Eu_{0.01}\ (PO_4)_3\ Cl$	1,34964	0,38	1,81	10,2712	7,65	10,264	7,6397	0,070	0,135
44	$Sr_{4.99}\ Eu_{0.01}\ (PO_4)_3\ Cl$	1,17998	0,38	1,81	9,878	7,1893	9,9354	7,2729	0,581	1,163
45	$Ca_2\ Pb_3\ (AsO_4)_3\ Cl$	1,114	0,46	1,81	10,14	7,185	10,213	7,2993	0,720	1,591
46	$Pb_5\ (VO_4)_3\ Cl$	1,19	0,54	1,81	10,3174	7,3378	10,143	7,345	1,690	0,098
47	$Ca_{10}\ (VO_4)\ (PO_4)_5\ (OH)_2$	1	0,407	1,37	9,467	6,904	9,4768	6,8992	0,104	0,070
48	$Ca_{10}\ (VO_4)_2\ (PO_4)_4\ (OH)_2$	1	0,433	1,37	9,535	6,927	9,6201	6,9144	0,893	0,182
49	$Ca_{10}\ (VO_4)_3\ (PO_4)_3\ (OH)_2$	1	0,46	1,37	9,586	6,943	9,7417	6,925	1,624	0,259
50	$Ca_{10}\ (VO_4)_4\ (PO_4)_2\ (OH)_2$	1	0,487	1,37	9,649	6,986	9,7822	6,9433	1,380	0,611
51	$Ca_{10}\ (VO_4)_5\ (PO_4)\ (OH)_2$	1	0,513	1,37	9,695	6,986	9,7733	6,9676	0,808	0,263
52	$Pb_{10}\ (PO_4)_6\ Br_2$	1,19	0,38	1,96	10,062	7,359	9,9766	7,2274	0,849	1,788
53	$Ca_{10}\ (PO_4)_{5.83}\ (SiO_4)_{0.17}\ (OH)_{1.83}$	1	0,381	1,37	9,41763	6,88545	9,4113	6,8725	0,067	0,188
54	$Ca_{10}\ (PO_4)_{5.65}\ (SiO_4)_{0.35}\ (OH)_{1.65}$	1	0,381	1,37	9,41869	6,88683	9,4118	6,8732	0,073	0,198
55	$Ca_{10}\ (PO_4)_{5.48}\ (SiO_4)_{0.52}\ (OH)_{1.48}$	1	0,382	1,37	9,42158	6,89155	9,4123	6,8739	0,098	0,256

Table 4.14 (continued)

	Apatite formula	Average Radii A	Average Radii B	Average Radii C	a	c	a output	c output	error% (a)	error% (c)
56	$Ca_{10}(PO_4)_{5.30}(SiO_4)_{0.70}(OH)_{1.30}$	1	0,382	1,37	9,42332	6,89703	9,4129	6,8746	0,111	0,325
57	$Ca_{10}(PO_4)_{5.84}(SiO_4)_{0.16}(OH)_{1.84}$	1	0,381	1,37	9,4082	6,8828	9,4112	6,8725	0,032	0,150
58	$Na\ Y_9(SiO_4)_6\ O_2$	0,912	0,4	1,4	9,334	6,759	9,3192	6,3835	0,159	5,556
59	$Sr_9\ La(PO_4)_5(SiO_4)\ F_2$	1,165	0,383	1,33	9,723	7,282	9,7299	7,2786	0,071	0,047
60	$Sr_8\ La_2(PO_4)_4(SiO_4)_2\ F_2$	1,15	0,387	1,33	9,727	7,277	9,7117	7,2552	0,157	0,300
61	$Sr_6\ La_4(PO_4)_2(SiO_4)_4\ F_2$	1,12	0,393	1,33	9,732	7,27	9,6737	7,2083	0,599	0,849
62	$Sr_4\ La_6(SiO_4)_6\ F_2$	1,09	0,4	1,33	9,737	7,265	9,6342	7,1596	1,056	1,451
63	$Sr_{10}(PO_4)_6\ O$	1,18	0,38	1,4	9,753	7,276	9,7902	7,3029	0,381	0,370
64	$Sr_9\ La(PO_4)_5(SiO_4)\ O$	1,165	0,383	1,4	9,756	7,272	9,7743	7,2784	0,188	0,088
65	$Sr_8\ La_2(PO_4)_4(SiO_4)_2\ O$	1,15	0,387	1,4	9,761	7,267	9,7577	7,254	0,034	0,179
66	$Sr_6\ La_4(PO_4)_2(SiO_4)_4\ O$	1,12	0,393	1,4	9,768	7,258	9,7226	7,2048	0,465	0,733
67	$Sr_4\ La_6(SiO_4)_6\ O$	1,09	0,4	1,4	9,771	7,255	9,6853	7,1535	0,877	1,399
						Average Percent Errors of Outputs:			0,631	0,817

Table 4.15 Comparison of average percent errors for outputs a and c and unit cell volumes obtained from Tables 4.11 to 4.14.

Learning method	Average percent error for a	Average percent error for c	Average percent error for unit cell volume
BR	0.570	0.792	1.542
LM	0.721	0.846	1.748
SCG	0.631	0.817	1.854

Table 4.16 Prediction of lattice parameters and volumes of possible apatites generated by using Bayesian regularization.

#	**Apatite formula**	**Average Radii A**	**Average Radii B**	**Average Radii C**	**a output**	**c output**	**Vol. (unit cell)**
1	$Ag_5 (PO_4)_3 OH$	0,94	0,38	1,37	9,3161	6,6695	1498,6
2	$Ag_5 (PO_4)_3 F$	0,94	0,38	1,33	9,2903	6,6754	1491,7
3	$Ag_5 (PO_4)_3 Cl$	0,94	0,38	1,81	9,5945	6,5677	1565,3
4	$Ag_5 (PO_4)_3 Br$	0,94	0,38	1,96	9,684	6,5178	1582,5
5	$Ag_5 (VO_4)_3 OH$	0,94	0,54	1,37	9,7162	6,8043	1663,1
6	$Ag_5 (VO_4)_3 F$	0,94	0,54	1,33	9,6848	6,8151	1655,0
7	$Ag_5 (VO_4)_3 Cl$	0,94	0,54	1,81	10,113	6,6506	1761,0
8	$Ag_5 (VO_4)_3 Br$	0,94	0,54	1,96	10,256	6,5847	1793,2
9	$Ag_5 (CrO_4)_3 OH$	0,94	0,55	1,37	9,7007	6,8096	1659,1
10	$Ag_5 (CrO_4)_3 F$	0,94	0,55	1,33	9,6694	6,8207	1651,0
11	$Ag_5 (CrO_4)_3 Cl$	0,94	0,55	1,81	10,101	6,6529	1757,4
12	$Ag_5 (CrO_4)_3 Br$	0,94	0,55	1,96	10,247	6,5861	1790,4
13	$Ag_5 (AsO_4)_3 OH$	0,94	0,46	1,37	9,694	6,7485	1641,9
14	$Ag_5 (AsO_4)_3 F$	0,94	0,46	1,33	9,6638	6,7569	1633,7
15	$Ag_5 (AsO_4)_3 Cl$	0,94	0,46	1,81	10,043	6,62	1728,7
16	$Ag_5 (AsO_4)_3 Br$	0,94	0,46	1,96	10,16	6,5618	1753,6
17	$Fe_5 (PO_4)_3 OH$	0,61	0,38	1,37	9,147	5,4932	1189,9
18	$Fe_5 (PO_4)_3 F$	0,61	0,38	1,33	9,1078	5,5027	1181,8
19	$Fe_5 (PO_4)_3 Cl$	0,61	0,38	1,81	9,5202	5,3566	1256,9
20	$Fe_5 (PO_4)_3 Br$	0,61	0,38	1,96	9,6252	5,2981	1270,8

Table 4.16 (continued)

#	Apatite formula	Average Radii A	Average Radii B	Average Radii C	a output	c output	Vol. (unit cell)
21	$Fe_5 (VO_4)_3$ OH	0,61	0,54	1,37	9,8814	5,6184	1420,3
22	$Fe_5 (VO_4)_3$ F	0,61	0,54	1,33	9,8304	5,6319	1409,1
23	$Fe_5 (VO_4)_3$ Cl	0,61	0,54	1,81	10,388	5,4465	1521,6
24	$Fe_5 (VO_4)_3$ Br	0,61	0,54	1,96	10,533	5,3796	1545,2
25	$Fe_5 (CrO_4)_3$ OH	0,61	0,55	1,37	9,8796	5,6238	1421,2
26	$Fe_5 (CrO_4)_3$ F	0,61	0,55	1,33	9,828	5,6375	1409,8
27	$Fe_5 (CrO_4)_3$ Cl	0,61	0,55	1,81	10,395	5,4502	1524,7
28	$Fe_5 (CrO_4)_3$ Br	0,61	0,55	1,96	10,544	5,383	1549,4
29	$Fe_5 (AsO_4)_3$ OH	0,61	0,46	1,37	9,7147	5,5651	1359,8
30	$Fe_5 (AsO_4)_3$ F	0,61	0,46	1,33	9,6694	5,5767	1349,9
31	$Fe_5 (AsO_4)_3$ Cl	0,61	0,46	1,81	10,15	5,4088	1442,7
32	$Fe_5 (AsO_4)_3$ Br	0,61	0,46	1,96	10,271	5,3454	1459,9
33	$Mg_5 (PO_4)_3$ OH	0,72	0,38	1,37	9,1565	5,9189	1284,8
34	$Mg_5 (PO_4)_3$ F	0,72	0,38	1,33	9,1196	5,9275	1276,3
35	$Mg_5 (PO_4)_3$ Cl	0,72	0,38	1,81	9,519	5,7887	1358,0
36	$Mg_5 (PO_4)_3$ Br	0,72	0,38	1,96	9,6242	5,7307	1374,3
37	$Mg_5 (VO_4)_3$ OH	0,72	0,54	1,37	9,7763	6,0431	1495,3
38	$Mg_5 (VO_4)_3$ F	0,72	0,54	1,33	9,7285	6,0563	1484,0
39	$Mg_5 (VO_4)_3$ Cl	0,72	0,54	1,81	10,278	5,8694	1605,3
40	$Mg_5 (VO_4)_3$ Br	0,72	0,54	1,96	10,43	5,7996	1633,4
41	$Mg_5 (CrO_4)_3$ OH	0,72	0,55	1,37	9,7693	6,0481	1494,4
42	$Mg_5 (CrO_4)_3$ F	0,72	0,55	1,33	9,721	6,0615	1483,0
43	$Mg_5 (CrO_4)_3$ Cl	0,72	0,55	1,81	10,279	5,8721	1606,3
44	$Mg_5 (CrO_4)_3$ Br	0,72	0,55	1,96	10,434	5,8018	1635,3
45	$Mg_5 (AsO_4)_3$ OH	0,72	0,46	1,37	9,6615	5,9915	1448,0
46	$Mg_5 (AsO_4)_3$ F	0,72	0,46	1,33	9,6184	6,0025	1437,7
47	$Mg_5 (AsO_4)_3$ Cl	0,72	0,46	1,81	10,094	5,8379	1540,0
48	$Mg_5 (AsO_4)_3$ Br	0,72	0,46	1,96	10,22	5,7733	1561,2
49	$Co_5 (PO_4)_3$ OH	0,65	0,38	1,37	9,1468	5,6516	1224,2
50	$Co_5 (PO_4)_3$ F	0,65	0,38	1,33	9,1082	5,6609	1215,9
51	$Co_5 (PO_4)_3$ Cl	0,65	0,38	1,81	9,5181	5,5165	1293,9
52	$Co_5 (PO_4)_3$ Br	0,65	0,38	1,96	9,6236	5,4579	1308,7
53	$Co_5 (VO_4)_3$ OH	0,65	0,54	1,37	9,8397	5,7758	1447,8
54	$Co_5 (VO_4)_3$ F	0,65	0,54	1,33	9,7895	5,7892	1436,4
55	$Co_5 (VO_4)_3$ Cl	0,65	0,54	1,81	10,347	5,6021	1552,8
56	$Co_5 (VO_4)_3$ Br	0,65	0,54	1,96	10,496	5,5338	1578,3

Table 4.16 (continued)

#	Apatite formula	Average Radii A	Average Radii B	Average Radii C	a output	c output	Vol. (unit cell)
57	$Co_5 (CrO_4)_3 OH$	0,65	0,55	1,37	9,8359	5,781	1448,0
58	$Co_5 (CrO_4)_3 F$	0,65	0,55	1,33	9,7852	5,7946	1436,5
59	$Co_5 (CrO_4)_3 Cl$	0,65	0,55	1,81	10,352	5,6054	1555,2
60	$Co_5 (CrO_4)_3 Br$	0,65	0,55	1,96	10,504	5,5367	1581,6
61	$Co_5 (AsO_4)_3 OH$	0,65	0,46	1,37	9,692	5,7235	1391,9
62	$Co_5 (AsO_4)_3 F$	0,65	0,46	1,33	9,6472	5,7349	1381,8
63	$Co_5 (AsO_4)_3 Cl$	0,65	0,46	1,81	10,129	5,5672	1478,8
64	$Co_5 (AsO_4)_3 Br$	0,65	0,46	1,96	10,252	5,503	1497,4
65	$Zn_5 (PO_4)_3 OH$	0,74	0,38	1,37	9,1622	5,9929	1302,5
66	$Zn_5 (PO_4)_3 F$	0,74	0,38	1,33	9,1259	6,0013	1294,0
67	$Zn_5 (PO_4)_3 Cl$	0,74	0,38	1,81	9,5206	5,8645	1376,2
68	$Zn_5 (PO_4)_3 Br$	0,74	0,38	1,96	9,6254	5,8068	1392,9
69	$Zn_5 (VO_4)_3 OH$	0,74	0,54	1,37	9,7611	6,1175	1509,0
70	$Zn_5 (VO_4)_3 F$	0,74	0,54	1,33	9,7142	6,1305	1497,8
71	$Zn_5 (VO_4)_3 Cl$	0,74	0,54	1,81	10,259	5,9444	1619,8
72	$Zn_5 (VO_4)_3 Br$	0,74	0,54	1,96	10,412	5,8745	1648,8
73	$Zn_5 (CrO_4)_3 OH$	0,74	0,55	1,37	9,7532	6,1224	1507,8
74	$Zn_5 (CrO_4)_3 F$	0,74	0,55	1,33	9,7059	6,1357	1496,5
75	$Zn_5 (CrO_4)_3 Cl$	0,74	0,55	1,81	10,258	5,947	1620,2
76	$Zn_5 (CrO_4)_3 Br$	0,74	0,55	1,96	10,415	5,8765	1650,3
77	$Zn_5 (AsO_4)_3 OH$	0,74	0,46	1,37	9,6555	6,0658	1464,1
78	$Zn_5 (AsO_4)_3 F$	0,74	0,46	1,33	9,613	6,0766	1453,8
79	$Zn_5 (AsO_4)_3 Cl$	0,74	0,46	1,81	10,085	5,9135	1557,1
80	$Zn_5 (AsO_4)_3 Br$	0,74	0,46	1,96	10,211	5,8491	1578,9

Table 4.17 Prediction of lattice parameters and volumes of apatites which were approximately formulated by using data from literature.

	Apatite formula	Average Radii A	Average Radii B	Average Radii C	a	c	a output	c output	error% for (a)	error% for (c)	Reference
1	$Ca_{9.75}\,Y_{0.25}\,(PO_4)_6\,(OH)_{1.75}\,F_{0.25}$	0,9975	0,38	1,365	9,406	6,874	9,3969	6,8433	0,097	0,447	[98]
2	$Ca_{9.5}\,Y_{0.5}\,(PO_4)_6\,(OH)_{1.75}\,F_{0.25}$	0,995	0,38	1,365	9,408	6,877	9,3928	6,836	0,162	0,596	
3	$Ca_{9.25}\,Y_{0.75}\,(PO_4)_6\,(OH)_{1.75}\,F_{0.25}$	0,9925	0,38	1,365	9,384	6,86	9,3888	6,8286	0,051	0,458	
4	$Ca_{9.75}\,Al_{0.25}\,(PO_4)_6\,(OH)_2$	0,9885	0,38	1,37	9,4248	6,8812	9,3853	6,8162	0,419	0,945	[99]
5	$Ca_{9.5}\,Al_{0.5}\,(PO_4)_6\,(OH)_2$	0,977	0,38	1,37	9,4252	6,892	9,3677	6,782	0,610	1,596	
6	$Ca_{9.25}\,Al_{0.75}\,(PO_4)_6\,(OH)_2$	0,9655	0,38	1,37	9,4218	6,8807	9,3509	6,7475	0,753	1,936	
7	$Ca_{9.5}\,Mg_{0.82}\,(PO_4)_6\,(OH)_2$	0,9778	0,38	1,37	8,8133	6,8215	9,3688	6,7843	6,303	0,545	[41]
8	$Ca_{9.5}\,Zn_{0.31}\,(PO_4)_6\,(OH)_2$	0,9918	0,38	1,37	8,8972	6,8427	9,3905	6,8259	5,544	0,246	
9	$Ca_{9.5}\,La_{0.14}\,(PO_4)_6\,(OH)_2$	1,0004	0,38	1,37	9,3135	6,8346	9,4044	6,8512	0,976	0,243	
10	$Ca_{9.5}\,Y_{0.23}\,(PO_4)_6\,(OH)_2$	0,9976	0,38	1,37	8,9013	6,8548	9,3998	6,843	5,600	0,172	
11	$Ca_{9.5}\,In_{0.17}\,(PO_4)_6\,(OH)_2$	0,9965	0,38	1,37	8,832	6,8101	9,398	6,8397	6,409	0,435	
12	$Ca_{9.5}\,Bi_{0.10}\,(PO_4)_6\,(OH)_2$	1,0003	0,38	1,37	9,3442	6,8457	9,4042	6,8509	0,642	0,076	
13	$Ca_{9.8}\,Cd_{0.2}\,(PO_4)_6\,(OH)_2$	0,999	0,38	1,37	9,3716	6,8662	9,402	6,847	0,324	0,280	[100]
14	$Ca_{9.8}\,Mg_{0.2}\,(PO_4)_6\,(OH)_2$	0,9944	0,38	1,37	9,3938	6,8758	9,3946	6,8335	0,009	0,615	
15	$Ca_{9.8}\,Zn_{0.2}\,(PO_4)_6\,(OH)_2$	0,9948	0,38	1,37	9,3828	6,876	9,3953	6,8347	0,133	0,601	
16	$Ca_{9.7}\,Y_{0.2}\,(PO_4)_6\,(OH)_2$	0,9980	0,38	1,37	9,4072	6,877	9,4004	6,844	0,072	0,480	
17	$Ca_{9.55}\,Y_{0.3}\,(PO_4)_6\,(OH)_2$	0,9970	0,38	1,37	9,377	6,859	9,3987	6,841	0,231	0,262	
18	$Ca_{9.4}\,Y_{0.4}\,(PO_4)_6\,(OH)_2$	0,9959	0,38	1,37	9,399	6,8734	9,3971	6,838	0,020	0,515	
19	$Ca_{9.25}\,Y_{0.5}\,(PO_4)_6\,(OH)_2$	0,9949	0,38	1,37	9,388	6,8662	9,3954	6,8349	0,079	0,456	
20	$Ca_{9.1}\,Y_{0.6}\,(PO_4)_6\,(OH)_2$	0,9938	0,38	1,37	9,3496	6,8544	9,3937	6,8318	0,472	0,330	

Table 4.17 (continued)

	Apatite formula	Average Radii A	Average Radii B	Average Radii C	a	c	a output	c output	error% for (a)	error% for (c)	Reference
21	$Ca_{8.55}Y_{0.7}(PO_4)_6(OH)_2$	0,9924	0,38	1,37	9,3384	6,8448	9,3915	6,8278	0,569	0,248	
22	$Ca_{9.95}(PO_4)_{5.71}(CO_3)_{0.20}(OH)_2$	1	0,373	1,37	9,410	6,879	9,3535	6,8418	0,600	0,541	[103]
23	$Ca_{9.46}(PO_4)_5(CO_3)_{1.00}(OH)_{1.78}$	1	0,343	1,37	9,394	6,894	9,1013	6,8047	3.116	1,295	
24	$Ca_{9.88}(PO_4)_{5.76}(CO_3)_{0.24}F_{1.49}(OH)_{0.51}$	1	0,3712	1,3402	9,382	6,891	9,3241	6,8432	0,617	0,694	

Table 4.18 Comparison of the calculated and predicted volumes of apatites that are listed in Table 4.17.

	Apatite formula	V (unit cell)	V (predicted)	Error percent for volume	Reference
1	$Ca_{9.75}\ Y_{0.25}\ (PO_4)_6\ (OH)_{1.75}\ F_{0.25}$	1574,5	1564,5	0,639	[98]
2	$Ca_{9.5}\ Y_{0.5}\ (PO_4)_6\ (OH)_{1.75}\ F_{0.25}$	1575,9	1561,4	0,917	
3	$Ca_{9.25}\ Y_{0.75}\ (PO_4)_6\ (OH)_{1.75}\ F_{0.25}$	1564,0	1558,4	0,356	
4	$Ca_{9.75}\ Al_{0.25}\ (PO_4)_6\ (OH)_2$	1582,5	1554,4	1,773	[99]
5	$Ca_{9.5}\ Al_{0.5}\ (PO_4)_6\ (OH)_2$	1585,1	1540,8	2,793	
6	$Ca_{9.25}\ Al_{0.75}\ (PO_4)_6\ (OH)_2$	1581,4	1527,5	3,406	
7	$Ca_{9.5}\,Mg_{0.82}\,(PO_4)_6\,(OH)_2$	1371,8	1541,7	12,387	[41]
8	$Ca_{9.5}\,Zn_{0.31}\,(PO_4)_6\,(OH)_2$	1402,4	1558,4	11,123	
9	$Ca_{9.5}\,La_{0.14}\,(PO_4)_6\,(OH)_2$	1534,9	1568,8	2,209	
10	$Ca_{9.5}\,Y_{0.23}\,(PO_4)_6\,(OH)_2$	1406,2	1565,4	11,322	
11	$Ca_{9.5}\,In_{0.17}\,(PO_4)_6\,(OH)_2$	1375,3	1564,0	13,720	
12	$Ca_{9.5}\,Bi_{0.10}\,(PO_4)_6\,(OH)_2$	1547,5	1568,6	1,365	
13	$Ca_{9.8}\,Cd_{0.2}\,(PO_4)_6\,(OH)_2$	1561,3	1567,0	0,368	[100]
14	$Ca_{9.8}\,Mg_{0.2}\,(PO_4)_6\,(OH)_2$	1570,9	1561,5	0,598	
15	$Ca_{9.8}\,Zn_{0.2}\,(PO_4)_6\,(OH)_2$	1567,2	1562,0	0,336	
16	$Ca_{9.7}\,Y_{0.2}\,(PO_4)_6\,(OH)_2$	1575,6	1565,8	0,624	
17	$Ca_{9.55}\,Y_{0.3}\,(PO_4)_6\,(OH)_2$	1561,4	1564,5	0,200	
18	$Ca_{9.4}\,Y_{0.4}\,(PO_4)_6\,(OH)_2$	1572,1	1563,3	0,555	
19	$Ca_{9.25}\,Y_{0.5}\,(PO_4)_6\,(OH)_2$	1566,7	1562,0	0,299	
20	$Ca_{9.1}\,Y_{0.6}\,(PO_4)_6\,(OH)_2$	1551,3	1560,8	0,613	
21	$Ca_{8.55}\,Y_{0.7}\,(PO_4)_6\,(OH)_2$	1545,4	1559,1	0,889	
22	$Ca_{9.95}(PO_4)_{5.71}(CO_3)_{0.20}\,(OH)_2$	1577.0	1549.7	1.731	[103]
23	$Ca_{9.46}(PO_4)_5(CO_3)_{1.00}\,(OH)_{1.78}$	1575.1	1459.3	7.352	
24	$Ca_{9.88}(PO_4)_{5.76}(CO_3)_{0.24}F_{1.49}(OH)_{0.51}$	1570.4	1540.3	1.917	

4.4 Formula Extraction for BR Method

Formulas can be derived by using weights, biases and activation functions of the neural network. Formulas for hexagonal lattice parameters a and c were derived by using BR method to show how predictions were made.

Table 4.19 The weights between the input and hidden layer for lattice parameter a

i	$E_i=C_1*R_A+C_2*R_B+C_3*R_C+C_4$			
	C_1	C_2	C_3	C_4
1	-0.29121	-0.37429	-0.93008	-0.68189
2	2.1243	-0.84122	-0.72689	-1.3309
3	-1.0465	-2.5549	0.6731	1.4169
4	-0.075195	-4.125	-0.091451	1.1377

Table 4.20 The weights between the input and hidden layer for lattice parameter c

i	$E_i=C_1*R_A+C_2*R_B+C_3*R_C+C_4$			
	C_1	C_2	C_3	C_4
1	-0.52211	-0.49087	-0.25122	0.054422
2	0.52211	0.49087	0.25122	-0.054422
3	1.0851	-0.95392	-0.34973	0.51105
4	-0.45506	-1.021	0.044623	0.29596

The equations in Tables 4.19 and 4.20 are dependent on R_A, R_B and R_C which are the average ionic radii for A,B and C sites, respectively. C_1, C_2 and C_3 are the weights corresponding to R_A, R_B and R_C, respectively. C_4 is the bias for each processing element. Coefficients of F_i in the Equations 4.4 and 4.5 are the weights between the hidden and output layers with the bias added as the last term. F_i is the activation function which is 'tansig' function from MATLAB in our study. Calculation of F_i is given in Eq.4.6.

$$Lattice\ \ parameter\ \ a = -3.5488 * F_1 + 2.0679 * F_2 + 2.1481 * F_3 - 4.6425 * F_4 + 3.6454 \quad (4.4)$$

$$Lattice\ \ parameter\ \ c = -1.8272 * F_1 + 1.8272 * F_2 + 2.1636 * F_3 - 1.9986 * F_4 + 1.7878 \quad (4.5)$$

$$F_i = \frac{2}{1+\exp(-2*E_i)} - 1 \qquad (4.6)$$

As an example, calculations of the lattice parameters of the first data of Table 4.11 with Formulas 4.4 and 4.5 are given below.

Inputs and outputs are as follows,

R_A=1.19 , R_B=0.38 , R_C=1.33 , a=9.76 , c=7.3

For lattice parameter a, calculation of E_1 is given as an example for the calculation E_i values as follows,

$$E_1 = -0.29121*1.19 - 0.37429*0.38 - 0.93008*1.33 - 0.68189 = -2.4077$$

$$F_1 = 2/(1+\exp(-2*(-2.0477))) = -0.9839$$

Other F_i values were calculated with the same method and lattice parameter **a** was calculated as follows,

$$a = -3.5488*(-0.9839) + 2.0679*(-0.0892) + 2.1481*(0.0956)$$
$$-4.6425*(-0.5655) + 3.6454 = 9.7836$$

$$Error\%\ for\ a = (9.7836 - 9.76)/9.76*100 = 0.242\%$$

For lattice parameter c,

$$E_1 = -0.52211*1.19 - 0.49087*0.38 - 0.25122*1.33 + 0.054422 = -1.0875$$

$$F_1 = 2/(1+\exp(-2(-1.0875))) = -0.7960$$

$$c = -1.8272*(-0.7960) + 1.8272*0.7960 + 2.1636*0.7508 - 1.9986*(-0.5184)$$
$$+1.7878 = 7.3572$$

$$Error\%\ for\ c = (7.3572 - 7.3)/7.3*100 = 0.784\%$$

By using formulas 4.4 and 4.5 predictions can be reproduced without using the network, so less time is spent by using only basic mathematical operations. In this

work, inputs were used without normalization, because same kind of variables were used and input values were around unity which is small. However, inputs should be normalized whenever their values are much larger than unity and different kinds of variables are available. Normalization will help to keep the weights small and sensitivity of the exponential term will be improved.

Formulas derived for lattice parameters a and c are not exact equations. They are the closest mathematical formulas obtained from the training dataset. This is a very important advantage of neural networks, because they can find reasonable solutions to problems even if there is no exact solution.

4.5 Discussion of Neural Networks' Applications on Nanotechnology

As a starting point in nanoscience, neural networks were used for investigating atomic and molecular properties. In the literature, there is a study which used local geometric arrangement of atoms like bond distances, bond angles, lattice constants and elastic properties to predict the functional relationships of potential energy surfaces [109]. Another interesting example can be the determination of optical properties of $Al_{80}Mn_{20}$ quasi-crystalline alloy using neural networks [110]. In this study, optical absorption variables refractive index (n) and extinction coefficient (k) of the quasi-crystalline alloy were calculated from reflectivity measurements at normal incidence in the range of 0.5 to 6.2 eV by using neural networks. The precision of the neural networks was found to be higher than calculations made by using Kramers-Kronig method. There are similar studies in the literature and this technique can be used for molecular structure and property studies by following some guidelines [111] regardless of the type of the application.

Another application area of neural networks is the prediction of nanocrystalline and nanomaterial properties. Crystallite size and lattice strain of the aluminum

matrix of the Al-8vol% SiC nanocomposite powders were predicted reasonably well by using various mechanical alloying parameters which are milling time, milling speed, ball to powder weight ratio and the amount of the process control agent [112]. Another study showed that it was possible to predict the purity of the perovskite type $SrTiO_3$ nanocrystals [113] with neural networks.

The examples given above show that neural networks are highly successful tools for molecular structure-property studies and prediction of the properties of nanomaterials. In addition, neural networks can also be used for solving problems encountered with the characterization tools. There are two important studies considering this issue. In the first study [114], samples needed to be characterized by Fourier Transform Infrared Sprectroscopy (FTIR) had different discrete bands which were overlapping. To identify the bands from FTIR spectra, neural networks method provided a solution by using the correlation between FTIR bands and crystallographic data like X-ray diffraction results. Second study was about high resolution electron microscopy (HREM) analysis [115]. There is a certain amount of noise in HREM images because of amorphous covering of samples needed for analysis and noise suppression performance of neural networks was the best among the investigated methods. In addition, local composition and thickness of III-V group semiconductors were determined from HREM images by neural networks.

Databases for nanomaterials are still being constructed by the addition of new experimental results continuously, but some relations will take a long time to physically model because of the complex nature of these materials. By using neural networks, quantitative inputs such as nanosized grains and weight precent of nanoparticles added can be used as inputs combined with ordinary variables like time, temperature, pressure etc. to effectively predict mechanical, electrical and thermal properties of the nanomaterials. Neural networks' prediction

accuracy is restricted with the accuracy of the experimental results retrieved [107], so precise experimental data is crucial for better results.

CHAPTER 5

CONCLUSION AND FURTHER SUGGESTIONS

In this work, several learning methods were experimented with different hidden layers, neuron numbers and activation functions for the neural networks application. It was found that neural networks is a strong statistical tool for non-linear regression problems such as prediction of lattice parameters of apatites from their ionic radii.

Datasets were created by collecting data from JCPDS database and literature. Only MLP network was used with single hidden layer for backpropagation algorithms because of its accurate prediction capabilities. It was seen that the smallest possible training dataset with the simplest network assembly should be used to improve the generalization capabilities of the network.

Several backpropagation algorithms with generalization methods were used to achieve approximately 98% prediction accuracy. Among the learning methods, LM, SCG and BR methods resulted in the correlation coefficients of higher than 0.99 proving that precise lattice parameter predictions were possible by using them.

Among acceptable learning methods, BR achieved the highest prediction accuracy for test dataset with multiple substitutions and charge differences. According to average errors of lattice parameters for the training dataset, BR method was not the best. However, it produced the best results for testing datasets. This showed that, training accuracy was not enough to make decisions

on the prediction capabilities of the network. Error functions and algorithms that work to simplify the network were also important for success.

Volume calculations from the predicted lattice parameters produced acceptable results for stoichiometric and slightly substituted apatites with BR, SCG and LM methods, but it was not reliable enough for highly substituted apatites with charge differences to be used in scientific applications.

Hexagonal lattice parameters of some possible apatites were predicted with the BR method. First prediction was for comparison with a previous work on this subject [9] and results closely matched with each other. After testing the accuracy of the network with the test dataset involving multiple substitutions and different charges and comparing the results with other learning methods, it was safe to predict new possible apatites. Ag, Fe, Mg, Co and Zn ions were used to create a dataset of possible apatites because of their common use in materials science. This dataset may be useful to researchers who wish to use common elements for applications involving apatites.

Finally, it was shown that it is possible to predict approximate formula of apatites with known percent of chemicals added by comparing predicted and experimental lattice parameters. However, prediction of some non-stoichiometric apatites were not reliable enough, probably because of increased point defects like vacancies and inadequacy of the network to model complex B sites. Also, shifts in lattice parameters should be considered between unsintered and sintered sprecimens while making these predictions and calculated if there is a reference available.

In this study, it was shown that neural networks is a powerful tool for the prediction of lattice parameters from their ionic radii and it can be used for revealing complex relationships in various engineering applications given that

enough experimental data exists and input-output variables are determined carefully. The lattice parameters found can be useful for other computational studies involving stabilities of apatites as well as interfacial stability of apatite coatings. In addition, these parameters may be useful for bulk forms if they can be combined with properties like solubility and thermal stability for various applications like detoxification of wastes.

REFERENCES

1. T. Tamm, M. Peld, "Computational Study of Cation Substitutions in Apatites", Journal of Solid State Chemistry, 179 (2006) 1581-1587.
2. B. Wopenka, J.D. Pasteris, "A Mineralogical Perspective on the Apatite in Bone", Materials Science and Engineering C 25 (2005) 131-143.
3. S. Peroos, Z. Du, N.H de Leeuw "A Computer Modelling Study of the Uptake, Structure and Distribution of Carbonate Defects in Hydroxyapatite", Biomaterials 27 (2006) 2150-2161.
4. M.I. Dominguez, J. Carpena, D. Borschnek, M.A. Centeno, J.A. Odriozola, J. Rose, "Apatite and Portland/Apatite Composite Cements Obtained Using a Hydrothermal Method for Retaining Heavy Metals", Journal of Hazardous Materials 150 (2008) 99-108.
5. J.C. Goes, S.D. Figueiro, A.M. Oliviera, A.A.M. Macedo, C.C. Silva, N.M.P.S. Ricardo, A.S.B. Sombra, "Apatite Coating on Anionic and Native Collagen Films by an Alternate Soaking Process", Acta Biomaterialia 3 (2007) 773-778.
6. E. Pecheva, T. Petrov, C. Lungu, P. Montgomery, L. Pramatarova, "Stimulated in Vitro Bone-Like Apatite Formation by a Novel Laser Processing Technique", Chemical Engineering Journal 137 (2008) 144-153.
7. S. Zhang, Y.S. Wang, X.T. Zeng, K. Cheng, M. Qian, D.E. Sun, W.J. Weng, W.Y. Chia, "Evaluation of Interfacial Shear Strength and Residual Stress of Sol-Gel Derived Fluoridated Hydroxyapatite Coatings on Ti6Al4V Substrates", Engineering Fracture Mechanics 74 (2007) 1884-1893.
8. J.C. Elliott, *Structure and Chemistry of the Apatites and Other Calcium Orthophosphates*, Elsevier, (1994).

9. P. Wu, Y.Z. Zeng, C.M. Wang, “Prediction of Apatite Lattice Constants from their Constituent Elemental Radii and Artificial Intelligence Methods”, Biomaterials 25 (2004) 1123-1130.
10. S. Malinov, W. Sha, “Software Products for Modelling and Simulation in Materials Science”, Computational Materials Science 28 (2003) 179-198.
11. M. Svetina, L. Colombi Ciacchi, O. Sbaizero, S. Meriani, A. Devita “Deposition of Calcium Ions on Rutile (110): A First-Principles Investigation”, Acta Materialia 49 (2001) 2169-2177.
12. R. Astala, M.J. Stott, “First Principles Investigation of Mineral Component of Bone: CO_3 Substitutions in Hydroxyapatite”, Chemistry of Materials 17 (2005) 4125-4133.
13. N. Zotov, A. Ludwig, “First-Principles Calculations of the Elastic Constants of Fe-Pt Alloys”, Intermetallics 16 (2008) 113-118.
14. R. Bhowmik, K.S. Kati, D. Kati, “Molecular Dynamics Simulation of Hydroxyapatite-Polyacrylic Acid Interfaces”, Polymer 48 (2007) 664-674.
15. S. Serajzadeh, “Prediction of Temperature Distribution and Required Energy in Hot Forging Process by Coupling Neural Networks and Finite Element Analysis”, Materials Letters 61 (2007) 3296-3300.
16. S. Samarasinghe, *Neural Networks for Applied Sciences and Engineering*, Taylor&Francis, (2007).
17. H.K.D.H. Bhadeshia, “Neural Networks in Materials Science”, ISIJ (The Iron and Steel Institute of Japan) International, 39 (1999) 966-979.
18. R.P. Cherian, L.N. Smith, P.S. Midha, “A Neural Network Approach for Selection of Powder Metallurgy Materials and Process Parameters”, Artificial Intelligence in Engineering 14 (2000) 39-44.
19. M. Çöl, H.M. Ertunç, M. Yılmaz, “An Artifical Neural Network Model for Toughness Properties in Micro-Alloyed Steel in Consideration of Industrial Production Conditions”, Materials and Design 28 (2007) 488-495.

20. H. Man, T. Furukawa, M. Hoffman, S. Imlao, “An Indirect Implicit Technique for Modelling Piezoelectric Ceramics”, Computational Materials Science, doi: 10.1016 / j.coomatsci.2008.01.008.
21. M.S. Ozerdem, S. Kolukisa, “Artificial Neural Network Approach to Predict Mechanical Properties of Hot Rolled, Nonresulfurized, AISI 10xx Series Carbon Steel Bars”, Journal of Materials Processing Technology I99 (2008) 437-439.
22. E.M. Bezerra, A.C. Ancelotti, L.C. Pardini, J.A.F.F. Rocco, K. Iha, C.H.C. Ribeiro, “Artificial Neural Networks Applied to Epoxy Composites Reinforced with Carbon and E-glass Fibers: Analysis of the Shear Mechanical Properties”, Materials Science and Engineering A 464 (2007) 177-185.
23. M. Abendroth, M. Kuna , “Determination of Deformation and Failure Properties of Ductile Materials by Means of the Small Punch Test and Neural Networks” , Computational Materials Science 28 (2003) 633-644.
24. Z. Zhang, K. Friedrich, “Artificial Neural Networks Applied to Polymer Composites: A Review”, Composites Science and Technology 63 (2003) 2029-2044.
25. L.A. Dobrzanski, M.D Trzaska, “Computer Simulation of Hard Magnetic Composite Materials Nd-Fe-B Properties”, Journal of Materials Processing Technology 192-193 (2007) 595-601.
26. E. Mahdi, H.E. Kadi, “Crushing Behaviour of Laterally Compressed Composite Elliptical Tubes: Experiments and Predictions Using Artificial Neural Networks”, Composite Structures 83 (2008) 399-412.
27. A. Bezazi, S.G. Pierce, K. Worden, E.H. Harkati, “Fatigue Life Prediction of Sandwich Composite Materials Under Flexural Tests Using a Bayesian Trained Artificial Neural Network”, International Journal of Fatigue 29 (2007) 738-747.

28. A.M. Hassan, A. Alrashdan, M.T. Hayajneh, A.T Mayyas, “Prediction of Density, Porosity and Hardness in Aluminum-Copper Based Composite Materials Using Artificial Neural Network”, Journal of Materials Processing Technology, doi: 10.1016/ j.jmatprotec.2008.02.066.
29. R.M. Patrikar, “Modeling and Simulation of Surface Roughness”, Applied Surface Science 228 (2004) 213-220.
30. A.C. Basheer, U.A. Dabade, S.S. Joshi, V.V. Bhanuprasad, V.M. Gadre, “Modeling of Surface Roughness in Precision Machining of Metal Matrix Composites using ANN”, Journal of Materials Processing Technology, doi: 10.1016 / j.jmatprotec.2007.04.121.
31. Amethyst Galleries, Inc., http://www.galleries.com/minerals/phosphat/apatite/apatite.htm, last visited on 26 December 2008.
32. C. Rey, C. Combes, C. Drouet, H. Sfihi, A. Barroug, “Physico-chemical Properties of Nanocrystalline Apatites: Implications for Biominerals and Biomaterials”, Materials Science and Engineering C 27 (2007) 198-205.
33. M. Clara, F. Magalhaes, P.A. Williams, “Apatite Group Minerals: Solubility and Environmental Remediation”, Thermodynamics, Solubility and Environmental Issues, T. M. Letcher (editor) Elsevier B.V. (2007).
34. P.J. Panteix, I. Julien, P. Abelard, D. Bernache-Assollant, “Influence of Cationic Vacancies on the Ionic Conductivity of Oxyapatites”, Journal of the European Ceramic Society 28 (2008) 821-828.
35. C. Hoen, V. Rheinberger, W. Holand, E. Apel, “Crystallization of Oxyapatite in Glass-Ceramics”, Journal of the European Ceramic Society 27 (2007) 1579-1584.
36. P.J. Panteix, E. Bechade, I. Julien, P. Abelard, D. Bernache-Assolant, “Influence of Anionic Vacancies on the Ionic Conductivity of Silicated Rare Earth Apatites”, Materials Research Bulletin, doi: 10.1016/j.materresbull.2007.05.030.

37. V. Louis-Achille, L. De Windt, M. Defrancccschi, “Local Density Calculation of Structural Properties and Cohesive Energy for $ScPO_4$ and the apatite $Ca_{10}(PO_4)_6F_2$”, Journal of Molecular Structure (Theochem) 426 (1998) 217-224.
38. L. Leon-Reina, J.M. Porras-Vazquez, E.R. Losilla, M.A.G. Aranda, “Interstitial Oxide Positions in Oxygen-Excess Oxy-apatite”, Solid State Ionics 177 (2006) 1307-1315.
39. S.M. Best, A.E. Porter, E.S. Thian, J. Huang, “Bioceramics: Past, Present and for the Future”, Journal of the European Ceramic Society, doi: 10.1016/j.jeurceramsoc.2007.12.001.
40. Joint Committee on Powder Diffractions Standard (JCPDS) Database, Rigaku Qualitative Analysis ICDD (The International Centre for Diffraction Data) Software.
41. T.J. Webster, E.A. Massa-Schlueter, J.L. Smith, E.B. Slamovich, “Osteoblast Response to Hydroxyapatite Doped with Divalent and Trivalent Cations”, Biomaterials 25 (2004) 2111-2121.
42. S. Sprio, A. Tampieri, E. Landi, M. Sandri, S. Martorana, G. Celotti, G. Logroscino, “Physico-chemical Properties and Solubility Behaviour of Multi-substituted Hydroxyapatite Powders Containing Silicon”, Materials Science and Engineering C 28 (2008) 179-187.
43. R.H. Doremus, “Review Bioceramics”, Journal of Materials Science 27 (1992) 285-297.
44. J.C. Elliott, P.E. Mackie, R. A. Young, “Monoclinic Hydroxyapatite”, Science, 180 (1973) 1055-1057.
45. R. Atsala, M.J. Stott, “First Principles Investigation of Mineral Component of Bone: CO_3 Substitutions in Hydroxyapatite”, Chemistry of Materials 17 (2005) 4125-4133.
46. B. Sutter, D.W. Ming, A. Clearfield, L. R. Hossner, “Mineralogical and Chemical Characterization of Iron-, Manganese-, and Copper- Containing

Synthetic Hydroxyapatites", Soil Science Society of America Journal 67 (2003) 1935-1942.

47. M.I. Kay, R.A. Young, A.S. Posner, "Crystal Structure of Hydroxyapatite", Nature 204 (1964) 1050-1052.
48. J.B. Park, J.D. Bronzino, " Biomaterials: Principles and Applications", CRC Press (2003).
49. A.S. Posner, A. Perloff, A.F. Diorio, "Refinement of the Hydroxyapatite Structure", Acta Crystallographica 11 (1958) 308-309.
50. Z.Y. Li, W.M. Lam, C. Yang, B. Xu, G.X. Ni, S.A. Abbah, K.M.C. Cheung, K.D.K. Luk, W.W. Lu, "Chemical Composition, Crystal Size and Lattice Structural Changes After Incorporation of Strontium Into Biomimetic Apatite", Biomaterials 28 (2007) 1452-1460.
51. M.E. Fleet, X. Liu, "Site Preference of Rare Earth Elements in Hydroxyapatite [$Ca_{10}(PO_4)_6(OH)_2$]", Journal of Solid State Chemistry 149 (2000) 391-398.
52. T. Ikoma, A. Yamazaki, S. Nakamura, M. Akao, "Preparation and Structure Refinement of Monoclinic Hydroxyapatite", Journal of Solid State Chemistry 144 (1999) 272-276.
53. John von Neumann Institute for Computing, www.fz-juelich.de/wscsm/pdf/allen.pdf, last visited on 26 December 2008.
54. D. Marx, J. Hutter, "Ab Initio Molecular Dynamics: Theory and Implementation", NIC (John von Neumann Institute for Computing) Series 3 (2000) 329-477.
55. J.S. Tse, "Ab Initio Molecular Dynamics with Density Functional Theory", Annual Review of Physical Chemistry 53 (2002) 249-90.
56. S.S. Rao, *Finite Element Method in Engineering*, Elsevier, (2004).
57. D.P. Landau, K. Binder, *A Guide to Monte Carlo Simulations in Statistical Physics*, Cambridge University Press, (2000).

58. G.A. Mansoori, *Principles of Nanotechnology: Molecular-Based Study of Condensed Matter in Small Systems*, World Scientific Publishing Company (2005).
59. Ashcroft Moore Software, www.usingneuralnetworks.com/what-is-a-neural-network.html, last visited on 26 December 2008.
60. P.A. Lucon, R.P. Donovan, "An Artificial Neural Network Approach to Multiphase Continua Constitutive Modeling", Composites: Part B 38 (2007) 817-823.
61. D.J. Scott, P.V. Conovey, J.A. Kilner, J.C.H. Rossiny, N. McN. Alford, "Prediction of the Functional Properties of Ceramic Materials from Composition Using Artificial Neural Networks", Journal of the European Ceramic Society 27 (2007) 4425-4435.
62. C. Karatas, A. Sozen, S. Erguney, "Modelling of Residual Stresses in the Shot Peened Material C-1020 by Artificial Neural Network", Expert Systems with Applications, doi: 10.1016/j.eswa.2008.02.012.
63. M.A. Meyers, P. Chen, A.Y. Lin, Y. Seki, "Biological Materials: Structure and Mechanical Properties", Progress in Materials Science, 53 (2008) 1-206.
64. C. Rey, C. Combes, C. Drouet, A. Lebugle, H. Sfihi, A. Barroug, "Nanocrystalline Apatites in Biological Systems: Characterisation, Structure and Properties", Materialwissenschaft und Werkstofftechnik, 38 (2007) 996-1002.
65. Neural Network Fundamentals for Scientists and Engineers, http://www.cibse.org/pdfs/neural.pdf, last visited on 26 December 2008.
66. A. Meyer-Bäse, *Pattern Recognition for Medical Imaging*, Elsevier Academic Press, (2004).
67. N.K. Sinha, M.M. Gupta, *Soft Computing and Intelligent Systems: Theory and Applications*, Academic Press, (2000).

68. Cooperative Institute for Mesoscale Meteorological Studies, http://www.cimms.ou.edu/~schultz/snowdensity/figs/fig4b.JPG, last visited on 26 December 2008.
69. Missouri University of Science and Technology, http://web.mst.edu/~ganeshv/clip_image002.JPG, last visited on 26 December 2008.
70. A. Heiat, "Comparison of Artificial Neural Network and Regression Models for Estimating Software Development Effort", Information and Software Technology 44 (2002) 911-922.
71. H. Demuth, M. Beale M. Hagan, *Matlab Neural Network Toolbox 6 Users Guide*, The Mathworks Inc., (2008).
72. K.J. McGarry, S. Wermter, J. MacIntyre, "Knowledge Extraction from Radial Basis Function Networks and Multilayer Perceptrons", IJCNN (International Joint Conference on Neural Networks) 4 (1999) 2494-2497.
73. A.M. Ibrahim, *Fuzzy Logic for Embedded Systems Applications*, Newnes, (2004).
74. Worcester Polytechnic Institute, http://davis.wpi.edu/~matt/courses/soms/#Introduction, last visited on 26 December 2008.
75. D. Isa, V.P. Kallimani, L.H. Lee, "Using the Self Organizing Map for Clustering of Text Documents", Expert Systems with Applications, doi:10.1016/j.eswa.2008.07.082.
76. N.C. Yeo, K.H. Lee, Y.V. Venkatesh, S.H. Ong, "Colour Image Segmentation Using the Self-Organizing Map and Adaptive Resonance Theory", Image and Vision Computing 23 (2005) 1060-1079.
77. Epina GmbH, http://www.lohninger.com/helpcsuite/kohonen_network_-_background_information.htm, last visited on 26 December 2008.
78. The MathWorks, Inc., http://www.mathworks.com/access/helpdesk/help/toolbox/nnet/logsig.gif, last visited on 26 December 2008.
79. The MathWorks, Inc., http://www.mathworks.com/access/helpdesk/help/toolbox/nnet/tansig.gif, last visited on 26 December 2008.

80. Willamette University, http://www.willamette.edu/~gorr/classes/cs449/precond.html, last visited on 26 December 2008.
81. The University of Lousiana at Lafayette, http://www.ucs.louisiana.edu/~isb9112/dept/phil341/IMG00006.GIF, last visited on 12 October 2008.
82. The MathWorks, Inc., http://www.mathworks.com/access/helpdesk/help/toolbox/nnet/, last visited on 26 December 2008.
83. D.R. Lide, *Handbook of Chemistry and Physics*, Taylor&Francis (2003).
84. Z. Evis, "Reactions in Hydroxylapatite-Zirconia Composites", Ceramics International 33 (2007) 987-991.
85. The International Centre for Diffraction Data, http://www.icdd.com/resources/webpdf/explain.htm, last visited on 26 December 2008.
86. I.R. Gibson, S.M. Best, W. Bonfield, "Chemical Characterization of Silicon-Substituted Hydroxyapatite", Journal of Biomedical Materials Research, 44 (1999) 422-428.
87. A. Onda, S. Ogo, K. Kajiyoshi, K. Yanagisawa, "Hydrothermal Synthesis of Vanadate/Phosphate Hydroxyapatite Solid Solutions", Materials Letters 62 (2008) 1406-1409.
88. P.E. Kazin, O.R. Gazizova, A.S. Karpov, M. Jansen, Y.D. Tretyakov, "Incorporation of 3d-Metal Ions in the Hexagonal Channels of the $Sr_5(PO_4)OH$ Apatite", Solid State Sciences 9 (2007) 82-87.
89. M. Masaoka, A. Kyono, "Single Crystal Growth of Lead Vanado-Chlorapatite $Pb_5(VO_4)_3Cl$ Using Flux Method", Materials Letters 60 (2006) 3922-3926.
90. H.P. Beck, M. Douiheche, R. Haberkorn, H. Kohlmann, "Synthesis and Characterization of Chloro-Vanado-Apatites $M_5(VO_4)_3Cl$ (M=Ca, Sr, Ba)", Solid State Sciences 8 (2006) 64-70.
91. K. Boughzala, E.B. Salem, A.B. Chrifa, E. Gaudin, K. Bouzouita, "Synthesis and Characterization of Strontium-Lanthanum Apatites", Materials Research Bulletin 42 (2007) 1221-1229.

92. B. Hamdi, H.E. Feki, J. Savariault, A.B. Salah, "Synthesis and Distribution of Cations in Substituted Lead Phosphate Lacunar Apatites", Materials Research Bulletin 42 (2007) 299-311.
93. T. Tian, D. Jiang, J. Zhang, Q. Lin, "Synthesis of Si-substituted Hydroxyapatite by a Wet Mechanochemical Method", Materials Science and Engineering C 28 (2008) 57-63.
94. S.I. Gallant, *Neural Network Learning and Expert Systems*, The MIT Press, (1993).
95. Mineralogy Database, http://webmineral.com/data/Svabite.shtml, last visited on 26 December 2008.
96. Mineralogy Database, http://webmineral.com/data/Johnbaumite.shtml, last visited on 26 December 2008.
97. Z. Evis, R.H. Doremus, "Hot-pressed Hydroxylapatite/Monoclinic Zirconia Composites with Improved Mechanical Properties", Journal of Materials Science, 42 (2007) 2426-2431.
98. B. Basar, Z. Evis, "Structural Investigation of Nanohydroxyapatite Doped with Y^{3+} and F^{-} Ions", Materials Science and Technology, doi: 10.1179/174328408X317255.
99. Z. Evis, "Al^{3+} Doped Nano-Hydroxyapatites and Their Sintering Characteristics", Journal of the Ceramic Society of Japan, 114 (2006) 1001-1004.
100. C. Ergun, T.J. Webster, R. Bizios, R.H. Doremus, "Hydroxylapatite with Substituted Magnesium, Zinc, Cadmium, and Yttrium. I. Structure and Microstructure", Journal of Biomedical Materials Research 59 (2002) 305-311.
101. B.D. Cullity, S. R. Stock, *Elements of X-ray Diffraction (Third Edition)*, Prentice Hall, (2001).

102. K. Xu, M. Xie, L.C. Tang, S.L. Ho, “Application of Neural Networks in Forecasting Engine Systems Reliability”, Applied Soft Computing 2 (2003) 255-268.
103. M. Veiderma, K. Tonsuaadu, R. Knubovets, M. Peld, “Impact of Anionic Substitutions on Apatite Structure and Properties”, Journal of Organometallic Chemistry 690 (2005) 2638-2643.
104. H. Okuyucu, A. Kurt, E. Arcaklioglu, “Artificial Neural Network Application to the Friction Stir Welding Alumnium Plates”, Materials and Design 28 (2007) 78-84.
105. M.S. Ozerdem, S. Kolukisa, “Artificial Neural Network Approach to Predict the Mechanical Properties of Cu-Sn-Pb-Zn-Ni Cast Alloys”, Materials and Design, doi:10.1016/j.matdes.2008.05.019.
106. H.F. Zhao, M. Chen, Y. Jin, “Determination of Interfacial Properties between Metal Film and Ceramic Substrate with an Adhesive Layer”, Materials and Design 30 (2009) 154-159.
107. W. Sha, K.L. Edwards, “The Use of Artificial Neural Networks in Materials Science Based Research”, Materials and Design 28 (2007) 1747-1752.
108. S. Yoshitake, V. Narayan, H. Harada, K.D.H. Bhadeshia, D.J.C. Mackay, “Estimation of the γ and γ' Lattice Parameters in Nickel-Base Superalloys Using Neural Network Analysis”, ISIJ (The Iron and Steel Institute of Japan) International 38 (1998) 495-502.
109. A. Bholoa, S.D. Kenny, R. Smith, “A New Approach to Potential Fitting Using Neural Networks”, Nuclear Instruments and Methods in Physics Research B 255 (2007) 1-7.
110. Ch. Bourouis , A. Meddour, A.K. Moussaoui, “Determination of Optical Properties of $Al_{80}Mn_{20}$ Quasi-Crystalline Alloy Using Neural Networks”, Journal of Molecular Structure: THEOCHEM 777 (2006) 45-51.

111. R. Leardi, *Nature-Inspired Methods in Chemometrics: Genetic Algorithms and Artificial Neural Networks*, Elsevier, (2003).
112. M.R. Dashtbayazi, A. Shokuhfar, A. Simchi, "Artificial Neural Network Modeling of Mechanical Alloying Process for Synthesizing of Metal Matrix Nanocomposite Powders", Materials Science and Engineering A 466 (2007) 274-283.
113. R. Qing-Li, C. Quan-Xi, "Predictive Model Based on Artificial Neural Net for Purity of Perovskite-type $SrTiO_3$ Nanocrystalline", Transactions of Nonferrous Metals Society of China 16 (2006) 865-868.
114. M. Severcan, F. Severcan, P.I. Haris, "Estimation of Protein Secondary Structure from FTIR Spectra Using Neural Networks", Journal of Molecular Structure 565-566 (2001) 383-387.
115. H. Kirschner, R. Hillebrand, "Neural Networks for HREM Image Analysis", Information Sciences 129 (2000) 31-44.

APPENDIX A

PEAKS OF STANDARD, DRY AND SINTERED HYDROXYAPATITES

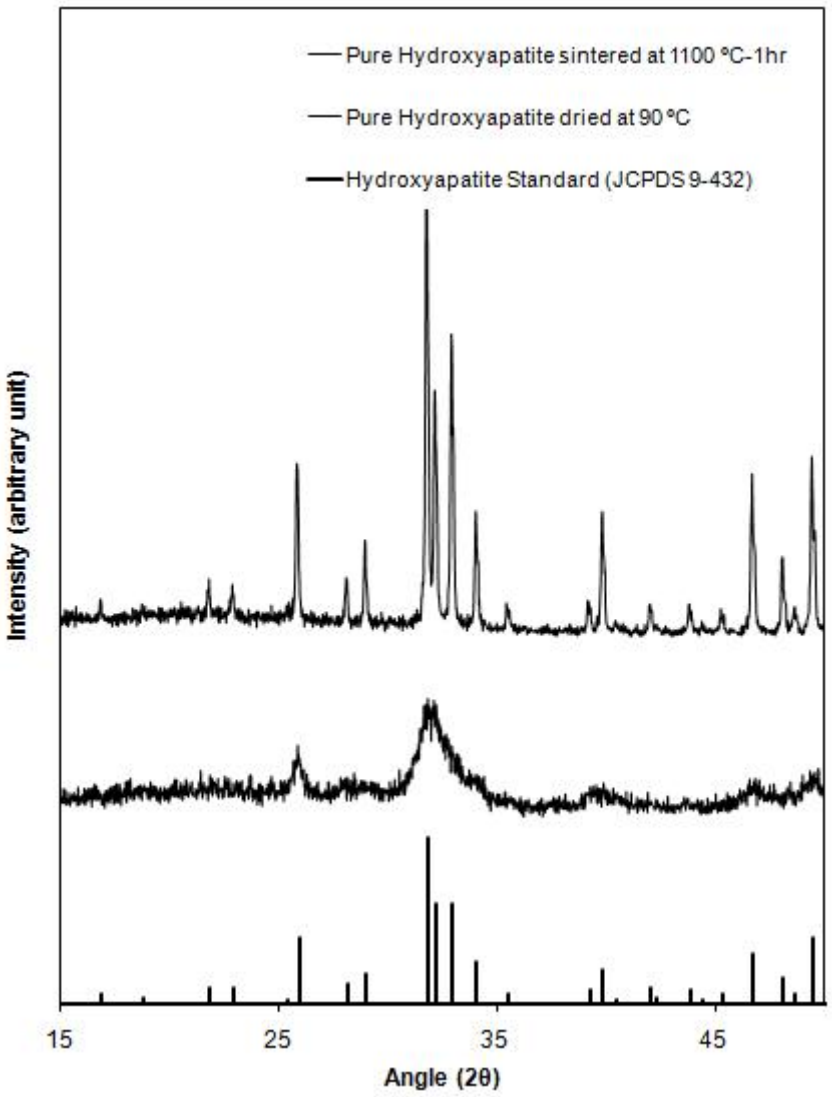

Figure A.1 Peaks of standard, dry and sintered hydroxyapatites [97].

APPENDIX B

CALCULATION OF HYDROXYAPATITE LATTICE PARAMETERS WITH A REFERENCE

Table B.1 Miller indices (hkl) of HAp and their corresponding 2θ values for reference and experimental samples.

(hkl) values	2θ (reference from JCPDS #9-432)	2θ (experimental)
002	25,8783	25,8219
211	31,7737	31,7075
112	32,1966	32,1188
300	32,9024	32,8494
202	34,0487	33,9975
310	39,8195	39,7356
222	46,7127	46,6206
213	49,4690	49,3937
321	50,4942	50,4094
004	53,1448	53,1100

Matlab code for this calculation is given in two parts below:

First part:

```
a=9.418;
```

```
c=6.884;
lambda=1.5418;
ratio=a/c;
n=10;  % number of inputs
hkl=zeros(n,3);
two_theta=zeros(n,1);
```

(hkl) and 2θ (experimental) values should be imported to hkl and two_theta matrices after first part of the code is written. a, c, lambda (λ) and n values were taken from the reference card of JCPDS #09-0432 and these numbers should be determined according to the specific reference. Than, second part of the code should be executed to obtain final lattice parameters.

Second part:

```
theta=zeros(n,1);
for i=1:n
theta(i,1)= two_theta(i,1)/2;
end
s=zeros(n,1);
for i=1:n
s(i,1)=hkl(i,1)^2+hkl(i,2)^2+hkl(i,1)*hkl(i,2);
end
l2=zeros(n,1);
for i=1:n
l2(i,1)=hkl(i,3)^2;
end
alpha=zeros(n,1);
for i=1:n
```

```
alpha(i,1)=(ratio^2)*l2(i,1);
end
beta=zeros(n,1);
for i=1:n
beta(i,1)=4/3*s(i,1);
end
gamma=zeros(n,1);
for i=1:n
gamma(i,1)=lambda/2/sin(2*pi/360*theta(i,1));
end
asub=zeros(n,1);
csub=zeros(n,1);
for i=1:n
if beta(i,1)>alpha(i,1)
asub(i,1)=gamma(i,1)*sqrt(beta(i,1)+alpha(i,1));
csub(i,1)=0;
elseif beta(i,1)<alpha(i,1)
asub(i,1)=0;
csub(i,1)=gamma(i,1)*sqrt(beta(i,1)/(ratio^2)+(l2(i,1)));
elseif beta(i,1)==alpha(i,1)
asub(i,1)=0;
csub(i,1)=0;
end
end
j=0;
for i=1:n
if asub(i,1) ~= 0
j=j+1;
end
```

```
end
k=0;
for i=1:n
if csub(i,1) ~= 0
k=k+1;
end
end
asub_average=sum(asub)/j;
csub_average=sum(csub)/k;
ratio_new=asub_average/csub_average;
while ratio_new ~= ratio
ratio=ratio_new;
for i=1:n
alpha(i,1)=(ratio^2)*l2(i,1);
end
for i=1:n
if beta(i,1)>alpha(i,1)
asub(i,1)=gamma(i,1)*sqrt(beta(i,1)+alpha(i,1));
csub(i,1)=0;
elseif beta(i,1)<alpha(i,1)
asub(i,1)=0;
csub(i,1)=gamma(i,1)*sqrt(beta(i,1)/(ratio^2)+(l2(i,1)));
elseif beta(i,1)==alpha(i,1)
asub(i,1)=0;
csub(i,1)=0;
end
end
j=0;
for i=1:n
```

```
if asub(i,1) ~= 0
j=j+1;
end
end
k=0;
for i=1:n
if csub(i,1) ~= 0
k=k+1;
end
end
asub_average=sum(asub)/j;
csub_average=sum(csub)/k;
ratio_new=asub_average/csub_average;
end
```

Results of this calculation:

a (calculated) = 9,444 ; c (calculated) = 6,8999
a/c (calculated) = 1,3687 (reference has a/c = 1,3681)

APPENDIX C

TRAINING CODES OF NEURAL NETWORKS

Bayesian Regularization

```
net=newff(minmax(p),[4,1],{'tansig','purelin'},'trainbr');
net.trainParam.show = 100;
net.trainParam.epochs = 1000;
net=init(net);
[net,tr]=train(net,p,t);
```

Gradient Descent with Momentum and Adaptive Learning Rate Backpropagation

```
net=newff(minmax(p),[7,1],{'tansig','purelin'},'traingdx');
net=init(net);
net.trainParam.show=100;
net.trainParam.mc=0.8;
net.trainParam.lr=0.05;
net.trainParam.epochs=5000;
net.trainParam.goal=1e-3;
[net,tr]=train(net,p,t);
```

Levenberg-Marquardt Backpropagation

```
net=newff(minmax(p),[4,1],{'tansig','purelin'},'trainlm');
net=init(net);
net.trainParam.show=20;
net.trainParam.epochs=400;
net.trainParam.goal=15e-4;
[net,tr]=train(net,p,t);
```

Resilient Backpropagation

```
net=newff(minmax(p),[6,1],{'tansig','purelin'},'trainrp');
net.trainParam.show = 100;
net.trainParam.epochs = 5000;
net.trainParam.goal = 1e-3;
[net,tr]=train(net,p,t);
```

Scaled Conjugate Gradient Backpropagation

```
net=newff(minmax(p),[7,1],{'tansig','purelin'},'trainscg');
net.trainParam.show = 100;
net.trainParam.epochs = 3000;
net.trainParam.goal = 177e-5;     (1e-3 for lattice parameter c)
[net,tr]=train(net,p,t);
```

General Post-Analysis Code:

```
a=sim(net,p);
[m,b,r]=postreg(a,t)
```